A MODEL FOR SIMIAN VIRUS 40 SMALL TUMOR ANTIGEN EXPRESSION IN DROSOPHILA MELANOGASTER

APPROVED BY SUPERVISORY COMMITTEE

Timothy Megraw, Ph.D.

Robert Hammer, Ph.D.

Hongtao Yu, Ph.D.

Hui Zou, Ph.D.

DEDICATION

I dedicate my thesis to everyone who filled my world with vivid colors. To the people who made me see stars when I closed my eyes and everything else was dark. Without you, life would not be worth living.

A MODEL FOR SIMIAN VIRUS 40 SMALL TUMOR ANTIGEN EXPRESSION IN DROSOPHILA MELANOGASTER

by

SHAILA KOTADIA

DISSERTATION / THESIS

Presented to the Faculty of the Graduate School of Biomedical Sciences

The University of Texas Southwestern Medical Center at Dallas

In Partial Fulfillment of the Requirements

For the Degree of

DOCTOR OF PHILOSOPHY

The University of Texas Southwestern Medical Center at Dallas

Dallas, Texas

September, 2008

A MODEL FOR SIMIAN VIRUS 40 SMALL TUMOR ANTIGEN EXPRESSION IN DROSOPHILA MELANOGASTER

SHAILA KOTADIA, Ph.D.

The University of Texas Southwestern Medical Center at Dallas, 2008

TIMOTHY MEGRAW, Ph.D.

Viruses of the DNA tumor virus family share the ability to transform vertebrate cells through the action of virus-encoded tumor antigens that interfere with normal cell physiology. They accomplish this very efficiently by inhibiting endogenous tumor suppressor proteins that control cell proliferation and apoptosis. Simian Virus 40 (SV40) encodes two oncoproteins, large tumor antigen (LT), which directly inhibits the tumor suppressors p53 and Rb, and small tumor antigen (ST), which interferes with serine/threonine protein phosphatase 2A (PP2A). We have constructed a Drosophila model for SV40 ST expression and show that ST induces supernumerary centrosomes, an

activity we also demonstrate in human cells. In early Drosophila embryos, ST also induced increased microtubule stability, chromosome segregation errors, defective assembly of actin into cleavage furrows, cleavage failure, a rise in cyclin E levels, and embryonic lethality. Using ST mutants and genetic interaction experiments between ST and PP2A subunit mutations, we show that all of these phenotypes are dependent on ST's interaction with PP2A. After characterizing the effects of ST on the cell cycle, we utilized the Drosophila model to further study ST. Through proteomics, we discovered ST binds the kinesin-1 motor, leading to inactivation of motor activity. Using genetic interactions, we showed that ST genetically interacts with a cyclin E mutant and overexpressed cyclin E. Together, these analyses demonstrate novel properties for ST and the validity and utility of Drosophila as a model for viral oncoprotein function *in vivo*.

TABLE OF CONTENTS

PRIOR PUBLICATIONS

Kotadia S, Kao LR, Comerford SA, Jones RT, Hammer RE, Megraw TL (2008). PP2A-dependent disruption of centrosome replication and cytoskeleton organization in Drosophila by SV40 small tumor antigen. Oncogene.

LIST OF FIGURES

LIST OF TABLES

LIST OF DEFINITIONS

ago – archipelago

AMP-PNP – adenosine 5′-(β,γ-imido)triphosphate

ATP – adenosine triphosphate

bp – basepairs

Cdk – Cyclin dependent kinase

Cdk2 – Cyclin dependent kinase 2

C. elegans - Caenorhabditis elegans

CIN – chromosomal instability

CNN – centrosomin

cycE – cyclin E

dpr1 – defective proboscis retention 1

eGFP – enhanced green fluorescent protein

EM – electron microscopy

FEZ1 – Fasciculation and elongation protein 1

GSK3 – Glycogen synthase kinase 3

GTP – guanine triphosphate

HBx – Hepatitis B virus oncoprotein X

HBxIP – Hepatitis B virus oncoprotein X interacting protein

hCdc4 – human Cdc4

HPLC/MS/MS – high performance liquid chromatography/mass spectrometry/mass spectrometry

HPV – Human papillomavirus

Hsc70 – Heat shock chaperone 70

HTLV-1- Human T-cell leukemia virus type-1

IP – immunoprecipitate

JIP – c-Jun N-terminal kinase interacting protein

JNK – c-Jun N-terminal kinase

kb – kilobasepairs

KHC – Kinesin heavy chain

LT – Large tumor antigen

MAP – microtubule associated protein

MAP – Mitogen activated protein

MAPK – Mitogen activated protein kinase

mRFP – monomeric red fluoresecent protein

MS – mass spectrometry

MTOC – microtubule organizing center

mts – microtubule star

NfI – Nuclear factor I

PCM – pericentriolar matrix

Plk4 – Polo like kinase 4

PP2A – Protein phosphatase 2A

Rb – Retinoblastoma protein

RNAi – RNA interference

RSA – regulator of spindle assembly

SCF – Skp/Cullin/F-box

ST – Small tumor antigen

SV40 – Simian virus 40

syt7 – synaptotagmin 7

tws – twins

wdb – widerborst

wrd – well-rounded

CHAPTER ONE

INTRODUCTION

A. Simian Virus 40

History of Simian Virus 40

Simian virus 40 (SV40) is naturally found in rhesus monkey populations, persists as a latent infection in the kidneys, and is asymptomatic (Poulin and DeCaprio 2006). SV40 was first discovered when polio vaccines were generated in rhesus and cynomolgous macaque kidney cells. SV40 was found to be a contaminant in some but not all polio vaccines when safety measures were taken to test the effect of the vaccine on green African monkey kidney cells, leading to SV40 exposure in some individuals vaccinated for polio virus (Sweet and Hilleman 1960). Furthering the controversy, SV40 was found to generate tumors in mice (Girardi, Sweet et al. 1962). Yet, recent studies show conflicting results that SV40 has the same consequence or even persists in humans (Poulin and DeCaprio 2006).

SV40, a member of the *Polyomaviridae* family, has a genome of approximately 5kb. The genome encodes for viral proteins 1-4, large tumor antigen (LT), small tumor antigen (ST), 17kT, and agnoprotein (Thimmappaya, Reddy et al. 1978; Sullivan and Pipas 2002; Daniels, Sadowicz et al. 2007). Viral proteins 1-4 are core proteins involved in virion assembly and cell lysis necessary for persistent infection. 17kT and agnoprotein have little known function. LT and ST, the most well characterized SV40 proteins, have

transforming potential (Sullivan and Pipas 2002). The SV40 early region encodes LT, ST, and 17kT due to alternative splicing (Figure 1-1a). LT and17kT contain splice sites, whereas the ST transcript does not have any introns. This splicing results in three proteins that share a common N-terminal domain and binding partner, and differ in the C-terminal region, conferring unique binding partners.

The transforming potential of SV40 requires the early region of the genome that encodes for LT and ST (Hahn, Dessain et al. 2002). Originally, it was believed that LT alone could cause transformation in human cell lines with other oncogenic stressors, however LT expression was not sufficient (Sager, Tanaka et al. 1983). This discovery prompted the field to explore the SV40 early region for potential proteins that may act with LT to induce tumorigenesis. Through these studies, ST was found to be required to cause transformation, while 17kT, the third early region protein, is dispensable. Therefore, LT and ST were further characterized to determine their transforming capabilities.

Large tumor antigen

LT is a 708 amino acid protein with several binding partners; the most important in transforming potential are p53 and retinoblastoma protein (Rb). In fact, p53 was initially discovered as a binding partner of LT, emphasizing the importance of DNA tumor viral proteins in discovering cellular pathways (Linzer and Levine 1979; Lane and Crawford 1980; McCormick and Harlow 1980). Levels of the transcriptional regulator p53 increase in response to cellular stress resulting in an upregulation of genes that either arrest the cell cycle or induce apoptosis (Aylon and Oren 2007). LT binds the DNA-binding domain of p53 and inhibits p53 from transcriptionally activating genes to allow

cell growth (Bargonetti, Reynisdottir et al. 1992; Jiang, Srinivasan et al. 1993). Rb was first shown as the tumor suppressor protein associated with human retinoblastoma. Rb functions as a transcriptional repressor that regulates progression from G1- to S-phase in several ways, for example, through repression of the E2F promoter, a transcriptional activator that controls cell cycle progression and DNA synthesis (Giacinti and Giordano 2006; Goodrich 2006). LT's LXCXE motif, a motif shared by other viral proteins, binds and inhibits Rb activity. This function is dependent on the LT J-domain, which binds heat shock chaperone 70 (Hsc70) (Ahuja, Saenz-Robles et al. 2005). Despite the ability to bind and block the activity of key tumor suppressor genes, LT alone cannot induce transformation. Instead ST was found to be crucial for tumorigenesis due to its ability to bind and inhibit protein phosphatase 2A (PP2A), an activity unique to ST.

Small Tumor Antigen

ST has two domains, a J domain and a PP2A-binding domain (Figure 1-1b). LT, ST, and 17kT share in common the J domain, which confers Hsc70 binding, and is dispensable for ST tumorigenic potential. Therefore, the PP2A-binding domain is necessary for transformation (Mumby 2007). The PP2A-binding domain, as the name suggests, binds and inhibits the phosphatase activity of PP2A.

PP2A is a phosphatase with three subunits, the scaffolding (A) subunit, the catalytic (C) subunit, and the regulatory (B) subunit (Janssens and Goris 2001). The A subunit binds both the catalytic and regulatory subunits, thereby serving as a scaffold for the holoenzyme. The C subunit contains the phosphatase activity and physically dephosphorylates substrates. Finally, the B subunit determines substrate specificity. Four

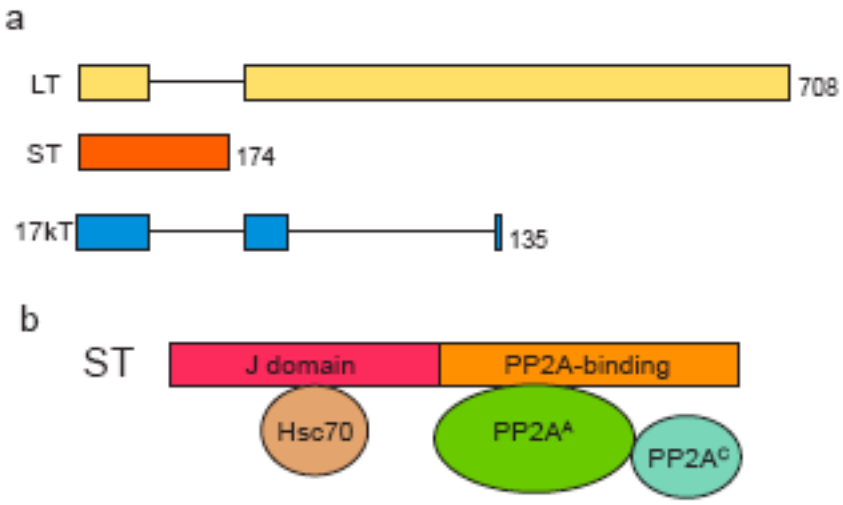

Figure 1-1. Simian virus 40 early region and small tumor antigen. (a) Simian virus 40 (SV40) early region encodes large tumor antigen (LT), small tumor antigen (ST), and 17kT due to alternative splicing. (b) ST has two domains: a J domain and a PP2A-binding domain. The J domain binds Heat shock chaperone 70 (Hsc70) and increases Hsc70 ATPase activity. The PP2A-binding domain binds Protein phosphatase 2A (PP2A) A and C subunits to disrupt phosphatase activity.

classes of the regulatory subunit exist, B, B', B'', and B''', and are defined not by sequence similarity but rather by A subunit binding sites. All four regulatory subunit classes bind the A subunit at overlapping sites, excluding multiple B subunits from binding the A subunit simultaneously (Cho and Xu 2007). Each regulatory subunit targets several proteins for dephosphorylation, resulting in greater than 75 substrates for PP2A, with more yet undiscovered, demonstrating the necessity of the phosphatase.

Recently the crystal structures for the PP2A holoenzyme and ST bound to the $PP2A^A$ subunit were solved (Chen, Xu et al. 2007; Cho, Morrone et al. 2007). These structures revealed that the second zinc-binding domain of ST binds to the HEAT repeats of the $PP2A^A$ subunit, the binding site of the B' regulatory subunit. These data confirm that ST displaces the regulatory subunit to block dephosphorylation of substrates. Furthermore, ST binding $PP2A^A$ in a similar region as regulatory subunits suggests that ST can act as a viral-type B subunit, possibly conferring new substrate specificities for the phosphatase. Thus far, two examples of ST targets have been identified, the increased specificity of PP2A activity towards Histone H1 and novel PP2A substrate specificity for the androgen receptor (Yang, Lickteig et al. 1991; Yang, Vitto et al. 2005). Therefore, while ST is often used as a tool to disrupt PP2A phosphatase activity, ST may also dephosphorylate novel substrates.

B. Centrosome Function

Overview

Centrosomes are organelles in the cell that function as microtubule organizing centers (MTOCs). A centrosome consists of two centrioles surrounded by an amorphous material, as depicted by electron microscopy (EM), known as the pericentriolar matrix (PCM). The PCM contains about one hundred proteins, including centrosomal proteins that function to polymerize and stabilize microtubules during mitosis. The main functions of the centrosome are to organize a bipolar spindle during mitosis and to organize microtubules in interphase (Azimzadeh and Bornens 2007).

Centrosome Duplication

Centrosome duplication occurs once per cell cycle. Licensing centrosome duplication is crucial to the cell's fidelity because increased centrosome numbers can result in multipolar spindles (Brinkley 2001; Nigg 2002; Sluder and Nordberg 2004). Multipolar spindles can generate aneuploidy due to chromosome missegregation. Further, centrosome amplification is often observed in cancerous cells, however it is unknown whether this is a cause or consequence of transformation. Centrosomal proteins have also been implicated as tumor suppressor genes or oncogenes (Fukasawa 2007).

One licensing mechanism for centrosome duplication is centriole engagement. Two centrioles are considered engaged when a cohesive protein physically connects them. At the metaphase to anaphase transition, the cohesive protein is cleaved by separase and centrioles disengage. Disengaged centrioles duplicate during S-phase resulting in two pairs of newly engaged centrioles (Tsou and Stearns 2006). The centrioles remain engaged from S-phase to metaphase and are unable to duplicate again. After S-phase, the centrosomes mature in G2 through PCM acquisition. Finally, the

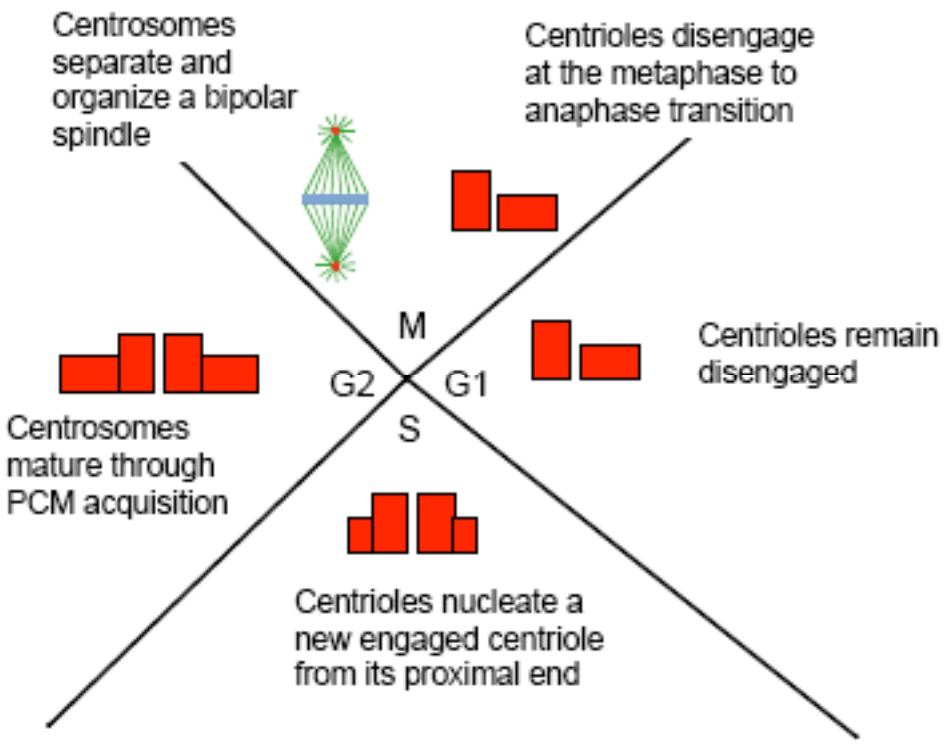

Figure 1-2. Centrosome duplication cycle. Centrioles become disengaged at the metaphase to anaphase transition in mitosis and remain disengaged in G1. New centrioles are nucleated from the proximal end of the centriole in S-phase and are engaged, preventing reduplication. The centrosomes mature in G2 and separate in mitosis to form a bipolar spindle in mitosis for accurate chromosome segregation.

centrosomes separate in mitosis to form a bipolar spindle for accurate chromosome segregation (summarized in Figure 1-2) (Nigg 2006).

A signaling pathway for centrosome duplication was recently identified in *Caenorhabditis elegans* (*C. elegans*). The five proteins involved in centrosome duplication were Spd-2, Zyg-1, Sas-4, Sas-5, and Sas-6 (O'Connell, Caron et al. 2001; Kirkham, Muller-Reichert et al. 2003; Leidel and Gonczy 2003; Delattre, Leidel et al. 2004; Kemp, Kopish et al. 2004; Pelletier, Ozlu et al. 2004; Leidel, Delattre et al. 2005). These proteins are conserved in Drosophila and humans, except for Sas-5 (Nigg 2006). The Zyg-1 homologue in Drosophila and humans is believed to be polo-like kinase 4 (Plk4). When these proteins are knocked down by RNA interference (RNAi) or in null mutants, centrioles fail to duplicate (Leidel and Gonczy 2003; Bettencourt-Dias, Rodrigues-Martins et al. 2005; Leidel, Delattre et al. 2005; Basto, Lau et al. 2006; Kleylein-Sohn, Westendorf et al. 2007). Conversely, when Sas-4, Sas-6, or Plk4 proteins are overexpressed, centrioles amplify (Leidel, Delattre et al. 2005; Peel, Stevens et al. 2007; Rodrigues-Martins, Riparbelli et al. 2007). The most dramatic example is Plk4 overexpression in the early Drosophila embryo. Not only do centrioles amplify, but *de novo* centrioles also form in the unfertilized embryo (Rodrigues-Martins, Riparbelli et al. 2007). Interestingly, when Plk4 was overexpressed in human cells, centrioles amplified in a floret-like arrangement where new procentrioles form in a circle around the parent centriole, whereas normally cells have two closely oriented centrosomes containing four centrioles (Duensing, Liu et al. 2007; Kleylein-Sohn, Westendorf et al. 2007). Unlike in *C. elegans*, other proteins are also involved in centrosome duplication in Drosophila and humans. One example is Cyclin dependent kinase 2/cyclin E (Cdk2/cycE), which

regulates DNA replication and centrosome duplication in S-phase. Depletion of Cdk2/cycE results in a block of centrosome reduplication (Hinchcliffe, Li et al. 1999; Lacey, Jackson et al. 1999). Manipulation of endogenous genes clearly affects centrosome duplication. Additionally, exogenous proteins, such as DNA tumor virus proteins, also affect centrosome duplication.

DNA tumor virus proteins affect on centrosome duplication

DNA tumor virus proteins can be used in scientific studies to disrupt functions of endogenous proteins, thereby permitting elucidation of cellular mechanisms. One process that is affected by viral oncoproteins is centrosome duplication. E7 from human papillomavirus (HPV), E1A from human adenovirus, Tax from human T cell leukemia virus type-1 (HTLV-1), and hepatitis B virus oncoprotein X (HBx) from hepatitis B all share in common the ability to induce centrosome amplification (Duensing, Lee et al. 2000; De Luca, Mangiacasale et al. 2003; Forgues, Difilippantonio et al. 2003; Yun, Cho et al. 2004; Ching, Chan et al. 2006; Wen, Golubkov et al. 2008). Interestingly, these DNA tumor virus proteins are oncogenic, suggesting that centrosome amplification may be a common mechanism used to transform cells.

HPV encodes two key viral oncoproteins, E6 and E7. In oncogenic HPV type 16 and 18, E7 binds to Rb, thereby blocking Rb inhibition of E2F (Wise-Draper and Wells 2008). E2F is then free to induce transcription of target genes and allow premature progression through the cell cycle. E6 binds and inhibits p53, another important cell cycle regulator (Wise-Draper and Wells 2008). Only oncogenic HPV E7 expression results in centrosome overduplication in mammalian cells, whereas E6 expression does not (Duensing, Lee et al. 2000). Furthermore, this effect is independent of Rb, but dependent

on Cdk2, and induces amplification similar to Plk4 overexpression (Duensing, Duensing et al. 2004; Duensing, Liu et al. 2007). These results suggest that E7 causes centrosome amplification by misregulating the pathway for centrosome duplication involving Plk4.

E1A of human adenovirus has been shown to misregulate a large variety of cellular processes to induce tumorigenesis. E1A binding partners include p300/Creb binding protein, an important transcriptional regulator, Rb/p107/p130, all related Rb proteins, and p21 and p27, Cdk inhibitors that regulate cell cycle progression (Frisch and Mymryk 2002). A novel binding partner of the E1A N-terminal region, specifically the first 36 amino acids, is the Ran GTPase. The Ran GTP-GDP cycle occurs through nucleotide exchange and hydrolysis on the Ran protein. Furthermore, full length E1A was found to induce centrosome amplification, dependent upon the first 36 amino acids, suggesting that E1A disruption of the Ran-GTP cycle misregulates the centrosome duplication cycle (De Luca, Mangiacasale et al. 2003).

HTLV-1 induces leukemogenesis through the oncoprotein Tax. Tax is necessary for HTLV-1-induced transformation, but is often lost as the tumors persist (Matsuoka and Jeang 2007). Tax promotes cell survival and proliferation through many cellular disruptions, including inhibition of the Akt and Nuclear factor κB pathways to prevent apoptosis, activation of Cdks and Cdk inhibitors to promote cell cycle progression, and inactivation of the spindle assembly checkpoint through Mad1 binding to cause aneuploidy (Matsuoka and Jeang 2007). Tax protein causes centrosome amplification *in vivo* in lymphocytes isolated from HTLV-1 patients (Nitta, Kanai et al. 2006). Additionally, T-cell lines overexpressing Tax protein have amplified centrosomes and a Cdk inhibitor reverses the phenotype. Another group discovered that Tax binds Tax1BP2,

a novel endogenous protein that when knocked down by RNAi results in centrosome amplification. Tax1BP2 localizes to the centrosome and a portion of Tax interacts with centrosomal Tax1BP2, suggesting that Tax is acting at the centrosome to increase centrosome numbers (Ching, Chan et al. 2006). These studies demonstrate how viral proteins disrupt centrosome duplication and also their potential in identifying novel endogenous proteins that regulate centrosome numbers.

Another example of disruption of endogenous proteins leading to centrosome amplification occurs with HBx protein expression. Hepatitis virus B is a major cause for hepatocellular carcinomas. HBx is encoded by the hepatitis B viral genome and is involved in viral mediated carcinogenesis. The main function of HBx is as a transcriptional activator for genes that induce signaling pathways that control cell cycle, proliferation, and apoptosis (Lupberger and Hildt 2007). HBx also causes genetic instability through centrosome amplification (Forgues, Difilippantonio et al. 2003; Yun, Cho et al. 2004; Wen, Golubkov et al. 2008). HBx increased centrosome numbers generated multinucleated cells and micronuclei through disruption of the Ras-Raf-mitogen-activated protein kinase pathway (Yun, Cho et al. 2004). Another study demonstrated that endogenous human HBx interacting protein (HBXIP) knockdown by RNAi results in centrosomal abnormalities. Furthermore, HBx mutants that cannot bind HBXIP, no longer localize to the centrosome and are ineffective at generating chromosomal aberrations, thus demonstrating that HBx interaction with HBXIP is essential for HBx-induced centrosome abnormalities (Wen, Golubkov et al. 2008). These examples illustrate that viral oncoproteins may use several pathways to disrupt

centrosome duplication or that these proteins may converge onto similar cell signaling pathways.

As discussed, several DNA tumor viral oncoproteins cause centrosome amplification, indicating that increased centrosome numbers may be a mechanism used to induce genetic instability and cellular transformation (Lavia, Mileo et al. 2003). These viral proteins give insight as to how centrosomes normally duplicate and enable the characterization of novel endogenous proteins that regulate the centrosome duplication cycle. These viral oncoproteins may converge onto a similar mechanism for disrupting centrosome duplication by inhibiting common proteins. One such protein is PP2A. E7, E1A, and Tax all bind and disrupt PP2A, similar to ST (Liao and Hung 2004; Pim, Massimi et al. 2005; Hong, Wang et al. 2007). Therefore, these proteins may share in common the ability to cause centrosome overduplication by affecting PP2A in addition to the mechanisms already discovered. Furthermore, recent studies have identified a role for PP2A activity at the centrosome.

PP2A and centrosomes

Many kinases have been identified for their involvement in centrosome duplication, most notably Plk4 and Cdk2, as mentioned above. However, little is known about phosphatase regulation of centrosome duplication. PP2A is an attractive candidate phosphatase for centrosome function due to its many substrates. Recent discoveries have implicated a role for PP2A at the centrosome.

In Drosophila, the $PP2A^{C}$ mutant was first identified for its role at the centrosome. The mutant has ~20% wild type zygotic activity and results in excess centrosomes in the late syncytial embryo and at cellularization, suggesting that the

centrosome cycle is no longer coupled to DNA replication. The excess centrosomes nucleate large asters, thereby giving the Drosophila $PP2A^C$ mutant the name *microtubule star* (Snaith, Armstrong et al. 1996). These phenotypes indicate that one role of PP2A is to control centrosome duplication and microtubule length in the Drosophila embryo. $PP2A^C$ and $PP2A^A$ RNAi in Drosophila S2 cells resulted in larger microtubule arrays associated with monopolar spindles or bipolar monoastral spindles, confirming the role of PP2A in regulating microtubule length (Chen, Archambault et al. 2007). The regulatory subunits in Drosophila consist of one B subunit and two B' subunits. The B subunit mutant is called *twins* and results in an increase in anaphase cells with lagging chromosomes and chromosomal bridges (Mayer-Jaekel, Ohkura et al. 1993). The B'-1 subunit mutant is termed *well-rounded* and was characterized in the neuronal system where synapses do not form properly and the cytoskeleton of the presynapse is irregular with a higher number of unbundled microtubules (Viquez, Li et al. 2006). Therefore, the B'-1 subunit may play a role in microtubule dynamics. The B'-2 subunit mutant is called *widerborst* and RNAi results in scattering of chromosomes along the mitotic spindle due to improper alignment along the metaphase plate (Chen, Archambault et al. 2007). Although, several of the PP2A subunits have a role in mitosis, only the $PP2A^A$ and $PP2A^C$ subunits have been directly implicated in centrosome regulation.

Recently, $PP2A^C$ was shown to localize to the centrosome in the early *C. elegans* embryo and in human cells. In *C. elegans* early embryogenesis, PP2A localizes the regulator of spindle assembly (RSA) complex to the centrosome. This complex is required for microtubule outgrowth from the centrosome (Schlaitz, Srayko et al. 2007).

Therefore, unlike Drosophila, when PP2A is depleted in the *C. elegans* embryo, microtubule outgrowth from the centrosome is diminished.

In human cells, $PP2A^C$ colocalizes at centrosomes with Aurora-A, an important mitotic regulator. $PP2A^C$ and Aurora-A interact and regulate each other's localization to the centrosome. Furthermore, phosphorylated Aurora-A interacts with PP2A, suggesting that PP2A dephosphorylates Aurora-A, thereby regulating Aurora-A stability (Horn, Thelu et al. 2007). PP2A may have a different role in centrosome duplication in human systems than in Drosophila. Moreover, human PP2A may be a more complex phosphatase than Drosophila PP2A due to the numerous members in each regulatory subunit family (Janssens and Goris 2001).

C. Dissertation Scope

Centrosome duplication is an important yet poorly understood process with severe implications when disrupted. Centrosome amplification, a phenotype commonly found in cancerous cells, can lead to multipolar spindles and aneuploidy. Initially, we aimed to characterize how centrosomes duplicate. To do so, we sought to create a Drosophila model for centrosome amplification. Due to tumor virus proteins causing centrosome amplification in mammalian cells, we hypothesized that the oncoproteins may cause a similar phenotype in Drosophila. Drosophila is an excellent model system and is experimentally advantageous due to its available genetic and biochemical tools. Therefore, we constructed Drosophila models for several viral oncoproteins: E6 from HPV, E7 from HPV, E1A from adenovirus, the SV40 early region, and ST from SV40.

We chose to characterize the SV40 early region because the mechanisms by which E7 and E1A cause centrosome amplification have been elucidated and E6 has been shown to not cause centrosome amplification. The SV40 early region, however, resulted in only detectable ST expression. Therefore, we constructed transgenic flies that expressed only ST or ST mutant proteins.

ST was found to cause centrosome amplification due to its PP2A-binding domain. Centrosome amplification is a novel phenotype associated with ST and is conserved in human cells. ST also caused larger and longer astral microtubules, cytoskeletal defects, chromosome segregation and alignment defects, and increased cyclin E levels in Drosophila syncytial embryos.

While trying to determine how ST causes centrosome amplification, we realized that our model revealed more information about ST protein function. We then verified our Drosophila model for ST by confirming PP2A-binding properties and conservation of centrosome amplification induced by ST expression in human cells, and utilized it to uncover new properties of ST. Biochemical assays revealed a novel binding partner for ST, the kinesin-1 motor. ST binds and inactivates kinesin-1. Through a genetic interaction, we show that ST and cycE interact in two ways. In an ST background, the heterozygous mutant cycE results in an enhancement of embryonic lethality and chromosome segregation and alignment defects. Overexpression of cycE in an ST background enhances many of the ST-associated phenotypes, most markedly the microtubule stability phenotypes. This indicates that ST has many properties that have not been uncovered utilizing mammalian systems, demonstrating the usefulness of the Drosophila model in further characterizing properties of viral oncoproteins.

A separate area of research focused on CG1674. CG1674, a novel Drosophila gene, causes centrosome amplification when knocked down by RNAi in Drosophila Kc cells. This phenotype is not conserved *in vivo* in the mutant we generated for CG1674. We made an ~75kb deletion of the fourth chromosome by P element excision and found that the missing region results in adult locomotion defects. Therefore, while CG1674 is possibly a regulator of centrosome duplication in Kc cells, it is dispensable for Drosophila development.

We have created the first Drosophila model for a tumor virus protein and studied the consequences of ST expression. We verified that the Drosophila model is an accurate representation of higher organisms by showing phenotypic conservation in mammals. The Drosophila model will be advantageous for further experiments in understanding ST pathogenesis. The use of Drosophila opens up a new avenue to characterize mechanisms of viral proteins' disruption of animal development, methods of causing disease, and interruption of normal cellular processes.

CHAPTER TWO

PP2A-DEPENDENT DISRUPTION OF CENTROSOME REPLICATION AND CYTOSKELETON ORGANIZATION IN DROSOPHILA BY SIMIAN VIRUS 40 SMALL TUMOR ANTIGEN

A. Introduction

Viruses of the DNA tumor virus family induce cell proliferation to promote the replication of the viral genome. Extensively investigated members of this family include HPV, adenovirus, polyomavirus, and SV40. By hijacking cell cycle and apoptosis regulation, viral oncoproteins transform cells. Investigation of DNA tumor virus oncoproteins has led to the identification of many fundamental mechanisms of tumor suppression (Lavia, Mileo et al. 2003; Ahuja, Saenz-Robles et al. 2005). By altering the activity of p53, Rb, and PP2A, three key tumor suppressors, SV40 can cause tumor formation in transgenic mouse models (Ahuja, Saenz-Robles et al. 2005; Arroyo and Hahn 2005).

A single transcript expressed from the early region of the SV40 genome encodes three proteins by alternative splicing: LT, ST, and 17kT (Sullivan and Pipas 2002). ST cooperates with LT to transform cells *in vitro* and *in vivo* (Skoczylas, Fahrbach et al. 2004). ST has two domains and two known binding partners: a domain with homology to dnaJ proteins, or J domain that binds Hsc70, and a PP2A binding domain. The oncogenic activity of ST requires PP2A binding, but not the J domain (Mungre, Enderle et al. 1994;

Saenz-Robles, Sullivan et al. 2001; Skoczylas, Fahrbach et al. 2004). Due to this property, ST has been used as a tool to assess PP2A's role in transformation (Chen, Possemato et al. 2004; Skoczylas, Fahrbach et al. 2004). By inhibiting PP2A, ST disrupts dephosphorylation of targets for transformation, including c-myc and RalA (Mumby 2007). The PP2A holoenzyme consists of three subunits, a scaffolding subunit (A), a regulatory subunit (B), and a catalytic subunit (C). In addition, there are four classes of regulatory subunits: B, B', B'', and B''', which confer substrate specificity (Janssens and Goris 2001; Sontag 2001). ST binds directly to $PP2A^{A}$, displacing B subunits from the holoenzyme but retaining the C subunit (Yang, Lickteig et al. 1991; Chen, Xu et al. 2007). The structure of $PP2A^{A}$ bound to ST was solved recently, revealing a direct association between several HEAT repeats of the A subunit with the second of two zinc-binding domains in ST, an association that is structurally similar to the B' subunit bound to the A subunit (Xu, Xing et al. 2006; Chen, Xu et al. 2007; Cho, Morrone et al. 2007; Cho and Xu 2007). Thus, ST might function as a PP2A B subunit (Cho, Morrone et al. 2007). Therefore, in addition to inhibiting activity toward normal substrates through competition with B subunits, ST may confer new substrate specificities to PP2A.

While DNA tumor virus oncoproteins disrupt pathways controlling the cell cycle and apoptosis, they also compromise mechanisms that prevent aberrant cell divisions, potentially leading to aneuploidy (Lavia, Mileo et al. 2003). For example, HPV E7 and adenovirus E1A induce centrosome overduplication, impacting genomic stability through an increase in the incidence of multipolar mitotic spindles (De Luca, Mangiacasale et al. 2003; Duensing and Munger 2003; Duensing, Duensing et al. 2004). While the transforming properties of ST have been extensively investigated, there is little

understanding of the impact that disruption of normal signaling caused by ST and other viral oncoproteins have on animal development. To address this question, we have constructed a *Drosophila melanogaster* model for SV40 ST pathogenesis; the first Drosophila model for expression of a viral oncoprotein. We show that ST causes increased centrosome numbers, chromosome segregation defects, aberrant cytoskeleton assembly, cytokinesis failures, and a rise in cyclin E levels. Using ST mutations and Drosophila mutant analysis, we show that the disruption of embryogenesis caused by ST requires PP2A subunits, confirming the ST-PP2A connection from vertebrate studies.

B. Results

Expression of the SV40 early coding region in the early embryo

The 2.7kb SV40 early region encodes the LT, ST, and 17kT proteins through alternative splicing (Figure 2-1a) (Sullivan and Pipas 2002). To express the early region of SV40 in early Drosophila embryos, we constructed transgenic flies that express this transcript under the control of the UAS-Gal4 system, a tool to control the spatial and temporal expression of ectopic proteins (Brand and Perrimon 1993). Expression in this system can be modulated by temperature within the range permissive for Drosophila growth, 16-29°C, with highest levels achieved at 29°C. In order to express early region proteins in the embryo maternally, the SV40 early region transcript was expressed during oogenesis using a *nanos*-Gal4 driver (Van Doren, Williamson et al. 1998). To detect early viral proteins by western blotting, we generated a polyclonal antibody in rabbits that recognizes ST, LT, and 17kT (Figure 2-1b and c, and unpublished data (S. Comerford

and R. Hammer)). Surprisingly, ST but not LT or 17kT expression from the SV40 early region was detected in embryos with this antibody (Figure 2-1c) or with two commercial antibodies (pAB108 and pAB419, not shown). A similar construct, expressed in mouse liver, produced ST and LT (Figure 2-1c) (Comerford, Clouthier et al. 2003). These results indicate that ST-encoding transcripts are the predominant mRNA species made in Drosophila embryos. This splicing bias was not simply due to genome position effect; since 3 independent lines showed exclusive expression of ST. ST expression in early embryos caused supernumerary centrosomes and lethality (Figures 2-1d and 2-2). In this report we focus on the effect of ST expression in early Drosophila development and the roles of PP2A subunits for its action.

ST induces centrosome overduplication, and cytoskeletal and cleavage defects that lead to embryonic lethality

To test whether ST causes the increased centrosome numbers and other phenotypes (see below) observed with the early region construct, and to eliminate a potential contribution from undetectable expression of LT and 17kT, transgenic flies that express an ST cDNA fused to a 3xFLAG tag at the C-terminus were generated (ST-FLAG). As a control, transgenic flies containing the FLAG tag vector were generated (vector). Comparison among several ST-FLAG transgenic lines showed that independent lines varied in expression levels, with embryonic lethality directly correlating with the level of ST-FLAG expressed (Figure 2-2a,b).

We next examined embryos that express ST-FLAG (hereafter referred to as ST embryos) for centrosome duplication, cytoskeleton, chromosome organization and cleavage defects by immunostaining embryos with antibodies to Centrosomin (CNN) and

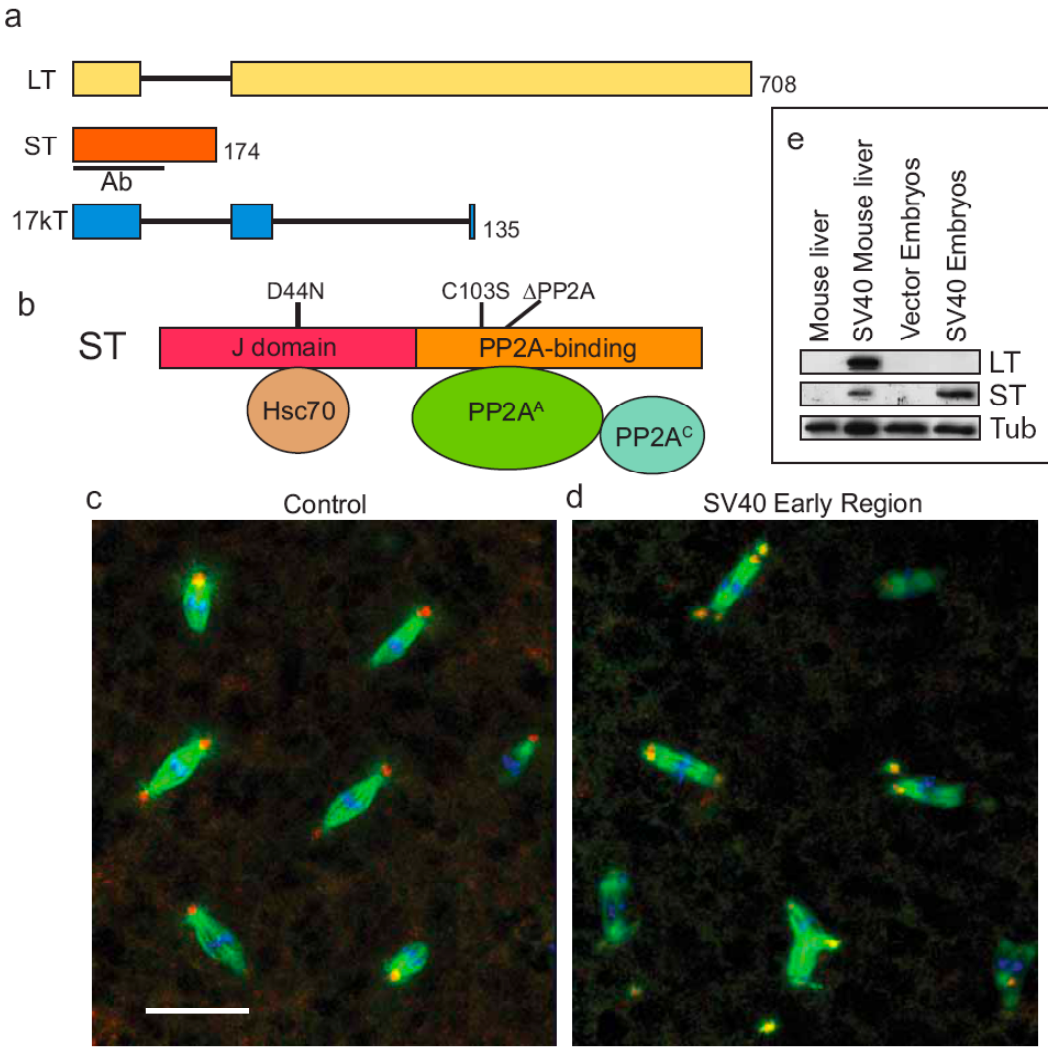

Figure 2-1. Centrosome abnormalities in Drosophila embryos expressing SV40 ST. (a) Schematic diagram of the SV40 early region gene products LT, ST, and 17kT, produced by alternative splicing. Black lines indicate introns. Size of each protein (in amino acids) and region used to raise antibodies (Ab) are indicated. (b) ST has two domains: a J domain and a PP2A-binding domain. The mutations used in this study are indicated. (c) SV40 early region-expressing embryos produce ST protein, but no detectable LT. Lysate

from mouse liver expressing SV40 early region (Comerford, Clouthier et al. 2003) is included as a positive control. (d) SV40 ST-expressing embryos exhibit supernumerary centrosomes and mitotic spindle abnormalities. Early cleavage stage embryos were stained for centrosomin (CNN) (red), a-tubulin (green), and DNA (blue). Note some of the spindle poles are located outside of the image stack shown. Scale bar: 25μm.

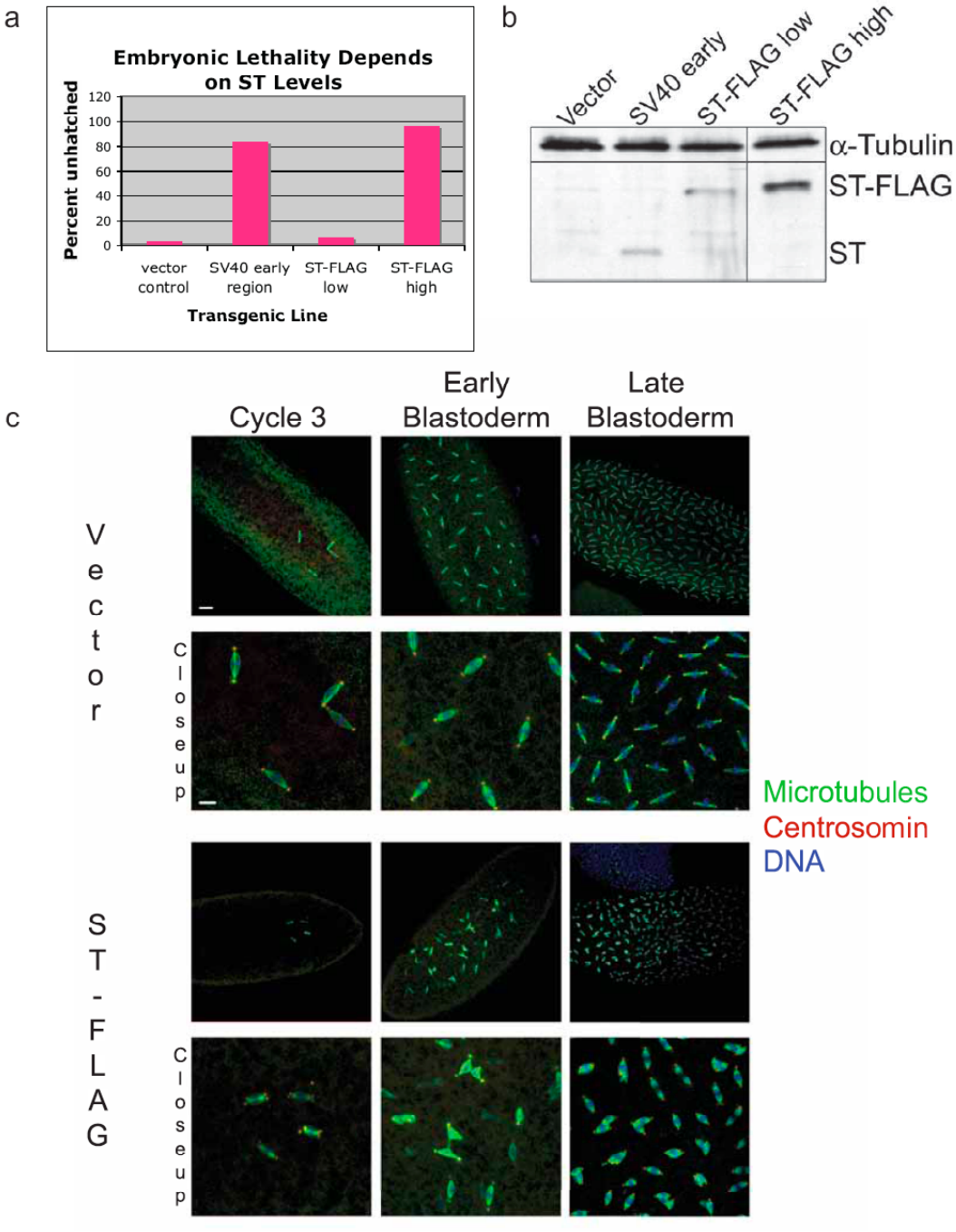

Figure 2-2. Embryonic lethality is correlated to ST-FLAG expression levels. Independent UASp-ST-FLAG transgenic lines showed variable lethality (a) that correlated directly

with the levels of expression of ST-FLAG from each line (b). Embryonic lethality, measured as percent of embryos that fail to hatch, is similar between a line that expresses "native" ST from the SV40 early region construct, and a line that expresses higher levels of ST-FLAG. This indicates that the C-terminal 3xFLAG tag reduced the activity of ST, yet we achieved high enough expression to overcome this. Importantly, ST-FLAG expression results in the same phenotypes as the SV40 early region: centrosome amplification, aneuploidy, large microtubule asters, actin/cleavage furrow defects, and lethality (Figures 2-3a-d). The blot in (b) was probed with anti-ST antibody and anti-a-tubulin as a loading control. All the lanes in (b) are from the same blot and same film exposure.

Whole embryo images of control and ST-FLAG embryos are shown in (c). Images of whole embryos at cycle 3, early syncytial blastoderm, and late syncytial blastoderm are shown with a higher magnification image shown below. Embryos were stained for CNN (red), a-tubulin (green), and DNA (blue). Scale bars: 25 μm top rows, 10 μm bottom rows.

α-tubulin to label centrosomes and microtubules, respectively, and with dyes for DNA and filamentous actin (Figure 2-3a-d). Normally, centrosomes duplicate with high fidelity once each cleavage cycle, ensuring a single centrosome at each spindle pole at mitosis (Figure 2-3a). ST not only caused centrosome overduplication by the first mitotic cycle (Figure 2-3b), but also caused other spindle assembly defects (eg. Figure 2-1d) including a failure to organize or maintain chromosomes within the spindle (Figure 2-3b, arrow). Often, the extra centrosomes in ST embryos were free, and not associated with a mitotic spindle (for example, Figure 2-1d). Thus, ST disrupts centrosome duplication and chromosome segregation from the earliest embryonic cleavage cycles.

Since induction of supernumerary centrosomes is a novel phenotype associated with ST, we asked whether ST elicited the same activity in mammalian cells. To test for centrosome duplication effects of ST in human cells, we transiently transfected U2OS cells with a plasmid that expresses native ST protein. Figures 2-3e-g show that ST-expressing U2OS cells also have increased centrosome numbers, with 23.2 +/- 3.9% (mean +/- SD) having >2 centrosomes, compared to 9.8 +/- 2.9% of control cells.
To examine the effects of ST on centrosome duplication within the time frame of a single cell cycle, we established a stable Drosophila cell line that expresses ST-FLAG under inducible control from the metallothionein promoter (Figure 2-3h). The doubling time of Kc cells is approximately 24 hrs at 25˚C, yet after only 20 hours of induction, ST-FLAG caused a significant increase in centrosome number within a single cell cycle from 21.2 +/- 1.6% (mean +/- SD) (uninduced) to 44.8 +/- 3.8% of cells that contain ≥4 centrosomes (Figure 2-3i and j). The excess centrosomes coalesced at the spindle poles in mitotic cells, resulting in bipolar spindles (Figure 2-3i). For this analysis, we restricted

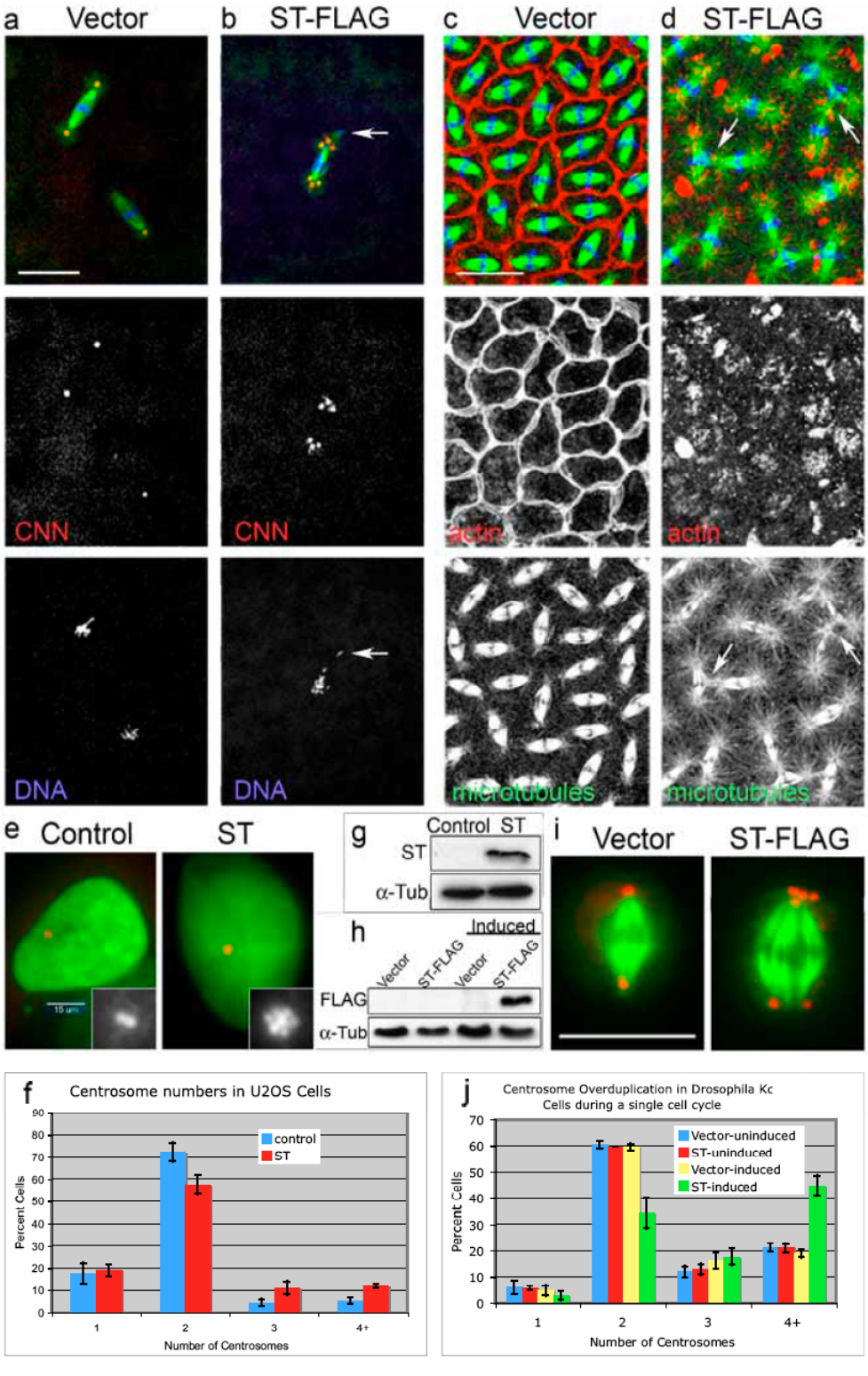
a Vector
b ST-FLAG
c Vector
d ST-FLAG
CNN
CNN
actin
actin
DNA
DNA
microtubules
microtubules
e Control
ST
g
Control ST
ST
α-Tub
h
Induced
Vector
ST-FLAG
Vector
ST-FLAG
FLAG
α-Tub
i Vector
ST-FLAG
f Centrosome numbers in U2OS Cells
control
ST
Percent Cells
Number of Centrosomes
j Centrosome Overduplication in Drosophila Kc Cells during a single cell cycle
Vector-uninduced
ST-uninduced
Vector-induced
ST-induced
Percent Cells
Number of Centrosomes

Figure 2-3. ST induces centrosome overduplication and cytoskeleton disruption. (a,b) Expression of FLAG-tagged ST causes centrosome overduplication and chromosome segregation errors from the earliest embryonic divisions. Spindles in ST-FLAG embryos have extra centrosomes at spindle poles and scattered arrangement of chromosomes, some displaced completely from the spindle (arrow in (b)). Embryos were stained for a-tubulin (green), CNN (red), and DNA (blue). At cortical cleavage stages (c,d) actin is not assembled properly into furrows, astral microtubules are larger and interact with neighboring spindles in ST embryos (arrows in (d)). (c,d) Embryos were stained for a-tubulin (green), filamentous actin (red), and DNA (blue). (e) In human U2OS cells, ST expression increases centrosome numbers. Cells transfected with pGFP-Histone (a marker for transfected cells) with or without the ST expression plasmid pCMV5/Smt (Sontag, Fedorov et al. 1993) were stained for g-tubulin (red) and GFP (green). Inset shows the centrosomes; note the flower-like arrangement of the multiple centrosomes in ST-expressing cells. (f) Quantitation of supernumerary centrosomes in human U2OS cells. 23.2 +/- 3.9% (mean +/- SD) of ST-expressing cells had greater than 2 centrosomes, versus 9.8 +/- 2.9% in control cells. n=200 cells per sample for 3 independent experiments. (g) Western blot for ST expression in U2OS cells. (h) Western blot for ST-FLAG expression in Drosophila Kc cells. Lanes labeled “Induced” were exposed to 1.0 mM $CuSO_4$ for 20 hrs. Detection of a-tubulin in each blot was used as a loading control. (i) Supernumerary centrosomes in Kc cells following induction of ST-FLAG. Cells were stained for a-tubulin (green) and CNN (red). (j) Quantitation of centrosome overduplication in Kc cells. Mitotic cells were counted following a 20 hr induction period. Four or more centrosomes were found in 44.8 +/- 3.8% (mean +/- SD)

of ST induced cells versus 21.2 +/- 1.6% for uninduced ST cells. n=200 cells per sample for three independent experiments. Bars: 25µm in a,b, 15µm in c,d,e, 10µm in i.

centrosome counts to mitotic cells, making it unlikely that tallied cells experienced cytokinesis during the 20-hour induction period. Flow cytometry was used to examine cell cycle effects of ST expression in Kc cells, yet no significant differences in cell cycle parameters or in the polyploid cell population were seen at 20 and 42 hours of induction of ST compared to the controls (Figure 2-4). Therefore, centrosome overduplication did not arise as an indirect perturbation of the cell cycle by ST. Moreover, double-staining of Kc cells for Cid, a kinetochore marker, and CNN showed that there was no increase in chromosome number coinciding with increased centrosome numbers (Figure 2-5). Thus, supernumerary centrosomes induced by ST are achieved by overduplication rather than through a failure of cytokinesis in Kc cells.

To examine microtubule and actin assembly, we stained ST embryos for microtubules and actin. Although centrosomes function primarily as MTOCs, they also play a critical role in organizing actin at the cortex and the assembly of cleavage furrows in syncytial Drosophila embryos during cleavage cycles 10-14 (Raff and Glover 1989; Rothwell and Sullivan 2000). We find that during cortical cleavage divisions the MTOC activity of centrosomes is enhanced in ST embryos, resulting in larger astral microtubule arrays containing longer microtubules (Figure 2-3d). Moreover, the organization of actin into cleavage furrows is severely aberrant in ST embryos, frequently failing to assemble into furrows, but rather organizing into clumps nearby the centrosomes (Figure 2-3d). Neighboring spindles, normally separated by cleavage furrows, come into direct contact with each other in ST embryos, with astral microtubules from one spindle integrating with the spindle microtubules of their neighbors (arrows in Figure 2-3d), a probable consequence of cleavage furrow failure (Rothwell and Sullivan 2000). Thus, in

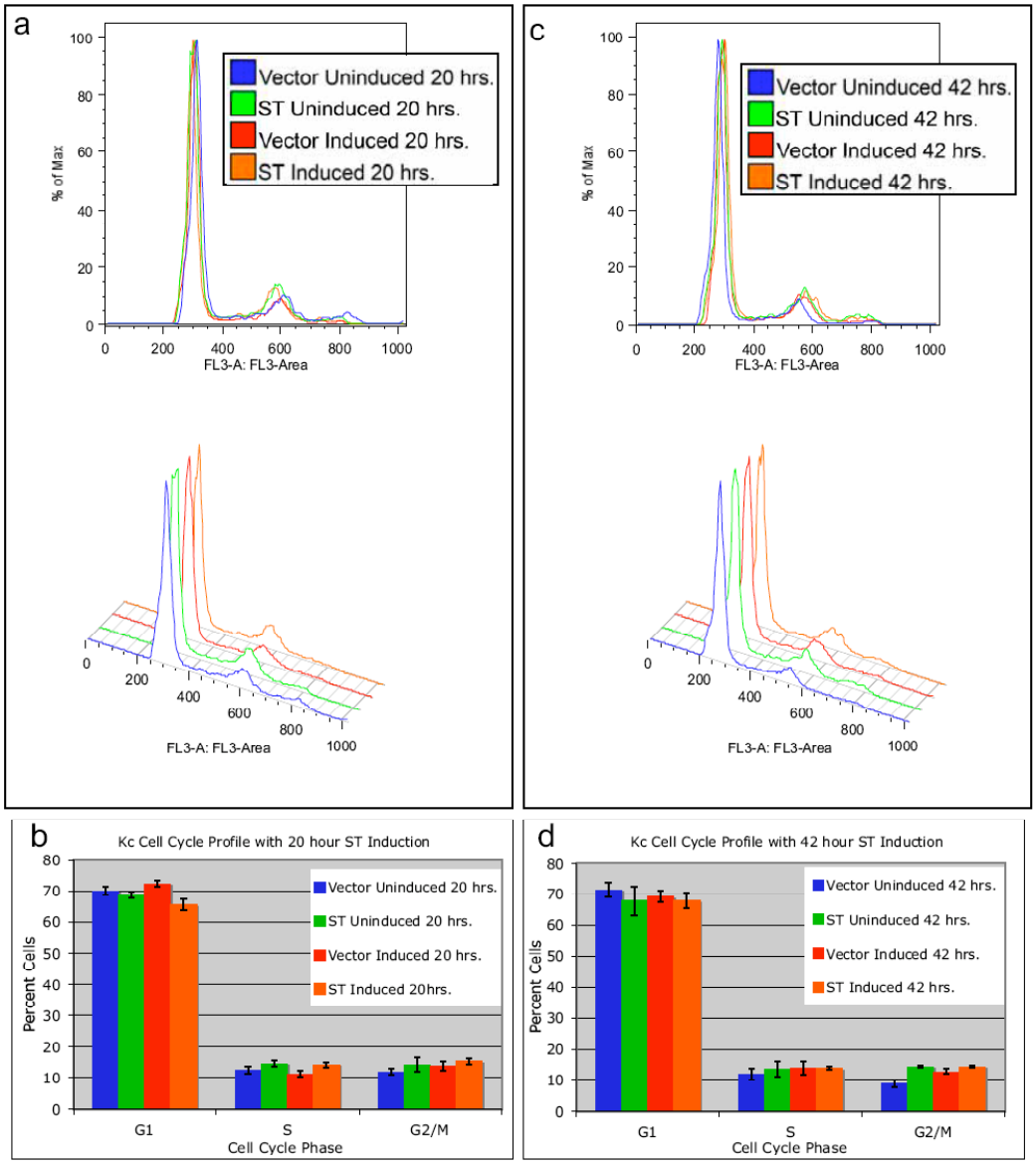

Figure 2-4. Cell cycle profiles of Kc cells following ST induction. Induction of vector or ST in stably-transfected Kc cell lines (as shown in Figure 2) showed no significant differences in the cell cycle stages at (a, b) 20 hours or (c, d) 42 hours. An example of a cell cycle profile for each sample is represented in (a, c) and the mean +/- SD of three profile measurements is represented in (b, d).

a

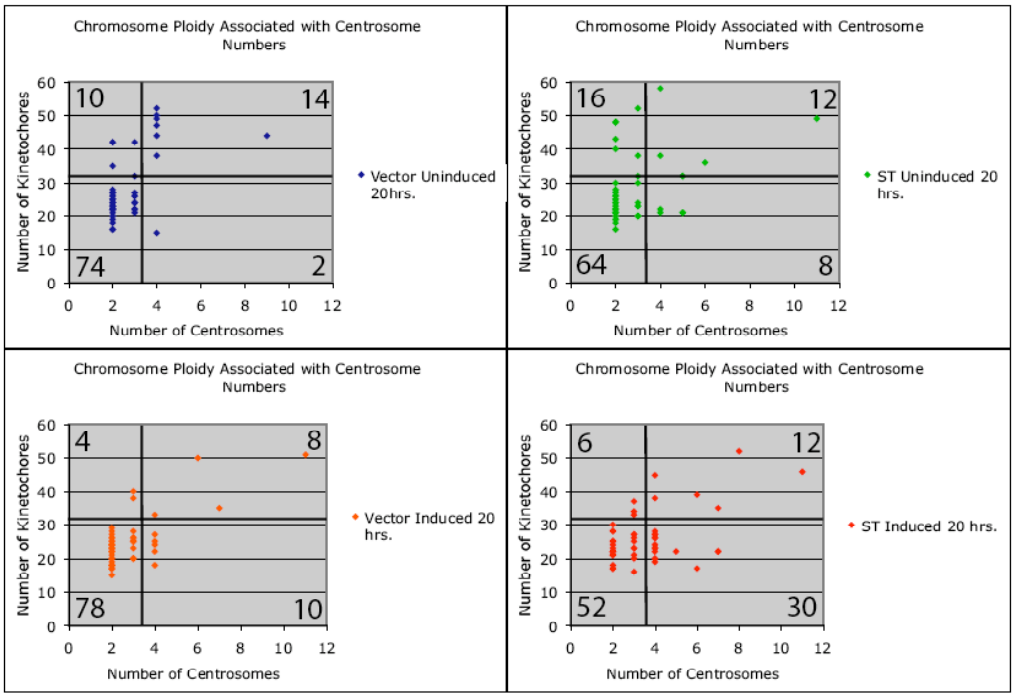

b

Sample:	Vector Uninduced 20 hrs.	ST Uninduced 20 hrs.	Vector Induced 20 hrs.	ST Induced 20 hrs.
Mean Number of Kinetochores	27.8	28.48	24.78	26.02

c

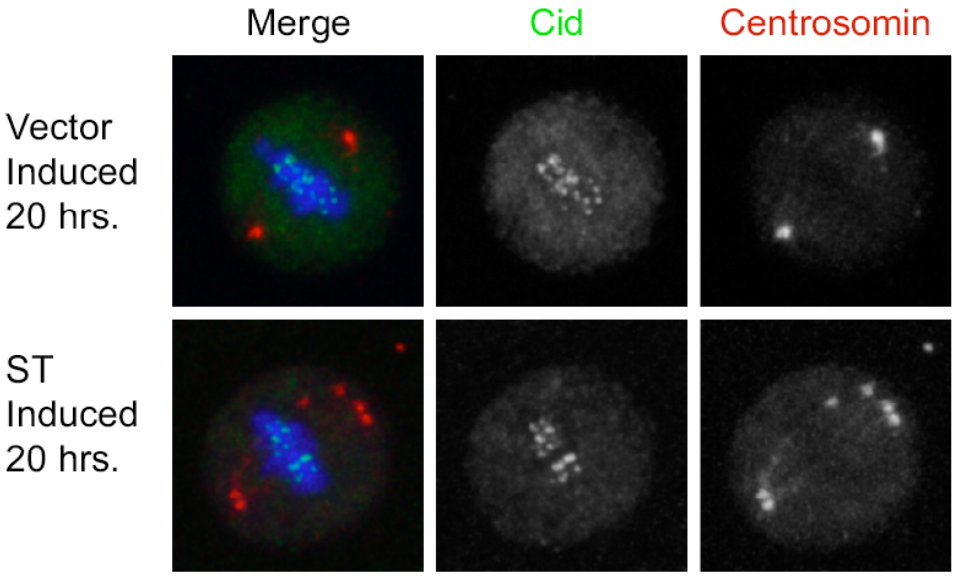

Figure 2-5. ST expression in Kc cells increases centrosome numbers without increasing chromosome numbers. Control and ST-expressing Kc cells, plus and minus induction with 1.0 mM $CuSO_4$ for 20 hrs, were stained with antibodies against CNN and Cid to label centrosomes and kinetochores, respectively. The results show that while centrosome numbers increase upon ST expression, the chromosome numbers do not increase. The scatter plot graphs in (a) show the centrosome and kinetochore counts for n = 50 cells. The horizontal bar in these graphs shows the number of kinetochores above and below 32 (the number expected for tetraploid Kc cells). The vertical line delineates 4+ centrosomes from <4 centrosomes. The numbers in each quadrant are the percent cells in each category. Note that approximately 30% of ST induced cells that are not polyploid have supernumerary centrosomes compared to 2-10% in the controls. The table in (b) shows the mean number of kinetochores for each sample shown in (a). Representative images of induced control and ST-expressing Kc cells stained for kinetochores and centrosomes are shown in (c). DNA is stained blue in the merged image.

late syncytial embryonic cleavage cycles, ST enhances microtubule stability and disrupts assembly of actin into cleavage furrows.

The disruption of actin assembly into cleavage furrows is predicted to have a severe impact on proper progression of cleavage cycles. To examine cleavage dynamics live, we imaged ST embryos using enhaced green fluorescent protein (eGFP)-tagged CNN and monomeric red fluorescent protein (mRFP)-tagged Histone to label centrosomes and chromosomes, respectively (Schuh, Lehner et al. 2007; Zhang and Megraw 2007). The fluorescent signals were too weak to image early cleavage deep within the embryo; however cortical cycles 10-13 were recorded by time-lapse confocal imaging. Control centrosomes split late in telophase and the nuclei divided synchronously as normal for cortical embryonic divisions (Figure 2-6a) (Callaini and Riparbelli 1990; Rothwell and Sullivan 2000). In ST embryos, cleavage cycles retained synchrony and progressed on a similar time scale as control embryos, demonstrating no delay in cycle completion. However, some nuclei failed to complete cleavage, causing daughter chromosomes to collapse back together after anaphase and producing polyploid nuclei associated with a double complement of 4 centrosomes that fail to enter the next cleavage cycle (Figure 2-6b). From this live imaging analysis we conclude that ST causes cytokinesis failure in embryonic cortical divisions.

ST activities in the embryo depend upon PP2A binding

To determine the relative contributions of PP2A and Hsc70 binding to the ST-associated embryonic phenotypes, we introduced independent mutations in the J domain and PP2A-binding domain (Figure 2-1b). To disrupt the J domain, we generated a mutation that changes the aspartic acid at amino acid 44 in the conserved HPD loop to

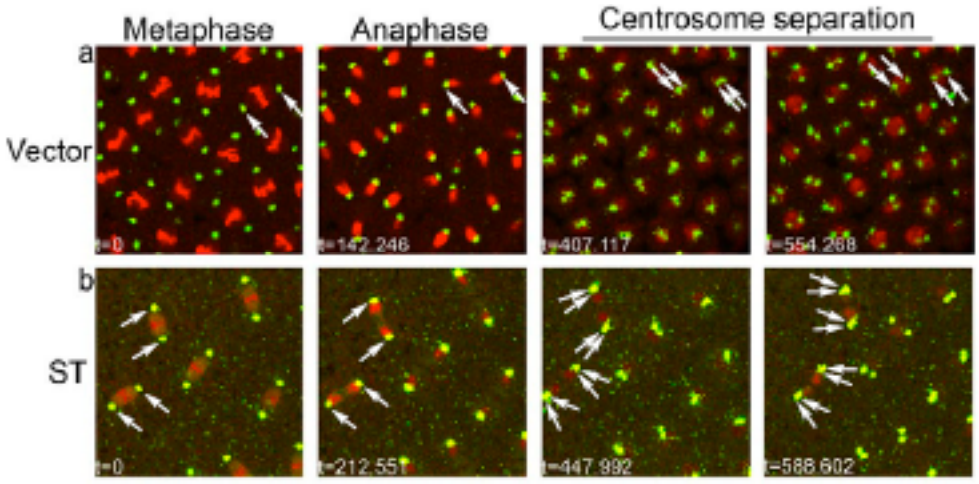

Figure 2-6. Live imaging of ST embryos shows cytokinesis failures. Syncytial blastoderm embryos that express eGFP-CNN to label centrosomes (green) and His2Av-mRFP to label chromosomes (red) were imaged by time-lapse confocal microscopy in (a) vector control embryos, and (b) ST embryos. In the vector time series (a), a pair of centrosomes is followed (arrows) through mitosis and centrosome splitting until cleavage is completed. In the ST series (b), two pairs of centrosomes (arrows) are followed through a cleavage cycle in which the nuclei collapse back onto each other and fuse during centrosome separation.

asparagine (ST^{D44N}). This mutation, when introduced into LT, disrupts the interaction of LT with Hsc70 (Sullivan, Cantalupo et al. 2000; Sullivan and Pipas 2002). To disrupt ST's ability to bind PP2A, we introduced two independent mutations into the PP2A-binding domain: a cysteine to serine amino acid substitution at position 103 (ST^{C103S}) and a nonsense mutation at position 111 ($ST^{\Delta PP2A}$). These mutations have been shown to block ST-PP2A association and PP2A inhibition completely ($ST^{\Delta PP2A}$) (Mateer, Fedorov et al. 1998) or by approximately 50% (ST^{C103S}) (Mungre, Enderle et al. 1994). Transgenic lines that express ST-FLAG and these mutants at similar levels (Figure 2-7a) were selected for phenotype analysis.

Since ST interacts directly with $PP2A^{AC}$ (Yang, Lickteig et al. 1991), association of ST and ST mutant proteins with PP2A was assayed in embryo extracts by immunoprecipitation (IP). The PP2A catalytic subunit ($PP2A^{C}$) co-IP'ed with ST and ST^{D44N} efficiently from embryo lysates (Figure 2-7a). In reciprocal binding assays, IP of $PP2A^{C}$ also precipitated ST (Figure 2-7b). However, IP of the two ST mutants predicted to disrupt interaction with PP2A showed either reduced (ST^{C103S}), or no binding to PP2A ($ST^{\Delta PP2A}$) (Figure 2-7a). These data show that the capacity of ST to bind PP2A is a property of mammalian cells that is conserved in Drosophila.

We next examined the effects of expression of ST mutants in embryos to compare their relative contribution to the spectrum of phenotypes associated with "wild type" ST expression. The first phenotype we quantified, lethality, was dependent on PP2A binding, but not on the J domain: expression of ST and ST^{D44N} in early embryos was deleterious, with ~70% of embryos failing to hatch. Expression of ST^{C103S} and $ST^{\Delta PP2A}$, on the other hand, had little affect on embryonic survival when compared to

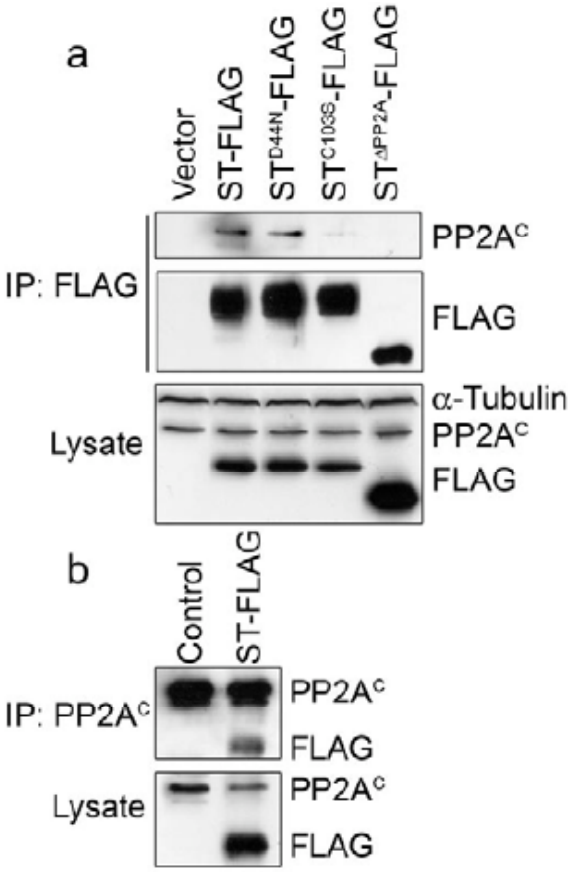

Figure 2-7. ST interacts with PP2A in Drosophila embryos. (a) $PP2A^C$ co-immunoprecipitates (co-IPs) with ST-FLAG, but poorly with ST PP2A-binding mutants ST^{C103S} and $ST^{\Delta PP2A}$. Western blotting of lysates shows that ST-FLAG and mutant derivatives are expressed at similar levels, except for $ST^{\Delta PP2A}$-FLAG, which is approximately 1.8 fold higher than the others. a-tubulin was used as a loading control. $PP2A^C$ co-IPs with ST-FLAG and ST^{D44N}-FLAG. A reduced amount of $PP2A^C$ co-IPs with ST^{C103S}-FLAG, and none is detected with $ST^{\Delta PP2A}$-FLAG. (b) ST-FLAG co-IPs with $PP2A^C$ from embryo lysates.

vector control embryos (Figure 2-8a). These results indicate that binding/inhibition of PP2A, but not association with Hsc70, is required for ST-induced lethality in early embryos.

To examine developmental delay or arrest as a possible cause for lethality, we compared embryonic stages among ST and ST mutants from a 3-hour embryo collection and found that most ST and ST^{D44N} embryos failed to progress beyond the early syncytial and blastoderm cleavage cycles of embryogenesis, whereas significantly greater numbers of the vector control, ST^{C103S}, and $ST^{\Delta PP2A}$ embryos progressed beyond the syncytial blastoderm to cellularization and gastrulation stages (Figure 2-8b). These data indicate that ST blocks or delays embryonic development during the early cleavage cycles, a stage in development that is dependent on rapid division and dynamic cytoskeletal rearrangements (Rothwell and Sullivan 2000).

Next, we compared ST embryos to those that express ST mutants to determine which phenotypes: increased centrosome numbers, microtubule aster size, and actin organization, are affected by ST mutations. We find that ST and ST^{D44N} cause supernumerary centrosomes in 55-60% of early embryos (Figure 2-8c). At mitosis, vector control embryos had normal bipolar spindles with one centrosome at each pole (Figure 2-8d), whereas ST and ST^{D44N} embryos assembled spindles with multiple centrosomes at spindle poles (Figure 2-8e and f). Supernumerary centrosomes occur rarely in ST^{C103S} and $ST^{\Delta PP2A}$ embryos (Figure 2-8c,g and h). Additionally, large astral microtubule arrays and disorganized cleavage furrows formed in ST and ST^{D44N} embryos compared to control embryos (Figure 2-8i-l). However, these effects were reduced or absent when the PP2A binding mutants ST^{C103S} and $ST^{\Delta PP2A}$ were expressed (Figure 2-8i,m and n). These results

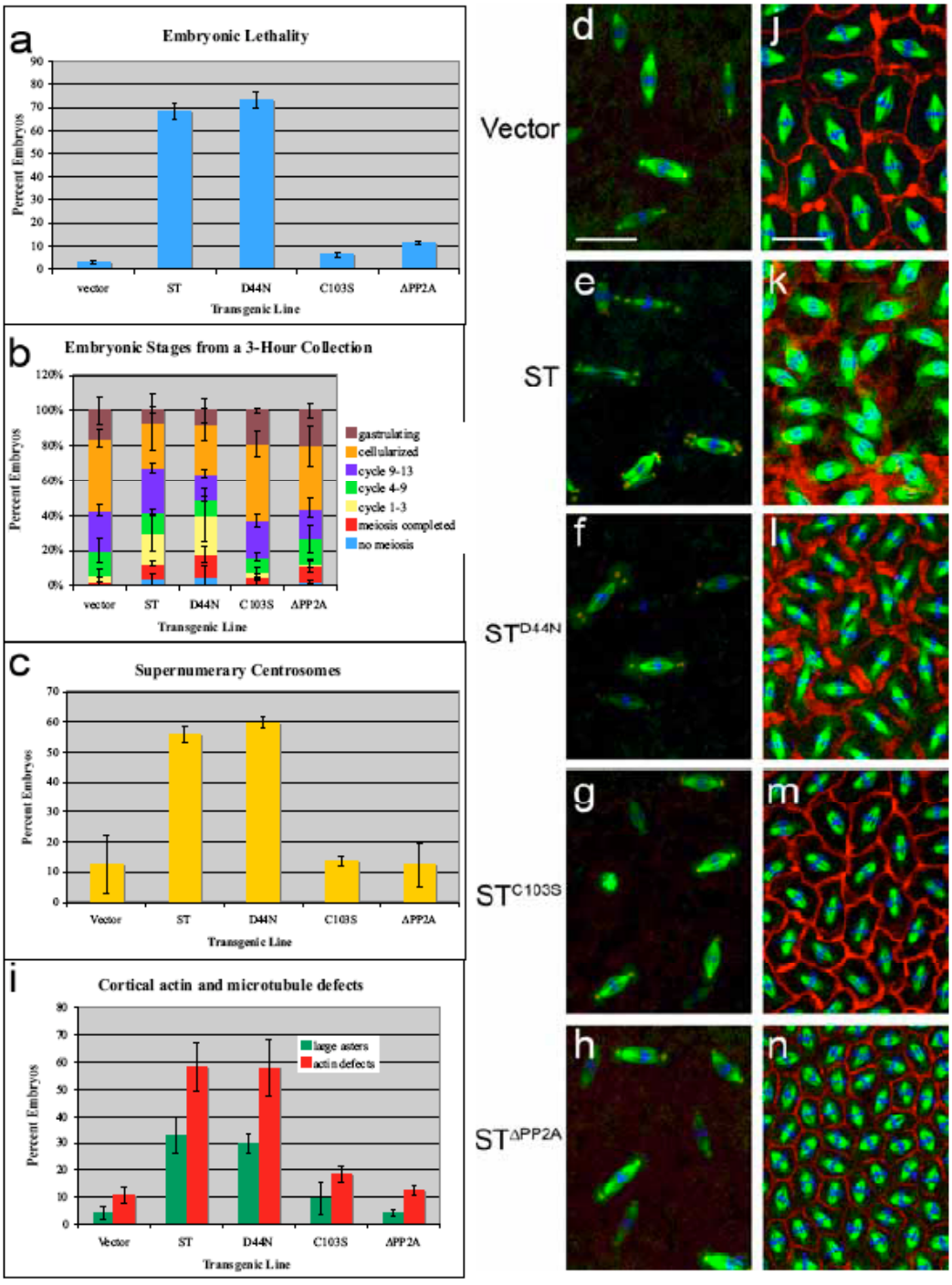
a
Embryonic Lethality
Percent Embryos
vector
ST
D44N
C103S
ΔPP2A
Transgenic Line
b
Embryonic Stages from a 3-Hour Collection
Percent Embryos
gastrulating
cellularized
cycle 9-13
cycle 4-9
cycle 1-3
meiosis completed
no meiosis
vector
ST
D44N
C103S
ΔPP2A
Transgenic Line
c
Supernumerary Centrosomes
Percent Embryos
Vector
ST
D44N
C103S
ΔPP2A
Transgenic Line
i
Cortical actin and microtubule defects
Percent Embryos
large asters
actin defects
Vector
ST
D44N
C103S
ΔPP2A
Transgenic Line
Vector
ST
ST^D44N
ST^C103S
ST^ΔPP2A
d
j
e
k
f
l
g
m
h
n

Figure 2-8. ST phenotypes are dependent on the PP2A-binding domain. (a) Approximately 70% of ST-FLAG (ST) and ST^{D44N}-FLAG (ST^{D44N}) embryos fail to hatch (y-axis is the percent of embryos that fail to hatch) at 29˚C. (b) The relative phases of embryogenesis among 3-hour collections of embryos from the indicated cross. Fewer ST and ST^{D44N} embryos progress to later embryonic stages compared to control and PP2A-binding mutant ST embryos. (c) Supernumerary centrosomes occur in 55-60% of ST and ST^{D44N} embryos, whereas ST^{C103S} and $ST^{\Delta PP2A}$ embryos are similar to control. (d-h) Multiple centrosomes are associated with spindle poles in ST and ST^{D44N} embryos. Control (d), ST (e) and ST mutant (f-h) embryos were stained for a-tubulin (green), CNN (red) and DNA (blue). (i) Larger astral microtubules and disruption of actin assembly into cleavage furrows occurs during cortical cycles with ST and ST^{D44N} embryos, but less so in ST^{C103S} and $ST^{\Delta PP2A}$ embryos. (j-n) Assembly of actin into cleavage furrows is disrupted by ST in a PP2A-dependent manner. Embryos were stained from control (j), ST (k) and ST mutants (l-n) for a-tubulin (green), actin (red) and DNA (blue). In ST and ST^{D44N} embryos, spindles collide with each other due to defective furrow assembly (k,l). The embryo in n is at a later cycle than those in j-m, which is why the spindles are smaller. Bars: 25µm in d-h, 15µm in j-n.

demonstrate that the centrosomal and cytoskeletal defects caused by ST are due to PP2A binding.

Genetic enhancement of ST by heterozygous PP2A subunit mutants

While our results show that PP2A-binding is required for ST embryonic phenotypes, we turned to genetic analysis to examine potential modifying effects that mutations in PP2A subunit genes may have on ST embryos. Drosophila have single genes encoding $PP2A^{C}$, $PP2A^{A}$, and $PP2A^{B}$ subunits, and two genes that encode $PP2A^{B'}$ subunits. $PP2A^{C}$ is encoded by the *microtubule star* (*mts*) gene, $PP2A^{A}$ by *PP2A-29B*, $PP2A^{B}$ by *twins* (*tws*), $PP2A^{B'-1}$ by *well-rounded* (*wrd*), and $PP2A^{B'-2}$ by *widerborst* (*wdb*). Mutations in all of these PP2A subunit genes were available or, in the case of *wdb*, generated here.

To generate a mutation in *wdb* in which $PP2A^{B'-2}$ expression is eliminated, we mobilized a P element transposon located at the 5' end of the *wdb* gene which resulted in a 1.9 kb deletion that removes both promoters (wdb^{12-1}, see Figure 2-9). Disruption of $PP2A^{B'-1}$ and $PP2A^{B'-2}$ expression in these mutants was confirmed using antibodies we generated specific to each B' subunit (Figure 2-9). The $wrd^{KG01108}$ mutant was viable, producing fertile adults. On the other hand, the wdb^{12-1} mutation was lethal, arresting development at late pupal stages. Both of these observations are consistent with published reports of *wdb* and *wrd* mutants (Hannus, Feiguin et al. 2002; Viquez, Li et al. 2006). We also generated a *wrd wdb* double mutant to test for genetic redundancy between these two $PP2A^{B'}$-encoding genes. The $wrd^{KG01108}$ wdb^{12-1} double mutant arrests development at an earlier stage than the single wdb^{12-1} mutant, dying as third instar larvae. This novel finding indicates that the two $PP2A^{B'}$ subunits are at least partially redundant

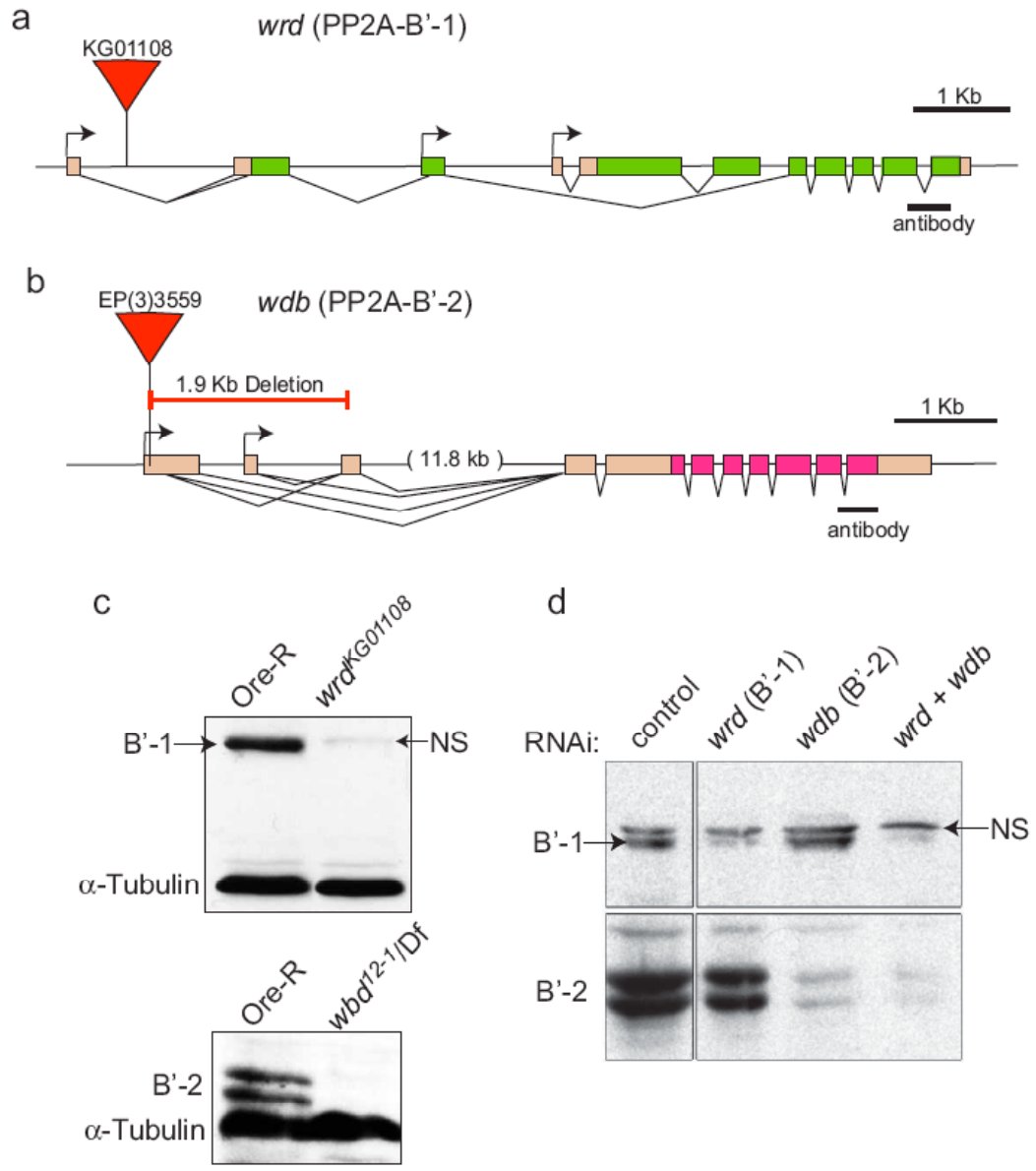

Figure 2-9. Mutations in the two PP2A$^{B'}$ subunits, *wrd* (B'-1) and *wdb* (B'-2), affect their expression. Schematic diagrams of the *wrd* (a) and *wdb* (b) genes and associated mutations are shown. While both subunit genes are highly conserved, we raised antibodies against the variant C-terminal regions. The *wrd*^{KG01108} and *wdb*$^{EP(3)3559}$ mutants

were obtained from the Bloomington Drosophila stock center. The 1.9 kb deletion in *wdb* (*wdb*$^{12\text{-}1)}$was generated by mobilization of EP(3)3559. (c) The two PP2A$^{B'}$ mutations used in this study, *wrd*^{KG01108} and *wdb*$^{12\text{-}1}$ have reduced levels of expressed B'-1 and B'-2 proteins, respectively. The *wrd*^{KG01108} sample is from a homozygous mutant ovary compared to a wild type (Ore-R) ovary. The *wdb*$^{12\text{-}1}$ mutant sample is from third instar larvae transheterozygous with a deficiency (Df(3R)R38.3) that deletes *wdb*, compared to wild type larvae. (d) RNAi knockdown of both gene products in Drosophila S2 cells confirms the specificity of the antibodies for each PP2A$^{B'}$ gene product. The band labeled "NS" in (c and d) is a non-specific protein recognized by the anti-PP2A$^{B'\text{-}1}$ antiserum and serves as a loading control in (d).

in function.

With the exception of the *wrd*^{KG01108} mutant, all the PP2A subunit mutations are homozygous lethal. In the heterozygous mutant state, all the PP2A subunit mutants are viable and healthy and can be maintained as heterozygous stocks.

To test for genetic interactions between ST and PP2A subunit genes, we crossed PP2A subunit mutants with ST-expressing flies to generate embryos that express ST and are heterozygous for each PP2A subunit mutation being tested. When tested at 25˚C, a temperature that results in lower ST expression and therefore increased embryo survival, approximately 20% of ST embryos fail to hatch into larvae (Figure 2-10a, compare to 68% lethality at 29˚C in Figure 2-8a). However, the addition of one mutant copy of *mts*, *PP2A-29B*, or *tws* enhanced ST embryonic lethality to >90%, while the *wrd wdb* double mutant enhanced ST-dependent lethality to 78% (Figure 2-10a). Whereas the *wrd wdb* double mutant enhanced ST lethality, the *wdb* and *wrd* single mutants exhibited little or no enhancement of ST-dependent lethality, again indicating redundancy between the two PP2A$^{B'}$ subunits in the early Drosophila embryo.

To determine if there were developmental stage, cell cycle phase, and PP2A subunit bias associated with the enhancement of ST pathology, we examined ST + PP2A$^{+/-}$ mutant embryos by immunostaining for centrosomes, microtubules, actin and DNA. By scoring embryonic stages among a 3-hour collection, we determined that ST + PP2A$^{+/-}$ mutations showed a delay or arrest of embryos at early cleavage cycles, including the *wrd wdb* double mutant, but less so for the single mutants for these PP2A$^{B'}$ genes (Figure 2-10b). There is a small increase in mitotic index in ST embryos compared to the control (Figure 2-10c). This mitotic delay is limited to the very early cleavage

cycles (cycles 1-9), prior to the cortical cycles (10-13) (data not shown). This accounts for our observation, by live imaging, of no difference in cortical cleavage cycle duration between control and ST embryos (Figure 2-6). Nevertheless, mutations in $PP2A^{C}$, $PP2A^{A}$, and the $PP2A^{B'}$ double mutant all enhanced the mitotic index (Figure 2-10c). Centrosome number increase by ST was enhanced by $PP2A^{C}$, $PP2A^{A}$, $PP2A^{B}$, and the $PP2A^{B'}$ double mutant but not by the individual $PP2A^{B'}$ mutants (Figure 2-10d-g). In addition to increased centrosome replication, PP2A subunit mutations also enhanced spindle abnormalities including aberrant microtubule assembly (Figure 2-10f), large spindles (Figure 2-10e), and chromosome scattering or loss from spindles (Figure 2-10e-g). At the cortex, the abundant centrosomes organize long microtubule asters associated with clusters of actin filaments (Figure 2-10h). Interestingly, while the centrosome replication, spindle microtubule, and chromosome arrangement defects were associated with $PP2A^{C}$, $PP2A^{A}$, $PP2A^{B}$, and the $PP2A^{B'}$ double mutants, enhancement of long astral microtubules at the cortex were seen with the $PP2A^{C}$, $PP2A^{A}$, and $PP2A^{B}$ mutants but not with the $PP2A^{B'}$ double or single mutants. This suggests that the microtubule stabilization imposed by ST is mediated through competition with the PP2A-ABC complex and not by the PP2A-AB'C complex. These strong genetic interactions between ST and PP2A subunit mutants unequivocally support a primary role for PP2A in ST-induced pathology *in vivo*.

Downstream effects of ST expression

PP2A has approximately 75 reported substrates, with likely more yet undiscovered (Janssens and Goris 2001). While ST binds to PP2A and disrupts normal PP2A activity in Drosophila embryos, it did not affect the expression levels of PP2A

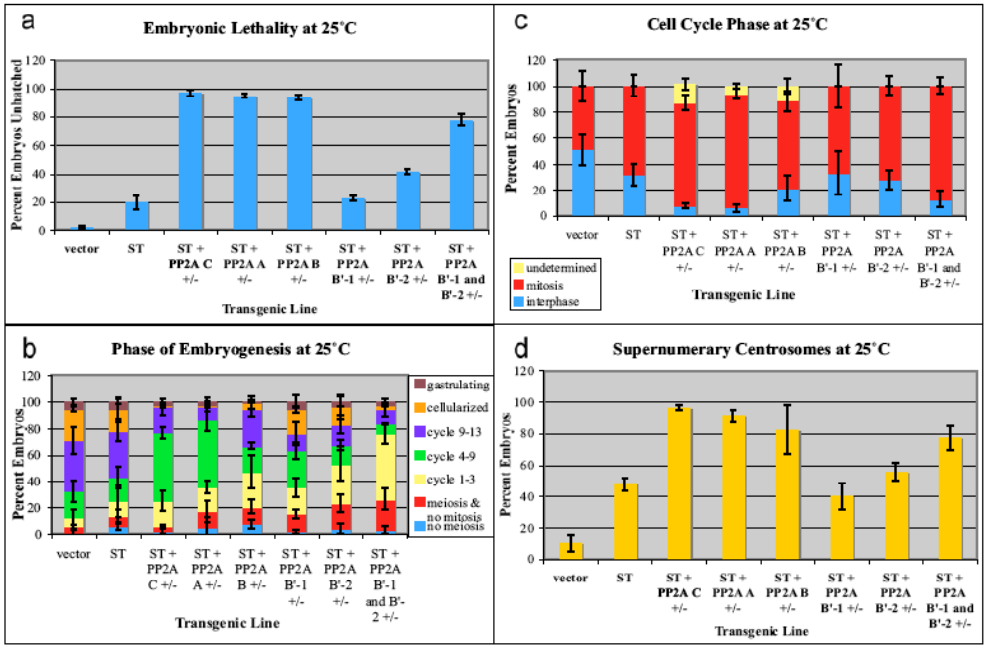
a
Embryonic Lethality at 25°C
Percent Embryos Unhatched
vector
ST
ST + PP2A C +/-
ST + PP2A A +/-
ST + PP2A B +/-
ST + PP2A B'-1 +/-
ST + PP2A B'-2 +/-
ST + PP2A B'-1 and B'-2 +/-
Transgenic Line
c
Cell Cycle Phase at 25°C
Percent Embryos
undetermined
mitosis
interphase
Transgenic Line
b
Phase of Embryogenesis at 25°C
Percent Embryos
gastrulating
cellularized
cycle 9-13
cycle 4-9
cycle 1-3
meiosis & no mitosis
no meiosis
Transgenic Line
d
Supernumerary Centrosomes at 25°C
Percent Embryos
Transgenic Line

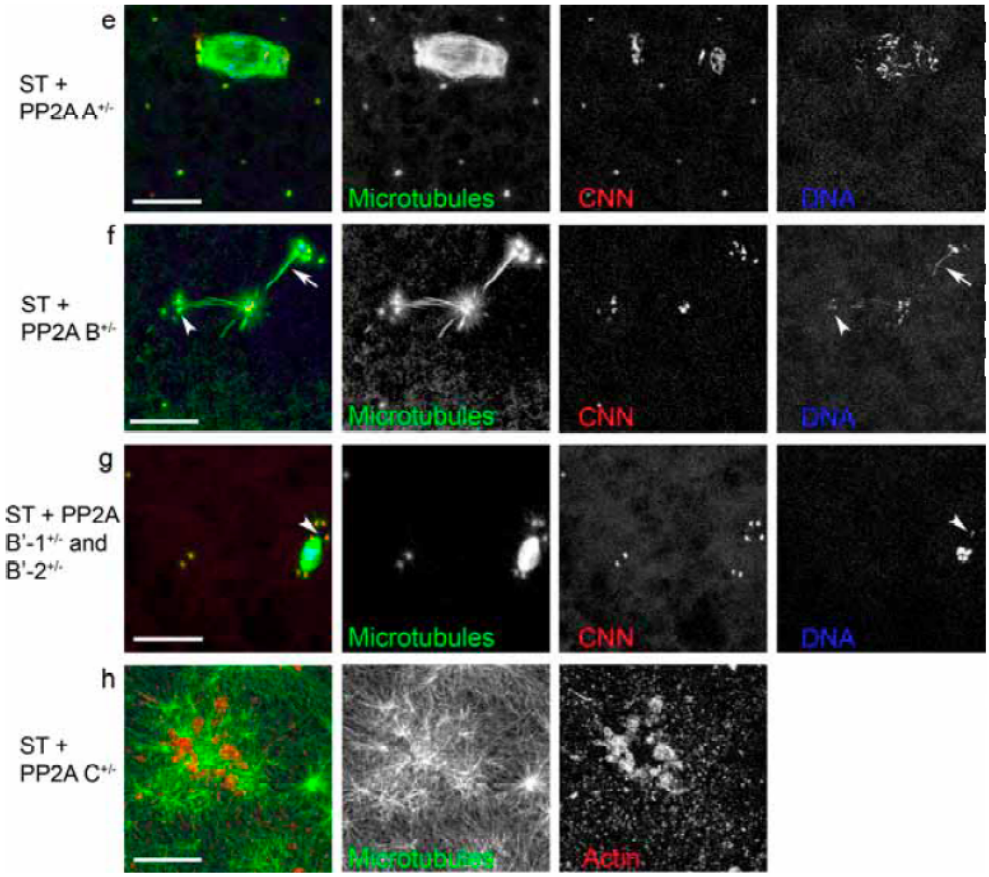
e
ST + PP2A A+/-
f
ST + PP2A B+/-
g
ST + PP2A B'-1+/- and B'-2+/-
h
ST + PP2A C+/-
Microtubules
CNN
DNA
Actin

Figure 2-10. ST embryonic phenotypes are enhanced by PP2A subunit-encoding mutations. Heterozygous *mts* ($PP2A^{C}$), *PP2A-29B* ($PP2A^{A}$), *tws* ($PP2A^{B}$), *wrd* ($PP2A^{B'-1}$), *wdb* ($PP2A^{B'-2}$), and the *wrd wdb* double mutant were introduced into ST embryos at 25˚C. (a) All mutations enhanced lethality except for $PP2A^{B'-1}$. (b) Inhibition of early embryonic development by PP2A subunit mutants. (c) The $PP2A^{C}$, $PP2A^{A}$, and $PP2A^{B'}$ double mutant increased the mitotic index. In some embryos, cleavage was disrupted to such a degree that cell cycle stage could not be determined ("undetermined"). (d) Supernumerary centrosomes was enhanced by all mutations except for the $PP2A^{B'}$ single mutants. Representative phenotypes include multiple centrosomes (e-g), ST + $PP2A^{A}$+/- showing a large spindle and scattered chromosomes (e), ST + $PP2A^{B}$+/- demonstrating linked spindles with aberrant microtubules and lagging chromosomes (f, arrow marks a lagging chromosome), ST + $PP2A^{B}$+/- and ST + $PP2A^{B'-1,B'-2}$+/- showing loss of chromosomes from the spindle or localized near centrosomes (f,g, arrowheads), and ST + $PP2A^{C}$+/- demonstrating large microtubule asters associated with clumps of actin filaments near the cortex (h). Bars: 25µm in e-g, 15µm in h.

subunits $PP2A^{C}$ (Figure 2-7) or $PP2A^{B'-2}$ (data not shown). A downstream target of ST action is increased cyclin A expression (Porras, Bennett et al. 1996; Schuchner and Wintersberger 1999; Goetz, Tzeng et al. 2001; Skoczylas, Henglein et al. 2005). We found that cyclin A levels were not altered in embryos by ST expression (data not shown). However, the levels of another G1/S cyclin and Cdk2 activator, cyclin E, were elevated in response to ST expression by 2.3 +/- 0.58 fold (mean +/- SD) at 29˚C (Figure 2-11).

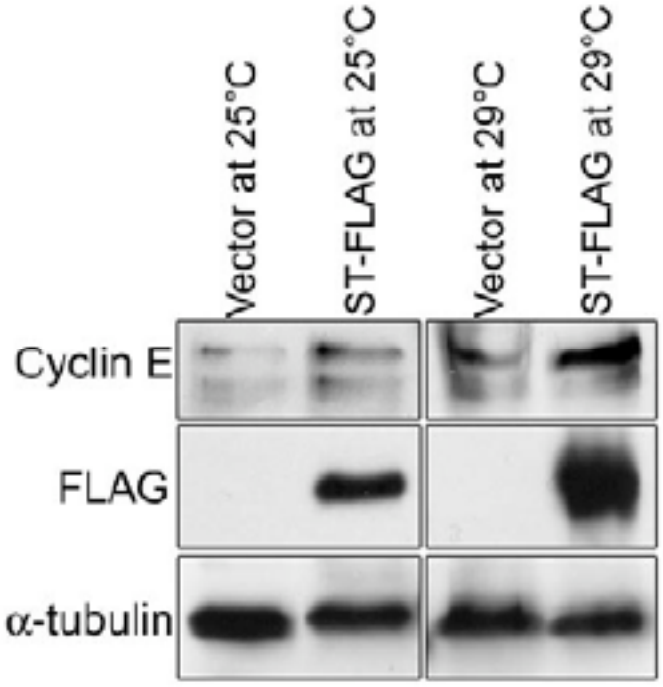

Figure 2-11. Cyclin E levels are elevated in ST embryos. Western blot of embryo lysates from ST embryos show that cyclin E levels are elevated in ST embryos at 25˚C, and more so at 29˚C when ST levels are also increased.

C. Discussion

SV40 ST, together with LT, promotes transformation through disruption of key regulators of cell proliferation and apoptosis (Saenz-Robles, Sullivan et al. 2001; Lavia, Mileo et al. 2003; Skoczylas, Fahrbach et al. 2004; Arroyo and Hahn 2005; Sontag and Sontag 2006). Here, we show that SV40 ST causes lethality when expressed in early Drosophila embryos. In addition, ST induces increased centrosome numbers in human and Drosophila cultured cells as well as in Drosophila embryos. Moreover, in Drosophila embryos ST expression induces multiple defects in cytoskeleton organization and in cleavage divisions including longer astral microtubules, defective microtubule organization into mitotic spindles, chromosome segregation defects, aberrant actin assembly into cleavage furrows, and cytokinesis failure. The phenotypes elicited by ST expression in embryos are due to disruption of PP2A, since mutations in the PP2A-binding domain but not the J domain of ST inhibit disruption of embryo development. Moreover, mutations in the genes that encode the PP2A C, A, B and B' subunits are strong enhancers of ST phenotypes, consistent with PP2A as the primary effector of ST pathogenesis in Drosophila embryos. In addition, the levels of cyclin E, a regulator of cell cycle entry and centrosome duplication, are elevated in ST embryos. These data establish the first Drosophila model for a viral oncoprotein, and show the efficacy of this model for genetic manipulation and for the potential to discover novel features of viral oncoprotein biology.

ST causes centrosome overduplication

Centrosomes play a dominant role in the assembly and organization of microtubules into the bipolar spindle apparatus at mitosis. Therefore, centrosome duplication must be tightly regulated to ensure spindle bipolarity and accurate chromosome segregation at cell division (Nigg 2002; Sluder and Nordberg 2004). Inaccurate chromosome segregation can lead to aneuploidy, a common feature of cancer cells. Supernumerary centrosomes are also a common feature of cancer cells, and centrosomal proteins have been implicated as tumor suppressors or oncogenes (Brinkley 2001; Pihan, Purohit et al. 2001; Lingle, Barrett et al. 2002; Nigg 2002; Fukasawa 2007).

The ability of ST to induce supernumerary centrosomes in Drosophila and human cells is a novel finding, and indicates conservation of this activity. Expression of ST in human cell culture was reported previously to block centrosome assembly and function (Gaillard, Fahrbach et al. 2001). This discrepancy with our findings may be attributed to differences in the levels of ST expressed and/or the cell type used, suggesting context-dependent effects of ST expression. We found that centrosome overduplication was potent in ST-naïve Drosophila Kc cells: a 20-hour induction of ST increased the incidence of supernumerary centrosomes from approximately 21% to 45%. While centrosome numbers can increase through overduplication or can arise as a consequence of failed cytokinesis, ST expression in Kc cells specifically affected centrosome duplication with little or no affect on cytokinesis. Interestingly, multiple centrioles induced by ST in U2OS cells appear to assemble around a single parent centriole, similar to that seen with overexpression of Plk4, a key regulator of centriole duplication (Duensing, Liu et al. 2007; Kleylein-Sohn, Westendorf et al. 2007). Increased centrosome numbers are elicited by ST through PP2A perturbation, since this activity is abolished by

ST mutations that block PP2A binding, and enhanced by PP2A subunit mutations. Other viral oncoproteins, including E7 from HPV type 16, E1A from adenovirus type 5, HBx from hepatitis type B virus, and Tax from HTLV-1, also induce supernumerary centrosomes (De Luca, Mangiacasale et al. 2003; Duensing and Munger 2003; Fujii, Zhu et al. 2006; Nitta, Kanai et al. 2006). Since E7, E1A and Tax bind to PP2A and affect its phosphatase activity, PP2A disruption may represent a shared mechanism for deregulating centrosome replication by viral oncoproteins (Liao and Hung 2004; Pim, Massimi et al. 2005; Hong, Wang et al. 2007).

Mutations in $PP2A^{C}$ (*mts*) cause uncoupling of centrosome and nuclear divisions, and longer astral microtubules that fail to attach to kinetochores (Snaith, Armstrong et al. 1996). While *mts* mutant embryos show excess centrosomes, increased centrosome numbers were not observed in $PP2A^{B}$ (*tws*) mutant cells (Mayer-Jaekel, Ohkura et al. 1993; Snaith, Armstrong et al. 1996). RNAi depletion of $PP2A^{C}$ and $PP2A^{A}$ in Drosophila S2 cells also showed elongated microtubules in mitotic cells (Chen, Archambault et al. 2007). However, depletion of PP2A A, C, or B subunits did not increase centrosome numbers in S2 cells, and even resulted in decreased numbers of centrosomes, a result that differs from ST expression in embryos, Drosophila Kc cells and human U2OS cells presented here (Chen, Archambault et al. 2007). These data suggest that, in addition to inhibiting activities toward normal PP2A substrates, ST may direct PP2A toward novel targets that regulate centrosome duplication. The idea of ST conferring new target specificities to PP2A is consistent with reports of ST increasing PP2A substrate specificity for Histone H1, and for novel targeting of PP2A to the androgen receptor (Yang, Lickteig et al. 1991; Yang, Vitto et al. 2005). Moreover, the

recently solved structures of PP2A AB'C heterotrimer and of the A-ST dimer, are consistent with ST acting as a viral-type PP2A B subunit, perhaps conferring a new range of substrate specificities (Xu, Xing et al. 2006; Chen, Xu et al. 2007; Cho, Morrone et al. 2007; Cho and Xu 2007). Thus, ST inhibits endogenous PP2A activity while bestowing novel target specificities.

While the targets of PP2A-ST that contribute to the phenotypes presented here are unknown, one downstream effector of ST appears to be cyclin E, whose levels we show are elevated in ST embryos. In other systems ST stimulates AP-1 transcription factor activity to promote transcription of cyclin D (Frost, Alberts et al. 1994; Watanabe, Howe et al. 1996), which is expected to then induce cyclin E expression to drive G1 cells into S phase (Reed 1997). Cyclin E/Cdk2 activity is required for centrosome duplication, and cyclin E + Cdk2 overexpression induces centrosome amplification (Tsou and Stearns 2006; Duensing, Liu et al. 2007; Nigg 2007). However, while Cdk2 + cyclin E overexpression can act synergistically with Plk4 overexpression, HPV-16 E7 expression, or proteasome inhibitors to induce centriole overduplication, cyclin E or Cdk2 + cyclin E overexpression alone has only a minor effect on centriole replication (Duensing, Duensing et al. 2004; Duensing, Liu et al. 2007). Thus, the elevation of cyclin E levels induced by ST expression is unlikely sufficient to account for the increased centrosome replication we observed, but may be a contributing factor.

Microtubule stability and actin organization

The major pool of cellular PP2A is associated with microtubules and centrosomes, showing the highest degree of association at S phase, when centrosome duplication occurs (Sontag, Nunbhakdi-Craig et al. 1995). Previous studies showed that

$PP2A^{C}$ mutant Drosophila embryos display longer, more stabilized microtubules, which is why the gene encoding the PP2A catalytic subunit was named "*microtubule star*" (Snaith, Armstrong et al. 1996). Consistent with a role for PP2A in promoting shorter microtubules, ST embryos have longer and more abundant astral microtubules. Moreover, this phenotype is dependent on PP2A binding and is strongly enhanced by PP2A subunit mutants, sometimes producing astral microtubules extending more than 100 μm in length. Interestingly, while the PP2A A, C, and B subunit mutants enhanced microtubule stability and actin disruption at cleavage furrows, the B' and double B' mutants did not. This suggests that the targets for PP2A that regulate these cytoskeletal dynamics are dependent more on the B subunit rather than on B'. Microtubule assembly at centrosomes requires γ-tubulin for nucleation and other regulators such as Aurora A kinase to promote microtubule polymerization or stability (Wiese and Zheng 2006). PP2A regulates Aurora A levels (Horn, Thelu et al. 2007) and the activity of the microtubule destabilizing phosphoprotein Op18/Stathmin (Tournebize, Andersen et al. 1997). The large asters in ST embryos may therefore be due to alterations in levels or activities of these factors. However, we found no changes in levels and/or centrosome localization of several MTOC regulators (γ-tubulin, CNN, Aurora A kinase, Msps, and D-TACC; data not shown). Elucidating the role of ST in microtubule stability will require the identification of PP2A substrates that regulate microtubule dynamics.

Actin assembly into cleavage furrows is severely aberrant in ST embryos, showing thicker bundles of actin cables and abnormal clumps of actin at the cortex. Enhancement of actin defects in ST embryos by PP2A A, C, and B subunit mutants resulted in clumping of actin assembly in the proximity of centrosomes, with furrow

assembly severely inhibited. The conserved small G protein regulators of actin, Cdc42 and Rac are activated by ST in MDCK cells, while Rho is inhibited (Nunbhakdi-Craig, Craig et al. 2003). Consistent with this, actin assembly into Drosophila cleavage furrows is regulated differentially by the active or inactive forms of Rho and Cdc42, but not Rac (Crawford, Harden et al. 1998). Thus, Cdc42 and Rho are potential targets of ST that disrupt actin organization into cleavage furrows in Drosophila embryos. Additionally, proteins that regulate actin dynamics and participate in actin organization into cytokinetic furrows are targets of PP2A, and therefore may be affected in ST embryos to promote cytokinesis failure (Sontag and Sontag 2006).

ST-induced aneuploidy

A hallmark of most solid tumors is aneuploidy/CIN, which is thought to be a causative factor in tumorigenesis (Rajagopalan and Lengauer 2004). Expression of ST in embryos caused an increase in lagging chromosomes at anaphase and also the scattering and loss of chromosomes on the spindle apparatus. These phenotypes are consistent with perturbation of PP2A, since mutations in $PP2A^{B}$ (*tws*) cause chromosomes to lag at anaphase (Mayer-Jaekel, Ohkura et al. 1993), and RNAi of $PP2A^{B'-2}$ (*wdb*) causes chromosome scattering on the spindle (Chen, Archambault et al. 2007). Both of these chromosome segregation defects were observed in ST embryos and enhanced by PP2A subunit gene mutations. Moreover, the increase in cyclin E levels induced by ST may also contribute to the chromosome segregation defects we observed, since elevated cyclin E expression increases susceptibility for tumor formation, not only due to its ability to drive cell proliferation, but also to generate CIN (Spruck, Won et al. 1999; Loeb, Kostner et al. 2005). In addition, as discussed above, supernumerary centrosomes are also

correlated to CIN and tumor progression (Brinkley 2001; Pihan, Purohit et al. 2001; Lingle, Barrett et al. 2002; Nigg 2002; Fukasawa 2007). Thus, ST expression may contribute to CIN by causing chromosome segregation errors that are exacerbated by centrosome overduplication, either or both of which may be enhanced by increased cyclin E expression.

We have created the first *Drosophila* model for expression of a viral oncoprotein. A unique advantage of this *in vivo* model for ST expression is the breadth of molecular genetic tools available for Drosophila research, and the relative rapidity of experimental implementation for investigating the determinants of ST pathology compared to mammalian models. Establishment of this model has revealed novel ST functions, including stimulation of centrosome duplication, stabilization of microtubules, chromosomal instability, and inhibition of cytokinesis, all of which could reflect fundamental mechanisms by which ST contributes to transformation. Furthermore, Drosophila has achieved utility as a model for investigation of mechanisms of tumorigenesis and metastasis through genetic screens (Brumby and Richardson 2003; Pagliarini and Xu 2003). Future experiments based on ST expression in somatic tissues will test tumor-promoting capabilities of ST and possibly pave the way for genetic dissection of ST pathways.

D. Materials and Methods

Fly Stocks and crosses

Transgenic flies were made by standard procedures. The PP2A mutants: *mts*$^{xe-2258}$ (PP2A^{C}), PP2A-29B^{EP2332} (PP2A^{A}), *tws*^{02414} (PP2A^{B}), *wrd*^{KG01108} (PP2A$^{B'-1}$), *wdb*$^{EP(3)3559}$ (PP2A$^{B'-2}$) and Df(3R)R38.3 were obtained from the Bloomington Stock Center. *wdb*$^{12-1}$ (PP2A$^{B'-2}$) is a 1.9 kb deletion generated by mobilization of a P element located in the 5' region of *wdb* (EP(3)3559) (Figure 2-9). Expression of transgenes from pUASp vectors in embryos was achieved by crossing transgenic lines to nos-GAL4VP16, which expresses GAL4VP16 in ovaries from the *nanos* promoter. Females from the cross were mated to wild-type males and incubated at either 25˚C or 29˚C (to vary the level of expression).

Plasmids

The SV40 early region (genomic sequence from positions 5763-2533) was cloned into the P element vector pUASp. ST cDNA and the ΔPP2A (also called "mut3") clone (gifts from Estelle Sontag) were amplified by PCR and cloned into pENTR/D-TOPO. Entry clones were then recombined into a vector containing a C-terminal 3X-FLAG tag (pPWF) using LR-recombination with the Gateway system (Invitrogen). ST cDNA in pPWF was named pST-FLAG. ST^{D44N} and ST^{C103S} were generated through site-directed mutagenesis with the ST Entry clone using QuikChange (Stratagene). The ST-expressing plasmid used for U2OS transfections was pCMV5/Smt (from E. Sontag). For expression of GST-ST fusion protein in *E. coli*, the ΔPP2A clone (which encodes amino acids 1-110) was cloned into the pGEX2* vector. The *wrd* (B56-1) and *wdb* (B56-2) sequences corresponding to amino acid regions 543-656 and 425-524, respectively, were cloned into pRSETB plasmid for expression in *E. coli* as 6XHis-tagged fusion proteins for antibody production in rabbits.

Cell culture, transfections, and flow cytometry

Kc167 cells were cultured in CCM3 (Hyclone) + Penicillin/Streptomycin medium. Stable cell lines were generated by co-transfection with pMT-GAL4 (Klueg, Alvarado et al. 2002) and either vector (pPWF) or pST-FLAG, and pCoPuro for drug selection using Effectene reagent (Qiagen). Cells were selected in the above medium + 2 μg/ml Puromycin (Sigma). Expression of ST-FLAG from these cells is induced by addition of $CuSO_4$, which activates expression of GAL4 transcription factor from the metallothionein promoter in pMT-GAL4. U2OS cells were cultured in DMEM + 10% FBS + Penn/Strep. Transient transfections into U2OS cells were performed using Lipofectamine 2000 (Invitrogen). pCMV5/Smt was co-transfected with pGFP-Histone (a marker for transfected cells), or pGFP-Histone was transfected alone as a control. Cells were processed for immunostaining and western blotting 46 hrs post-transfection. Cell cycle analysis was accomplished through DNA staining with propidium iodide (PI) and flow cytometry as described in *Current Protocols in Cytometry (2007)*. Cells were washed with PBS and fixed with 70% ice-cold ethanol. Ethanol was removed and the cells were resuspended to a final concentration ~10^6 ml^{-1} in PBS + PI/RNaseA/Triton X-100 (20 μg ml^{-1}, 200 μg ml^{-1} and 0.1% v/v respectively). Fluorescence was measured (Becton Dickinson, FACScan) for 15,000 cells per sample, and the data analyzed with FlowJo 8.7 software (Tree Star Inc, Ashland, OR) using a Watson Pragmatic fitting algorithm.

Immunofluorescent Staining

Embryos were collected on apple juice/agar plates for 3 hours. They were then fixed with methanol/heptane. For actin staining and optimal astral microtubule fixation,

embryos were fixed 2-3 min with 37% formaldehyde and the vitelline membrane removed by hand. Embryos were blocked in PBT (PBS + 0.1% Tween-20) + 5 mg/ml BSA for 1 hour at room temperature, incubated with primary antibodies in PBT + 5 mg/ml BSA overnight at room temperature, and incubated with secondary antibodies in PBT + 1 mg/ml BSA for two hours at room temperature. After each antibody application, embryos were rinsed twice in PBT and washed two times with PBT for twenty minutes. Embryos were left to settle onto a PBT/90% glycerol cushion overnight at 4°C prior to mounting. Embryos were imaged on a Leica SP2 confocal microscope using a 63X /NA1.4 oil immersion objective. Kc cells were fixed and stained as described (Kao and Megraw 2004). Human cells were seeded onto four-well slides and cultured overnight. Cells were fixed 46 hours post-transfection in methanol. After fixation, cells were blocked with 1% goat serum + 5 mg/ml BSA + 0.1% saponin for thirty minutes. Cells were then stained as described for Kc cells. U2OS and Kc cells were imaged on a Zeiss axioskop using a 63X /NA1.4 oil immersion objective and a Coolsnap FX CCD camera with Metamorph software.

Embryo Hatching

Embryos were collected on apple juice/agar plates, and then lined up on fresh apple juice/agar plates. The plates were kept at room temperature for two days and were then counted under a dissecting scope to score hatching.

Antibodies

Soluble GST-ST fusion protein (amino acids 1-110) from E. coli was purified by glutathione agarose chromatography. 6XHis-tagged B56-1 (amino acids 543-656) and B56-2 (amino acids 425-524) were purified from E. coli using immobilized Ni^{++} on

chelating sepharose fast flow (Amersham Biosciences). Antisera were raised in rabbits by Cocalico Biologicals, Inc. For immunostaining the following antibodies were used: Rabbit anti-centrosomin (Zhang and Megraw 2007) 1:2000, α-tubulin DM1a 1:1000 (Sigma), Alexa546-phalloidin 1:200 (Molecular Probes), gamma-tubulin GTU-88 1:500 (Sigma), GFP 1:1000 (Invitrogen), Draq5 1:1000 (Axxora). Secondary antibodies included Alexa 488 and 546 coupled goat antibodies used at 1:400 (Invitrogen). For western blotting the following antibodies were used: FLAG (M2 monoclonal from Sigma) 1:10,000, cyclin E (a gift from H. Richardson) 1:20, cyclin A clone A12 (Developmental Studies Hybridoma Bank (DSHB)) 1:5, cyclin B clone F2F4 (DSHB) 1:1000, anti-B56-1 1:10,000, anti-B56-2 1:10,000, anti-$PP2A^{C}$ clone 1D6 (Upstate Cell Signaling) 1:5000, anti-ST (UT450) 1:10,000, pAb280 1:1000 (Oncogene), pAb419 1:1000 (Oncogene), α-tubulin DM1a 1:10,000 (Sigma). HRP-conjugated anti-mouse and anti-rabbit secondary antibodies were diluted 1:20,000 (Jackson IRL, Inc). Western blots were processed with SuperSignal West Pico chemiluminescent substrate (Pierce).

Immunoprecipitation

Embryos were collected for 3 hours on apple juice/agar plates. After chorion removal with 50% bleach, embryos were washed with extraction buffer (EB; 50 mM Tris pH 8.0, 150 mM NaCl). Embryos were then homogenized in approximately two volumes of EB + 1X protease inhibitor cocktail (Sigma). The extract was centrifuged for 15 minutes at 16,000xg at 4˚C and the supernatant was transferred to a new tube. Approximately one-tenth volume of 10% NP-40 was added to the extract and the extract was centrifuged for 10 minutes as above and the supernatant again transferred to a new tube. The extracts were then snap frozen in liquid nitrogen and stored at -80°C. Upon

thawing, extracts were again centrifuged for 10 minutes as above. Colcemid (10 μM) was added to embryo extracts that were then incubated with anti-FLAG agarose (Sigma) pre-equilibrated with wash buffer (WB; 50 mM Tris pH 7.4, 150 mM NaCl) for two hours at 4°C. Following centrifugation, the pellet was washed five times over the course of 1 hr with WB + 0.5% Triton X-100 at 4°C, then twice more in WB. Protein was eluted with 20 μl 2X SDS-PAGE loading dye supplemented with fresh 2-mercaptoethanol (0.4 M) for 5 minutes at 95°C. All centrifugations were 10,600xg for 5 seconds, unless otherwise indicated. The $PP2A^C$ IP was performed similarly as the FLAG IP, except 1μg of $PP2A^C$ monoclonal 1D6 was incubated with embryo extract + 10 μM Colcemid for 1 hour at 4°C and then the antibody + extract was added to 20μl pre-equilibrated Protein A sepharose (Amersham Biosciences). The Protein A sepharose was washed and eluted as above for FLAG IP.

Live-Imaging

Movies were captured as described in (Zhang and Megraw 2007). The HandleExtraFileTypes.class plugin in Image J was used to convert the .avi files generated from the Leica software into stacks, which were then converted to Quicktime movies 15 frames per second with a Sorenson 3 Normal compression.

CHAPTER THREE

SMALL TUMOR ANTIGEN FORMS AN INDEPENDENT COMPLEX WITH KINESIN-1 AND SELECTIVELY INHIBITS MOTOR ACTIVITY

A. Introduction

Kinesin-1 is a plus-end microtubule motor protein used to transport cargo towards the periphery of the cell. Kinesin-1 is a heterotetramer consisting of two heavy chains and two light chains. The kinesin heavy chains compose the motor domains that bind directly to an α- and β-tubulin heterodimer and the kinesin light chains bind cargo. In kinesin-1's inactive state, the light chains fold back on the heavy chains to inhibit motor activity. Cargo proteins relieve the inhibition by changing the conformation of kinesin-1 (Horiuchi, Collins et al. 2007).

To move along the length of the microtubules, kinesin-1 hydrolyzes a molecule of ATP. When ATP is converted to ADP, kinesin-1 walks in ~8 nm steps with each head taking either 0 nm or ~17 nm steps, as determined by single-head labeling experiments (Yildiz, Tomishige et al. 2004). Kinesin-1 walks in a hand-over-hand fashion without dissociating from the microtubule filament for on average about one hundred steps (Hancock and Howard 1998; Asbury, Fehr et al. 2003). If ATP is replaced by a non-hydrolyzable analog, AMP-PNP, the motor no longer walks and instead remains bound to the microtubule (Asenjo, Weinberg et al. 2006).

Kinesin-1 is crucial for the cytoplasmic transport of cargo proteins, for example the transport of neuronal proteins along axons to the cell body. The significance of

kinesin-1 function is demonstrated in *Drosophila melanogaster* third instar larval motor neurons that branch from the ventral lobe of the brain. In weak kinesin heavy chain mutants, staining of the kinesin heavy and light chains show accumulations of kinesin-1 along the motor neurons. Similarly, staining for synaptotagmin, a neural specific cargo protein, results in focal accumulations of the protein along motor neurons. Finally, misregulation of kinesin-1 results in larval paralysis (Saxton, Hicks et al. 1991). The phenotypes associated with weak kinesin-1 mutants have been used to identify other mutants that regulate kinesin-1 activity or cargo linkage to kinesin-1.

Cargo proteins were recently shown to bind kinesin-1 to regulate motor activity by changing the conformation of the heterotetramer. One cargo protein is c-Jun N-terminal kinase (JNK)-interacting protein (JIP) 1, or JIP1. JIP1 is a linker protein between the kinesin light chain and its vesicular cargo. Another JIP protein, JIP3, also binds the kinesin light chain, however it does so at a distinct binding site from JIP1. The two proteins were shown to work cooperatively to allow efficient cargo transport and proper neuronal growth (Hammond, Griffin et al. 2008).

JIP1 also works with another protein, fasciculation and elongation protein zeta 1, or FEZ1, that binds the kinesin heavy chain. Individually, JIP1 and FEZ1 cannot activate kinesin-1, but when both proteins are bound to kinesin-1, the motor is activated. JIP1 and FEZ1 interact only in the presence of kinesin-1, suggesting that they work cooperatively to activate kinesin-1 (Blasius, Cai et al. 2007). These two proteins demonstrate regulation of both kinesin-1 subunits.

Cargo proteins regulate activity of kinesin-1; therefore signaling pathways that involve JIPs and FEZ1 also affect motor activity and neuronal development. JIPs bind

proteins in the JNK pathway, including JNK and mitogen activated protein (MAP) kinases (MAPK) (Yasuda, Whitmarsh et al. 1999; Kelkar, Standen et al. 2005). Using Drosophila genetic interactions, Horiuchi, *et al.* showed that overexpression of components of the MAPK signaling pathway, including fat facets and wallenda (MAPKKK), suppress axonal-transport-disruption phenotypes caused by JIP1, or Drosophila Aplip1, overexpression (Horiuchi, Collins et al. 2007). Consistent with the genetic interaction, Drosophila mutations in wallenda, hemipterous (MAPKK), and basket (JNK) cause synaptic protein accumulation. Another group showed that mouse JIP3, or Sunday Driver in Drosophila, interacts with JNK3 as a scaffolding protein that links JNK signaling to kinesin-1, and then transports the signaling pathway components along the axon to the cell body (Cavalli, Kujala et al. 2005). Both these examples confirm the JNK and MAP signaling pathways in the regulation of neuronal kinesin-1 motor activity and proper cytoplasmic signaling.

The role of kinesin-1 in trafficking cargo suggests that viral proteins can utilize kinesin-1 to their benefit. Moreover, many viruses manipulate motor proteins to move along microtubules (Greber and Way 2006). For example, some viruses use dynein, a minus-end directed motor, to transport viral particles toward the centrosome for virion assembly. Thus far, only one example has been shown where a virus relies on kinesin-1 for its life cycle (Schepis, Stauber et al. 2007). Vaccinia virus uses kinesin-1 for three different intermediates in the viral life cycle, DNA replication, trans golgi networking, and intracellular envelope viral egress. Here we show another viral protein, ST, mediates kinesin-1 activity by selective binding and inhibition of motor function.

B. Results

ST binds kinesin heavy chain

ST may have interacting partners other than PP2A and Hsc70 that have not been identified due to a lack of experimental tools available to detect protein-protein interactions, such as ST antibodies for IP. Moreover, tagging of ST is quite difficult. Indeed, we found that tagged ST has lowered activity compared to native ST (see Figure 2-2). Given these results, ST-FLAG (described in Chapter 2) was used to determine novel ST binding partners. ST-FLAG was IP'ed from Drosophila embryo extract using FLAG resin and the IP was analyzed by nano-high performance liquid chromatography/mass spectrometry/mass spectrometry (HPLC/MS/MS, hereafter referred to as MS). As a control, CNN exons 3 and 4 with a C-terminal FLAG tag, which results in a similar sized protein as ST-FLAG, was also IP'ed from embryo extract and analyzed by MS. After cross comparing the identified binding partners and isolating unique hits for each sample, several proteins were identified to bind to ST. The top two hits for ST were $PP2A^{C}$ and $PP2A^{A}$, thereby confirming the MS analysis (Table 3-1). Of the potential interacting partners, most interesting were the kinesin heavy and light chain, or the kinesin-1 motor. To confirm the interaction, IP with FLAG resin and western blotting were performed. As expected, ST binds to the kinesin heavy chain (Figure 3-1a). To further map the binding domain, the ST mutants, as described in Chapter 2, were utilized. Interestingly, the ST^{D44N} and ST^{C103S} mutants bind kinesin heavy chain as strongly as wild type ST (Figure 3-1a,b). Furthermore, the $ST^{\Delta PP2A}$ mutant weakly binds kinesin heavy chain compared to wild type ST. Conversely, the kinesin heavy chain IPs ST-FLAG (Figure 3-1c). These

Hit	Protein Name	Score	Note
7	microtubule star CG7109-PA [Drosophila melanogaster]	293	PP2A^C
29	phosphoprotein phosphatase (EC 3.1.3.16) 65K regulatory chain - fruit fly (Drosophila melanogaster)	99	PP2A^A
48	kinesin heavy chain	65	microtubule plus-end motor
60	MCM6 [Drosophila melanogaster]	58	minichromosome maintenance 6
71	mutagen-sensitive 209 CG9193-PA, isoform A [Drosophila melanogaster]	55	PCNA: DNA synthesis and DNA repair
91	Kinesin light chain CG5433-PA [Drosophila melanogaster]	45	microtubule plus-end motor
96	GA14559-PA [Drosophila pseudoobscura]	43	gamma-tubulin

Table 3-1. ST proteomic hits for MS analysis. ST-FLAG was IP'ed with FLAG resin. Beads were sent in for nano-HPLC/MS/MS analysis along with a control IP, CNN exons 3-4 with a C-terminal FLAG tag. The proteins pulled down for both samples were cross-compared and unique hits isolated. Only a subset of hits is represented here for ST-FLAG. The hit number indicates its position on the list of results and the score indicates the coverage value for the peptide in the original sample.

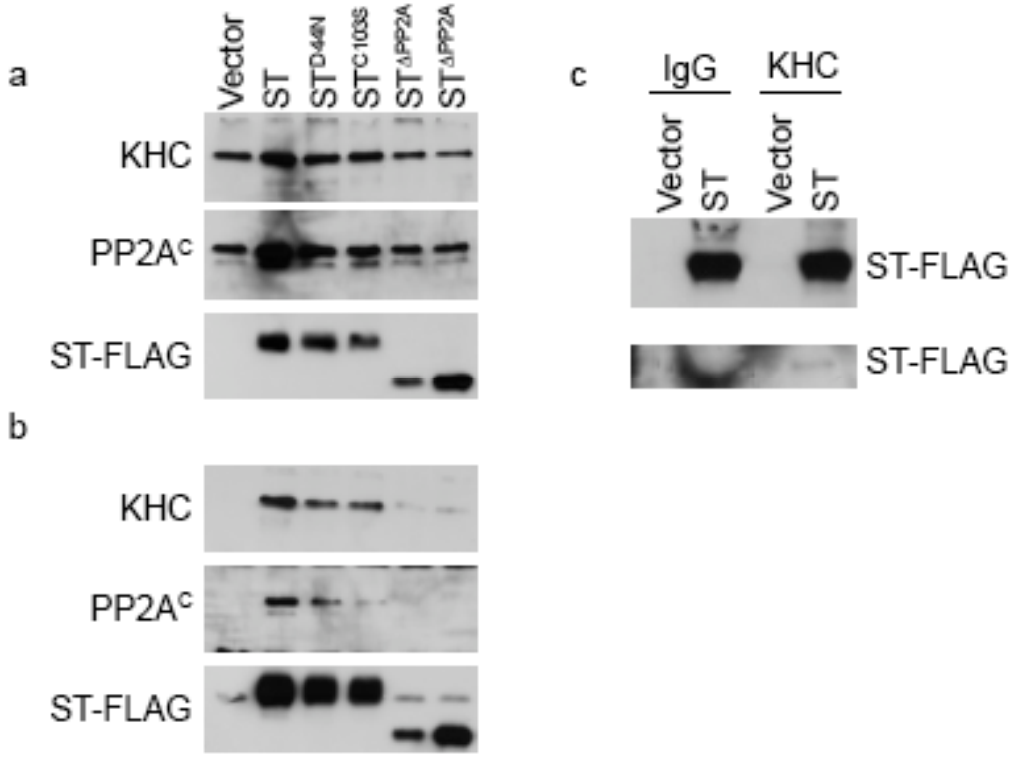

Figure 3-1. ST binds kinesin heavy chain (KHC) independent of Hsc70 and PP2A. (a) Embryos were collected for 3 hours and lysed. Western blotting of whole extract shows kinesin heavy chain, $PP2A^{C}$, and FLAG tagged protein expression. (b) Western blotting for kinesin heavy chain, $PP2A^{C}$, and FLAG tagged proteins from the FLAG IP of whole embryo extract. ST, ST^{D44N}, and ST^{C103S} bind kinesin heavy chain equally well while $ST^{\Delta PP2A}$ weakly binds and the vector does not bind. (c) Vector and ST-FLAG lysates were IP'ed with either Rb IgG or the kinesin heavy chain antibody. The upper western blot indicates lysate while the lower western blot indicates IP. Both blots were probed with an anti-FLAG Ab. Only the kinesin heavy chain IPs ST-FLAG, whereas Rb IgG does not.

results suggest kinesin heavy chain is a novel interactor of ST and binds independent of ST's two known binding partners.

ST inactivates the kinesin-1 motor

ST binds kinesin-1, however the result of this binding is unknown. As discussed above, when kinesin-1 is inactivated, larval paralysis and focal accumulation of kinesin-1 and cargo proteins occurs in larval motor neurons (Saxton, Hicks et al. 1991; Hurd and Saxton 1996). Moreover, mutations in genes that regulate kinesin-1 and cargo proteins phenocopy the kinesin-1 mutants (Horiuchi, Barkus et al. 2005; Pilling, Horiuchi et al. 2006; Horiuchi, Collins et al. 2007). To determine if ST has a similar effect on kinesin-1 activity, ST was expressed in the Drosophila central nervous system, including larval motor neurons, with the *elaV*-Gal4 driver (Robinow and White 1988; Robinow and White 1991; Berger, Renner et al. 2007). To obtain higher expression of ST, an untagged ST transgenic line was constructed. The line referred to as T/t-Amber was derived from T/t-pTre2, a plasmid containing the SV40 early region (the same coding region as the SV40 T/t line described in Chapter 2). An amber stop codon was inserted early in the second exon of LT at a TstI site, in the process deleting base pairs 4525-4557. Then T/t-Amber was inserted into the pUASp plasmid for use in Drosophila (Figure 3-2a). With the elaV-Gal4 driver, T/t-Amber only produces ST (Figure 3-2b) (Robinow and White 1988; Robinow and White 1991; Berger, Renner et al. 2007). For maximal expression, the crosses were maintained at 29°C. At this temperature, T/t-Amber is lethal, resulting in small, sickly larvae with brown spots along the outside of their body (Figure 3-3a). In order for the larvae to develop to the third instar stage, the crosses were kept at 25°C for

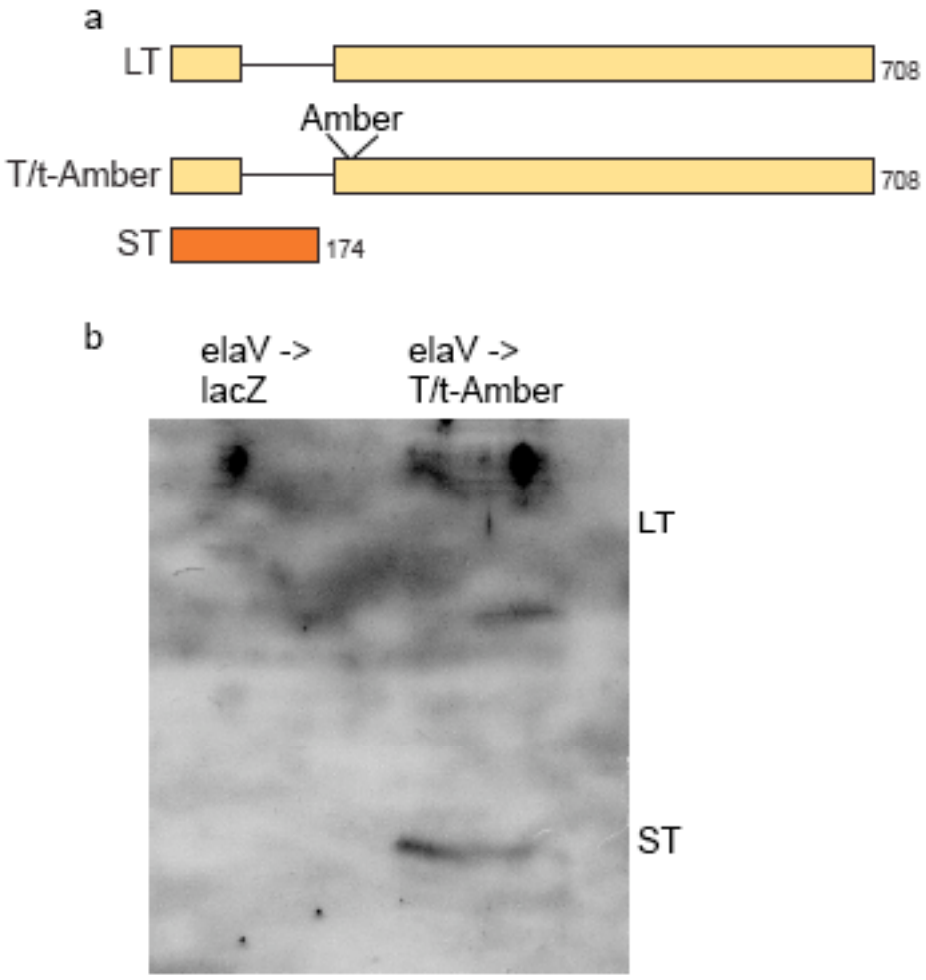

Figure 3-2. T/t-Amber only expresses ST protein. (a) Schematic of T/t-Amber. An amber stop codon was inserted into a TstI site early in the second exon of LT. This amber insert does not interfere with the ST coding region. (b) LacZ and T/t-Amber expression were driven in the Drosophila central nervous system using an ElaV-Gal4 driver. Western blotting of larval brains shows that only ST is made from the T/t-Amber transgenic line.

five days and then shifted to 29°C. A five-day time course revealed that after one day at 29°C, third instar larvae showed a phenotype comparable to five days at 29°C. LacZ, as a negative control, and T/t-Amber larval motor neurons were stained for synaptotagmin and the kinesin heavy chain. Synaptotagmin staining revealed focal accumulations of cargo along the T/t-Amber-expressing motor neurons as compared to the lacZ control; however lacZ sometimes also showed weak synaptotagmin focal accumulations (Figure 3-3b). These synaptotagmin focal accumulations were not present in all ST larval motor neurons, nor in all samples stained, suggesting that ST expression is not high enough to cause complete kinesin-1 inhibition similar to weak kinesin-1 mutants. Kinesin heavy chain staining did not result in the same accumulations as synaptotagmin (data not shown). Due to this result, we were interested in determining a possible genetic interaction between ST and kinesin-1 because many mutants that regulate kinesin-1 were discovered through genetic screens for enhancers of heterozygous kinesin heavy chain mutants. Therefore, T/t-Amber was expressed in either a khc^{6} or khc^{8} heterozygous mutant background. The khc^{6} mutant has a point mutation in the kinesin heavy chain and is lethal at the third instar larval stage (Saxton, Hicks et al. 1991). The khc^{8} mutant has a point mutation at arginine 210 that results in a stop codon in the kinesin heavy chain and is lethal in the early larval stages (Saxton, Hicks et al. 1991). While both the heterozygous kinesin heavy chain mutants alone do not have any kinesin accumulations, T/t-Amber with either of the heterozygous mutants result in long accumulations unlike any other characterized mutants, although this occurs at a similar penetrance as the synaptotagmin focal accumulations (Figure 3-3c). These data indicate that ST expression

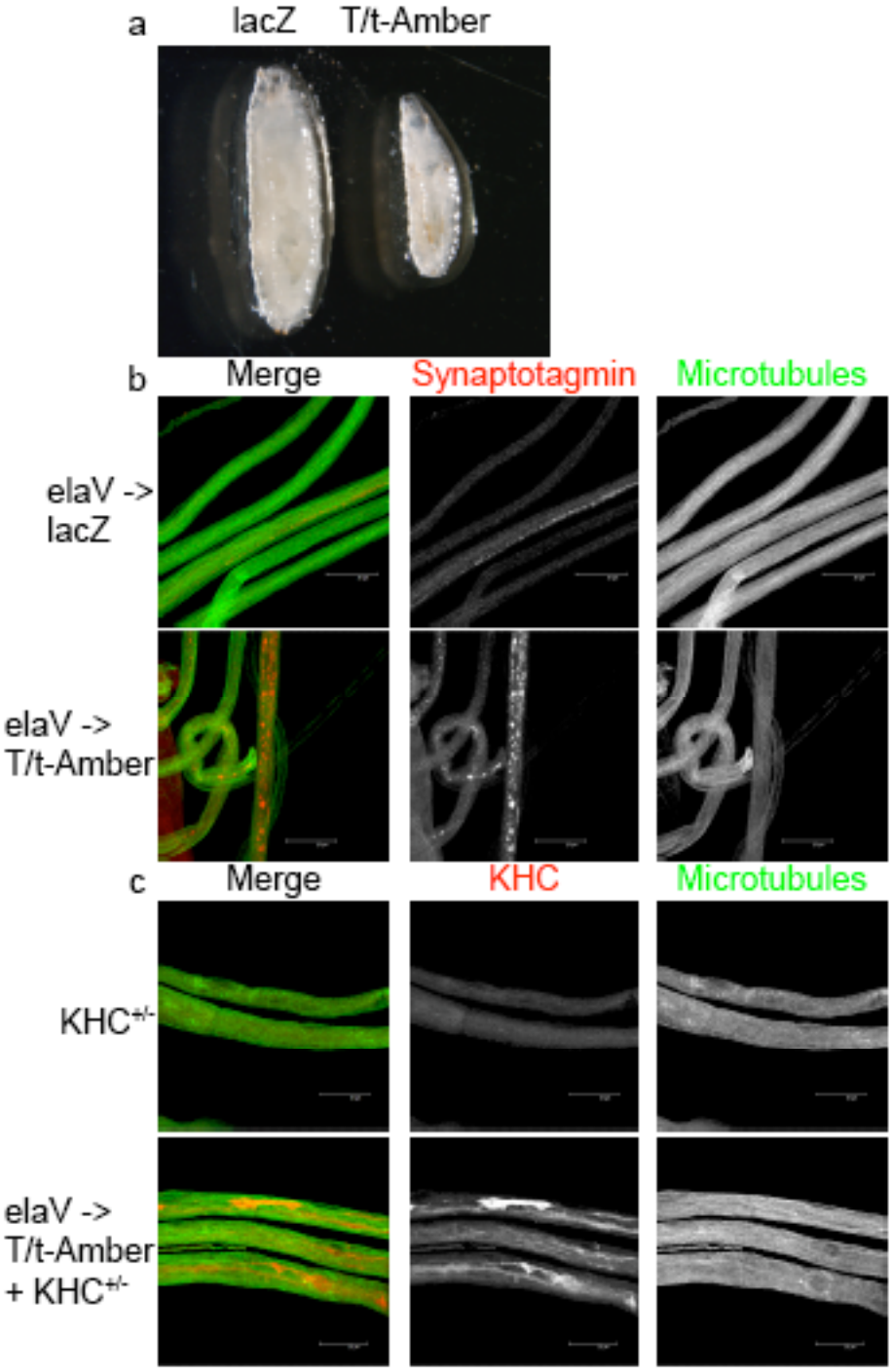
a
lacZ
T/t-Amber
b
Merge
Synaptotagmin
Microtubules
elaV -> lacZ
elaV -> T/t-Amber
c
Merge
KHC
Microtubules
KHC+/-
elaV -> T/t-Amber + KHC+/-

Figure 3-3. ST partially inactivates kinesin-1 in Drosophila larval motor neurons. (a) ElaV-Gal4 was used to drive either lacZ or T/t-Amber in the central nervous system. T/t-Amber larvae do not develop properly. Instead, they are smaller in size and have brown spots along their body, eventually turning completely brown and dying. (b) T/t-Amber larvae have focal accumulations of synaptotagmin in motor neurons as compared to lacZ larvae. LacZ larvae sometimes show background synaptotagmin staining that appears similar to focal accumulations. Larval motor neurons were stained for a-tubulin (green) and synaptotagmin (red). (c) T/t-Amber with a heterozygous kinesin heavy chain mutant show abnormal elongated accumulations of kinesin heavy chain as compared to a heterozygous kinesin heavy chain mutant. Larval motor neurons were stained for a-tubulin (green) and kinesin heavy chain (KHC) (red).

results in weak kinesin-1 misregulation in Drosophila larval motor neurons.

Kinesin-1 microtubule binding

To determine how ST inactivates kinesin-1, the microtubule binding property of kinesin-1 was assayed in Drosophila embryo extracts. Microtubules were first depolymerized with cold treatment and then repolymerized with GTP and Taxol. Microtubules polymerize when α- and β-tubulin bind GTP. When GTP is hydrolyzed to GDP, the tubulin association weakens promoting depolymerization (Desai and Mitchison 1997). Therefore, excess GTP promotes microtubule polymerization. Taxol further promotes polymerization by stabilizing microtubules (Thompson, Wilson et al. 1981; Wilson, Miller et al. 1985). Together, these two components allow the pelleting of microtubules and microtubule associated proteins, or MAPs. Kinesin heavy chain is one example of a MAP. As discussed in the introduction, kinesin-1 walks along microtubules by utilizing molecules of ATP. If AMP-PNP, a non-hydrolyzable analog of ATP, is used, kinesin-1 essentially becomes "stuck" on the microtubule. Using four conditions: 1) no GTP and no Taxol, 2) GTP and Taxol, 3) ATP, GTP, and Taxol, and 4) AMP-PNP, GTP, and Taxol, the binding of kinesin heavy chain to microtubules in the absence and presence of ST was determined (Figure 3-4). Without GTP and Taxol, microtubules do not polymerize and therefore do not pellet. In the three other conditions, microtubules efficiently pellet. In the wild type control, kinesin heavy chain binding to microtubules was not affected by the presence of ATP but is increased in the presence of AMP-PNP (Figure 3-4). When ST is expressed, kinesin heavy chain does not associate as strongly to microtubules compared to the wild type control, as demonstrated by the AMP-PNP sample (Figure 3-4). Therefore, ST disrupts kinesin-1 association with microtubules.

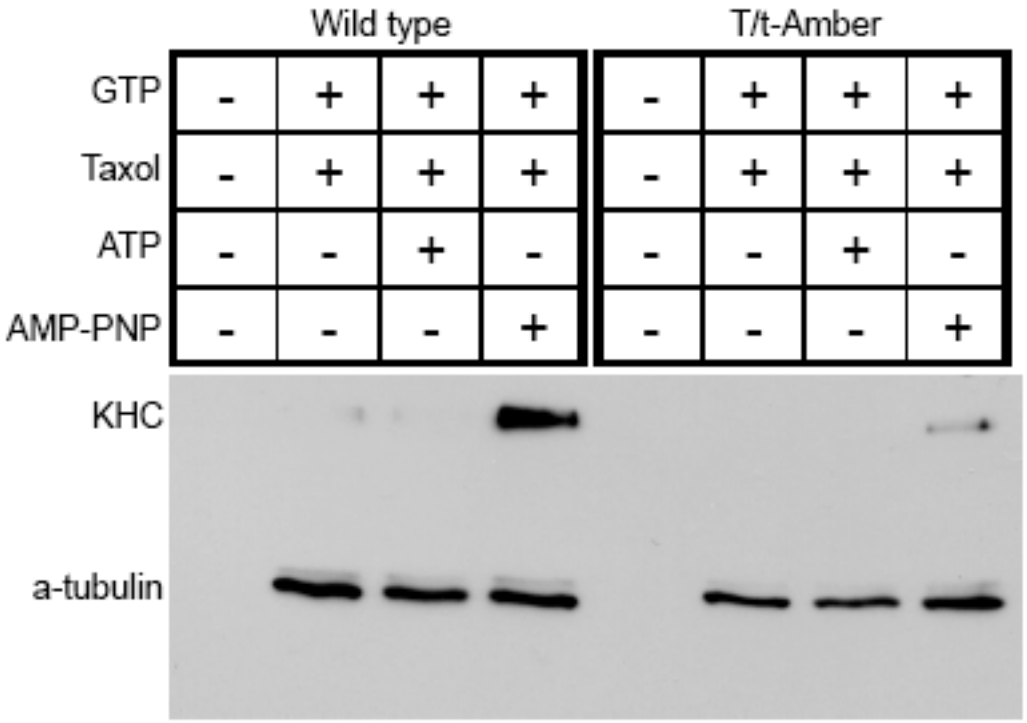

Figure 3-4. ST disrupts kinesin-1 association with microtubules. Microtubules (α-tubulin) were pelleted from wild type or T/t-Amber embryo extract and kinesin heavy chain (KHC) association with microtubules was determined by western blotting. Microtubules are pelleted with GTP and Taxol. ATP and AMP-PNP do not affect microtubule polymerization. ATP does not affect kinesin-1 association with microtubules, while AMP-PNP increases kinesin-1 association with microtubules. Note that with ST expression kinesin heavy chain weakly associates with microtubules.

C. Discussion

Using proteomics and MS analysis, we aimed to find ST interactors. This approach identified a novel binding partner for ST, the kinesin-1 motor. We further characterized the interaction between kinesin-1 and ST, however further experiments need to be performed to fully understand how and why ST inhibits kinesin-1.

A novel binding partner for ST

To identify novel ST binding partners, proteomics and MS analysis were implemented. ST-FLAG proved to be very beneficial in proteomic analysis because of the available tools used to pulldown FLAG-tagged proteins. Utilizing this method, we IP'ed ST, as well as its known binding partners, $PP2A^{A}$ and $PP2A^{C}$. We then confirmed the next highest confidence interacting partner, kinesin heavy chain. Interestingly, ST binds kinesin heavy chain independent of Hsc70 and PP2A, suggesting that the kinesin-1 motor could form an independent complex with ST. Alternatively, ST could be acting as a viral-type B subunit to target PP2A phosphatase activity towards kinesin-1. ST may bind kinesin-1 independently of PP2A, however PP2A must then also bind ST to affect kinesin-1 activity. Since most ST phenotypes are associated with the PP2A-binding domain, this hypothesis is a more likely possibility.

Both the kinesin heavy and light chains are regulated by phosphorylation, however little is known about which kinases are responsible for the modification (Hollenbeck 1993; Lee and Hollenbeck 1995). One study shows that this post-translational modification may control membrane organelle binding (Morfini, Szebenyi et al. 2002). The kinesin light chain is regulated by the kinase, glycogen synthase kinase 3,

or GSK3 (Morfini, Szebenyi et al. 2002). GSK3 activity inhibits fast anterograde axonal transport by disrupting kinesin-1 organelle binding without disrupting kinesin-1 ATPase activity or microtubule binding. Phosphatase activity most likely affects kinesin-1 regulation, however no phosphatases have been identified to dephosphorylate either the heavy or light chain (Gindhart 2006).

To determine if ST is acting as a viral-type B subunit, mutants that bind kinesin-1 but do not bind PP2A are necessary. The C103S and ΔPP2A mutants fit these criteria, however the transgenic flies constructed are tagged on the C-terminus. The ST-FLAG flies do not cause lethality with central nervous system expression at 29ºC, most likely because the tag interferes with ST activity. Therefore, the ST mutants could not answer the requirement of PP2A in causing the kinesin-1-associated phenotypes. Untagged mutant transgenic flies need to be constructed to formally test the necessity of PP2A in ST-inhibition of kinesin-1.

ST affect on kinesin-1 activity

If ST forms an independent complex with kinesin-1, then ST may manipulate kinesin-1 in one of four ways: 1) ST binds the kinesin-1 motor to disrupt kinesin-1 binding to microtubules, 2) ST binds the kinesin-1 motor to enhance kinesin-1 binding to microtubules, 3) ST acts as a cargo protein and uses the kinesin-1 motor to track along microtubules, or 4) ST binds cargo proteins bound to the kinesin-1 motor to track along microtubules.

Of these four possibilities, our results suggest that ST binds and inhibits kinesin-1 motor activity. First, ST expression resulted in focal accumulations of synaptotagmin along Drosophila larval motor neurons. Further, ST in a heterozygous kinesin heavy

chain mutant background resulted in unusual accumulations of kinesin heavy chain. However, both these accumulations are not nearly as robust as weak kinesin and cargo protein mutants, suggesting that ST is only partially or weakly inhibiting kinesin-1 activity. However, ST efficiently inhibits kinesin-1 microtubule binding in Drosophila embryo extract. The discrepancy between these results may be that when ST strongly inhibits kinesin-1, lethality occurs prior to third instar larval development. Maintaining crosses at a higher temperature increases ST expression in the central nervous system and larvae die in the first and second instar stages. Shifting up from 25°C to 29°C allows more third instar larvae to develop, however many larvae still die at earlier stages. Therefore, higher expression levels of ST may cause more focal accumulations of kinesin heavy chain and synaptotagmin in Drosophila larval motor neurons than we observed, however these levels kill larvae before the third instar stage, making it impossible to characterize kinesin-1 associated phenotypes.

The kinesin-1 heterotetramer is in an autoinhibitory state. Binding partners of the heavy and light chains can relieve this inhibition by changing the confirmation of the motor to permit microtubule binding (Horiuchi, Collins et al. 2007). For example, in mammalian cells, JIP1 and FEZ1 cooperatively bind the kinesin light chain and kinesin heavy chain, respectively, to allow kinesin-1 to bind to microtubules (Blasius, Cai et al. 2007). ST may compete for binding to kinesin-1 with FEZ1 or JIP1 or any other modifying partner for kinesin-1, thereby disrupting the interaction and inhibiting kinesin-1 from confirmationally changing to an active state. Alternatively, ST may bind kinesin in a different domain to keep kinesin-1 in an inactive state. Domain mapping experiments are necessary to determine where ST binds kinesin-1 and if this domain overlaps with

known binding partners of kinesin-1 or has a key regulatory function for kinesin-1 activity.

In this chapter, we show that ST binds and inactivates kinesin-1. Further studies need to be performed to determine the significance of this newfound property. ST may utilize PP2A to target kinesin-1 for dephosphorylation. Kinesin-1 has not been implicated as a tumor suppressor gene, however microtubule trafficking and transport are important for cellular processes, including cell signaling, chromosome and organelle movement, and cytoplasmic transport, therefore inhibiting kinesin-1 could have dire consequences, including a mode of transformation. Conversely, ST may inhibit kinesin-1 to allow SV40 survival and infection, similar to vaccinia virus, by allowing the virus to assemble and lyse at appropriate cytoplasmic locations.

D. Materials and Methods

Fly Stocks and crosses

Transgenic flies were made by standard procedures. The kinesin mutants, khc^{6} and khc^{8}, were obtained as a gift from W. Saxton and from the Bloomington Stock Center, respectively. Expression of transgenes from pUASp vectors in embryos and in larval motor neurons was achieved by crossing transgenic lines to nanos-Gal4VP16 and elaV-Gal4, respectively, which expresses GAL4VP16 in ovaries from the *nanos* promoter or Gal4 in the central nervous system from the *elaV* promoter. Larvae from the elaV-Gal4 crosses were collected after incubation at either 25˚C or 29˚C (to vary the level of expression).

Immunoprecipitation

Embryos were collected for 3 hours on apple juice/agar plates. After chorion removal with 50% bleach, embryos were washed with extraction buffer (EB; 50 mM Tris pH 8.0, 150 mM NaCl). Embryos were then homogenized in approximately two volumes of EB + 1X protease inhibitor cocktail (Sigma). The extract was centrifuged for 15 minutes at 16,000xg at 4˚C and the supernatant was transferred to a new tube. Approximately one-tenth volume of 10% NP-40 was added to the extract and the extract was centrifuged for 10 minutes as above and the supernatant again transferred to a new tube. The extracts were then snap frozen in liquid nitrogen and stored at -80°C. Upon thawing, extracts were again centrifuged for 10 minutes as above. Colcemid (10 μM) was added to embryo extracts that were then incubated with anti-FLAG agarose (Sigma) pre-equilibrated with wash buffer (WB; 50 mM Tris pH 7.4, 150 mM NaCl) for two hours at 4°C. Following centrifugation, the pellet was washed five times over the course of 1 hr with WB + 0.5% Triton X-100 at 4°C, then twice more in WB. Protein was eluted with 20 μl 2X SDS-PAGE loading dye supplemented with fresh 2-mercaptoethanol (0.4 M) for 5 minutes at 95°C. All centrifugations were 10,600xg for 5 seconds, unless otherwise indicated. The kinesin heavy chain IP was performed similarly as the FLAG IP, except 1μg of kinesin heavy chain antibody was incubated with embryo extract + 10 μM Colcemid for 1 hour at 4°C and then the antibody + extract was added to 20μl pre-equilibrated Protein A sepharose (Amersham Biosciences). The Protein A sepharose was washed and eluted as above for FLAG IP.

Proteomic Analysis

Immunoprecipitation was performed as above, except instead of eluting protein, beads were stored at 4°C. Beads were sent for nano-HPLC/MS/MS analysis at the University of Texas Southwestern Medical Center Protein Core Chemistry Facility.

Larval Motor Neuron Staining

Third instar larvae were dissected, fixed, and stained as in (Hurd and Saxton 1996).

Microtubule Sedimentation

Embryos were collected for 3 hours on apple juice/agar plates. After chorion removal with 50% bleach, embryos were washed with PEM (0.1 M Pipes pH 6.6, 5mM EGTA, 1mM $MgSO^4$). Embryos were then homogenized in approximately two volumes of PEM + 0.1 mM DTT + 1X protease inhibitor cocktail (Sigma). The extract was centrifuged for 15 minutes at 16,000xg at 4˚C and the supernatant was transferred to a new tube. The extracts were then snap frozen in liquid nitrogen and stored at -80°C. Upon thawing, extracts were kept on ice for 30 minutes and then centrifuged at 140,000xg for 30 minutes at 4˚C. Approximately one-tenth of the supernatant was set-aside for western blotting analysis. The supernatant was then kept at room temperature for 30 minutes in one of four conditions: 1) no GTP and no Taxol, 2) 0.1 mM GTP + 20 μM Taxol, 3) 0.1 mM ATP + 0.1 mM GTP + 20 μM Taxol, or 4) 0.1 mM AMP-PNP + 0.1 mM GTP + 20 μM Taxol. Extracts were then layered upon a sucrose cushion supplemented with the above conditions in a 1:1 ratio to extract and centrifuged at 80,000xg for 30 minutes at room temperature. The supernatant and pellet were separated and resuspended in 6X SDS-PAGE loading dye.

Antibodies

For immunostaining the following antibodies were used: Rabbit anti-kinesin heavy chain (Cytoskeleton) 1:500, Rabbit anti-synaptotagmin (Dsyt2, a gift from H. Bellen), 1:500, α-tubulin DM1a 1:1000 (Sigma). Secondary antibodies included Alexa 488 and 546 coupled goat antibodies used at 1:400 (Invitrogen). For western blotting the following antibodies were used: anti-ST (UT450) 1:5,000, Rabbit anti-kinesin heavy chain (Cytoskeleton) 1:2000, FLAG (M2 monoclonal from Sigma) 1:10,000, α-tubulin DM1a 1:10,000 (Sigma). HRP-conjugated anti-mouse and anti-rabbit secondary antibodies were diluted 1:20,000 (Jackson IRL, Inc). Western blots were processed with SuperSignal West Pico chemiluminescent substrate (Pierce).

Plasmid

The T/t-Amber-pTRE2 plasmid was constructed from the T/t-pTRE2 plasmid (a gift from R. Hammer). An amber stop codon, from a short linker region with the amber codon in three reading frames, was inserted into T/t (SV40 early region described in Chapter 2) using a TstI site, deleting base pairs 4525-4557 in T/t. The T/t region was then cloned into the pUASp plasmid using the KpnI 5'- and BamHI 3'-sites.

CHAPTER FOUR

SMALL TUMOR ANTIGEN GENETICALLY INTERACTS WITH CYCLIN E

A. Introduction

Progression through the cell cycle requires Cdks coupled to cyclins. One such complex is Cdk2/cycE that controls the transition from G1- to S-phase. In Drosophila, there are five different alternatively spliced transcripts of cycE that result in two cycE proteins. The long isoform of cycE is expressed throughout oogenesis, resulting in a maternal supply of the protein in early embryogenesis. The short isoform of cycE is expressed zygotically, starting at cycle 15, the first non-syncytial embryonic cycle (Richardson, O'Keefe et al. 1993). CycE is differentially regulated dependent on the cell type and mitotic cycle. In endoreduplicating cells, where after completion of mitosis there are several repeated S-phase cycles, cycE regulates its own activity to allow numerous rounds of DNA replication (Sauer, Knoblich et al. 1995). In ectopic studies performed in the Drosophila eye, zygotic and maternal cycE were shown to drive G1-arrested cells into S-phase (Richardson, O'Keefe et al. 1995). The same study demonstrated that a subset of G1-arrested cells in the developing eye did not enter S-phase with ectopic zygotic cycE expression but did so with maternal cycE (Richardson, O'Keefe et al. 1995). These results suggest that there are negative regulatory mechanisms controlling the activity and levels of zygotic cycE. Maternal cycE is a longer isoform and may contain important domains that permit it to overcome negative feedback. A lack of more studies of maternal cycE,

specifically in the early embryonic cycles, is due to defects in oogenesis in cycE mutants, resulting in sterile females (Doronkin, Djagaeva et al. 2003).

While cycE is known to regulate entry into S-phase, another function of cycE is to prevent CIN. One study showed that a T393A knockin mutation in mice results in increased cycE stability because cycE cannot be phosphorylated on a key site for E3 ligase recognition for ubiquitylation. The T393A mutant, in conjunction with a p21 mutation, a negative regulator of cycE, results in CIN (Loeb, Kostner et al. 2005). In rat embryonic fibroblasts and human breast epithelial cells, overexpressed cycE generates CIN (Spruck, Won et al. 1999). Presumably, cycE is carefully regulated and degraded after entry into S-phase to prevent any abnormal activity in later phases of the cell cycle that may result in CIN, however the mechanism by which cycE causes CIN is unknown.

The regulation of cycE is better characterized in mammalian systems, where post-translational modifications have been identified. CycE phosphorylation on a conserved TPXXS motif targets it for ubiquitylation by the Skp-Cullin-F-box (SCF) complex and subsequently regulates its turnover by the 26S proteasome. The specificity of the SCF complex is conferred through its E3 ligase, the F-box protein, which recognizes phosphorylated substrates. Human Cdc4 (hCdc4), or Drosophila archipelago (ago), is the F-box protein that targets cycE for ubiquitylation (Koepp, Schaefer et al. 2001; Moberg, Bell et al. 2001; Strohmaier, Spruck et al. 2001). Studies have shown that human cycE phosphorylation on threonine 380 and serine 384 are key sites for hCdc4 recognition (Clurman, Sheaff et al. 1996; Won and Reed 1996; Welcker, Singer et al. 2003). A more recent study found that isomerization between prolines 381 and 382 is also important for cycE recognition by the SCF complex (van Drogen, Sangfelt et al.

2006). The TPXXS motif is well conserved across species, suggesting that cycE phosphorylation and isomerization is a conserved mechanism important for its degradation.

As shown in Chapter 2, ST expression in Drosophila embryos results in increased cycE expression. In this chapter, the interaction between ST and cycE is further explored. A genetic interaction between ST and a heterozygous mutant cycE result in increased chromosome segregation defects. Overexpression of cycE in a wild type background causes many cell cycle defects, including centrosome overduplication and chromosome missegregation, while overexpression of cyclin E in an ST background causes an enhancement of ST-associated phenotypes, most notably larger and longer astral microtubules at the cortex of the embryo organized by free-floating centrosomes.

B. Results

Genetic Interaction between ST and cycE

ST expression at 29ºC results in a greater than two-fold increase in cycE protein (see Figure 2-11). However, due to the limitations in reagents for Drosophila cycE, the post-translational modification of the increased cycE is unknown. Therefore, cycE may be elevated due to increased transcription or improper post-translational regulation. To better understand the result of increased cycE expression in ST embryos, a genetic interaction between ST and cycE was tested. We hypothesized that if cycE protein is increased due to ST, then expressing a heterozygous mutant cycE in an ST background may suppress some of the ST-associated phenotypes.

To determine a genetic interaction between ST and cycE, one copy of the $cycE^{AR95}$ mutant (referred to here as $cycE^{+/-}$) was expressed in an ST embryonic background. The $cycE^{AR95}$ mutant was previously characterized and contains a stop codon at amino acid glutamine 365 in the cyclin box of the protein (Knoblich, Sauer et al. 1994). Heterozygous $cycE^{AR95}$ flies can be maintained as a stock and are healthy and viable. To test our hypothesis, we expressed the heterozygous cycE mutant in an ST background at 25ºC to lower expression of the ST transgene. ST + $cycE^{+/-}$ results in an increase of embryonic lethality from ~50% to nearly 100% (Figure 4-1a). The majority of the embryos arrest in cycles 1-3 of the syncytial embryonic cycles. Many of the embryos also exhibited only meiotic spindles or no visible meiotic products. A small percentage of embryos progressed past the syncytial divisions to cellularization and gastrulation. ST + $cycE^{+/-}$ embryos exhibit increased chromosome segregation and alignment defects (Figure 4-1b-d) but did not increase centrosome amplification (data not shown). In the ST + $cycE^{+/-}$ embryos, the chromosomes are misaligned during metaphase, lagging or prematurely separated, and scattered along the spindle, as well as chromosomes improperly localized near and around the centrosomes (Figure 4-1d). The same phenotype was also observed with another allele of cycE, $cycE^{k05007}$, a hypomorphic, homozygous lethal cycE mutant with a P-element insertion in an intron of all the cycE splice forms (data not shown). Therefore, instead of suppressing ST-associated phenotypes, the heterozygous cycE mutant enhances ST embryonic lethality and chromosome segregation and alignment defects.

Overexpression of cycE-Myc

Due to the genetic interaction between the cycE mutant and ST, we were

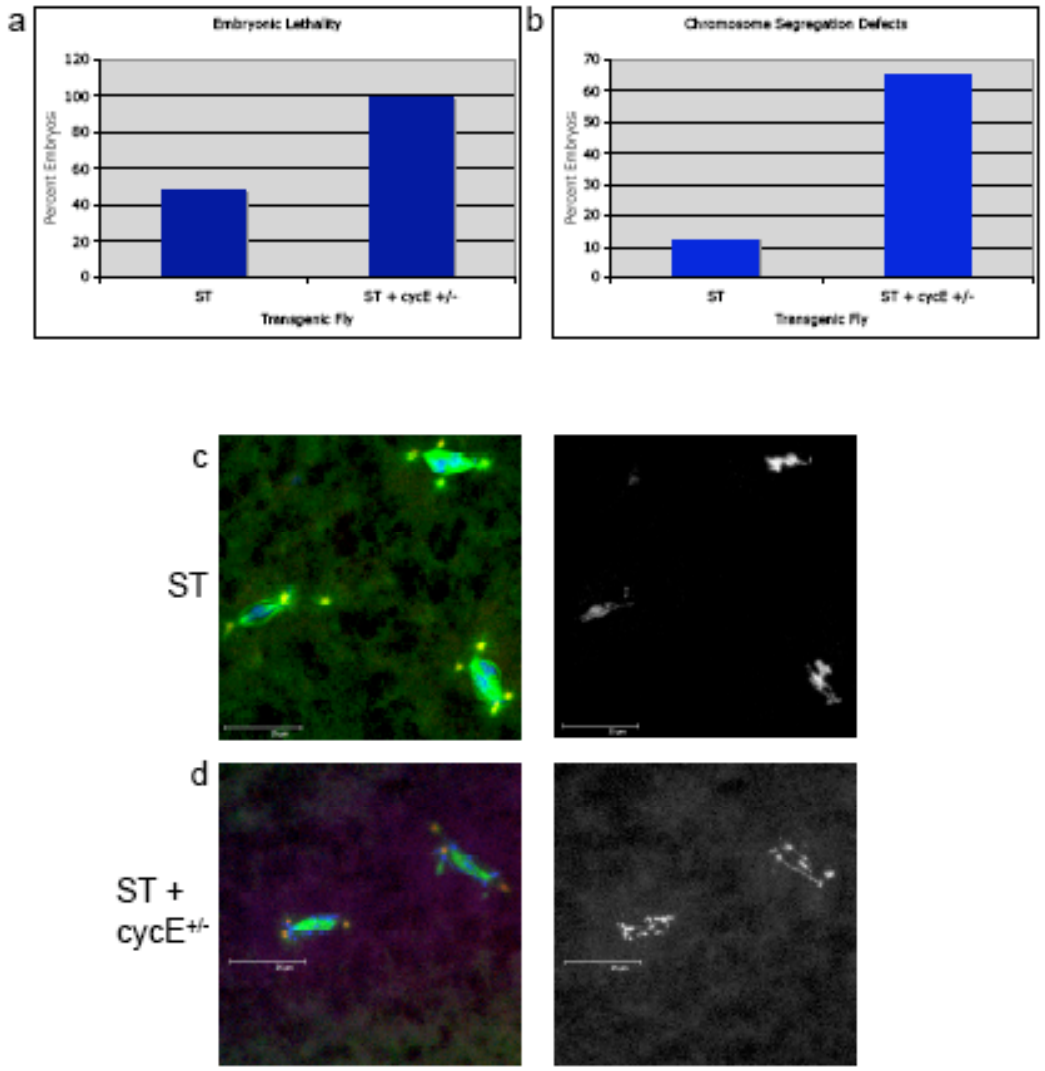

Figure 4-1. A heterozygous cycE mutant enhances ST phenotypes. Graphs depicting embryonic lethality (a) and chromosome segregation defects (b) for ST and ST + $cycE^{+/-}$ embryos at 25°C. (c) ST embryos show some chromosome segregation defects, while ST + $cycE^{+/-}$ embryos show chromosomes scattered all over the spindle, off the spindle, and near the centrosomes (d). Embryos were stained for a-tubulin (green), CNN (red), and DNA (blue).

interested in determining the consequence of overexpressing cycE in early Drosophila embryos with and without ST. To assay overexpression of cycE, we generated transgenic flies expressing maternal cycE. To generate high expression in the germline and a maternal supply of protein in the early embryo, the UASp promoter was used to express cycE (Rorth 1998). To facilitate experiments and due to the limited available antibody supply of cycE, the construct was tagged with a 6X-Myc tag on its C-terminus (hereafter referred to as cycE-Myc).

First, cycE-Myc overexpression in the early syncytial embryo was characterized. To obtain a maternal supply of cycE-Myc protein, a *nanos*-Gal4 driver was used (Van Doren, Williamson et al. 1998). At 25°C, on a small-scale test, none of the cycE trasnsgenic lines appeared to cause significant lethality. To obtain maximal expression levels, experiments were performed at 29ºC. Several lines resulted in nearly 100% embryonic lethality at this temperature. The embryos were then fixed and stained for α-tubulin to label microtubules, CNN to label centrosomes, and the Draq5 dye to label DNA to visualize mitotic divisions in the early syncytial blastoderm. Many of the embryos arrest early with only meiotic spindles. Most embryos that progress to mitotic divisions have cell cycle defects at cycles 9-11. A small percentage of embryos reach cellularization and gastrulation. CNN staining demonstrated that cycE-Myc overexpression results in centrosome amplification, reminiscent of Plk4 overexpression in the early embryo (Figure 4-2b) (Rodrigues-Martins, Riparbelli et al. 2007). CycE-Myc overexpression also results in chromosome segregation and replication defects (Figure 4-2b). Fragments of chromosomes are free-floating in the embryo with mini-microtubule spindles organized along the length of the chromosome. Finally, cycE-Myc

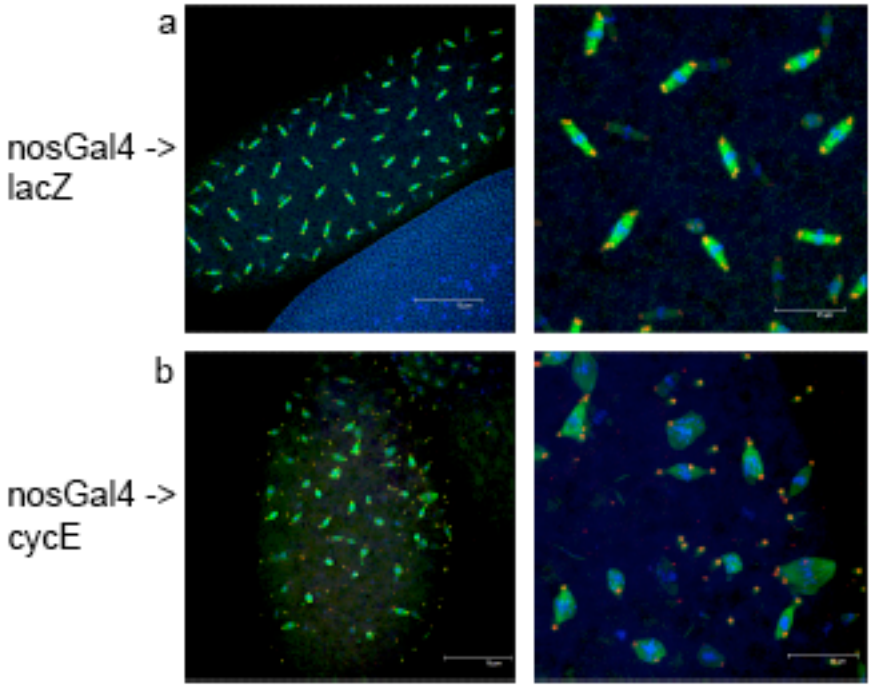

Figure 4-2. Overexpression of cycE-Myc in embryos results in cell cycle defects. (a) LacZ-expressing embryos have two centrosomes at the end of each spindle pole (due to premature centrosome duplication at 29ºC), bipolar spindles, and proper chromosome alignment. (B) Overexpressing cycE-Myc in embryos results in centrosome amplification, abnormally sized spindles, multipolar spindles, chromosome segregation and alignment defects, and free-floating centrosomes and DNA associated with microtubules. Embryos were stained for a-tubulin (green), CNN (red), and DNA (blue).

overexpression results in abnormally large and small mitotic spindles, suggesting that cycE-Myc may cause aneuploidy or CIN (Figure 4-2b). The abnormally sized spindles and chromosome segregation and alignment defects are reminiscent of previous studies that show that increased cycE result in CIN (Spruck, Won et al. 1999; Loeb, Kostner et al. 2005). However, the centrosomal result is somewhat surprising given that while in other systems cycE overexpression results in centrosome amplification, it is not quite to the extent that is observed in the early embryo, suggesting that the syncytial cycles are particularly sensitive to centrosome amplification (Hinchcliffe, Li et al. 1999; Lacey, Jackson et al. 1999; Mussman, Horn et al. 2000; Tsou and Stearns 2006).

Therefore, cycE-Myc may have different roles in centrosome duplication depending on the cell type. To determine if cycE-Myc can induce centrosome amplification in somatic tissues, cycE-Myc was overexpressed in the central nervous system, including the larval brain, as discussed in Chapter 3, using the elaV-Gal4 driver (Robinow and White 1988; Robinow and White 1991; Berger, Renner et al. 2007). Divisions in the neuroblasts, or dividing somatic cells in the third instar larval brain, are commonly used to look at centrosome fidelity because there are many mitotic divisions. Third instar larval brains overexpressing cycE-Myc were stained with α-tubulin to label microtubules, CNN to label centrosomes, and Draq5 dye to label DNA. CycE-Myc did not cause centrosome overduplication and no multipolar spindles were ever observed (Figure 4-3). Furthermore, Bld10p staining to mark centrioles gave similar results (data not shown). It is quite possible that cycE-Myc needs to be more highly expressed to induce centrosome overduplication. This critical level may not be reached because cycE-Myc was expressed from a UASp promoter instead of a UAST promoter, which is

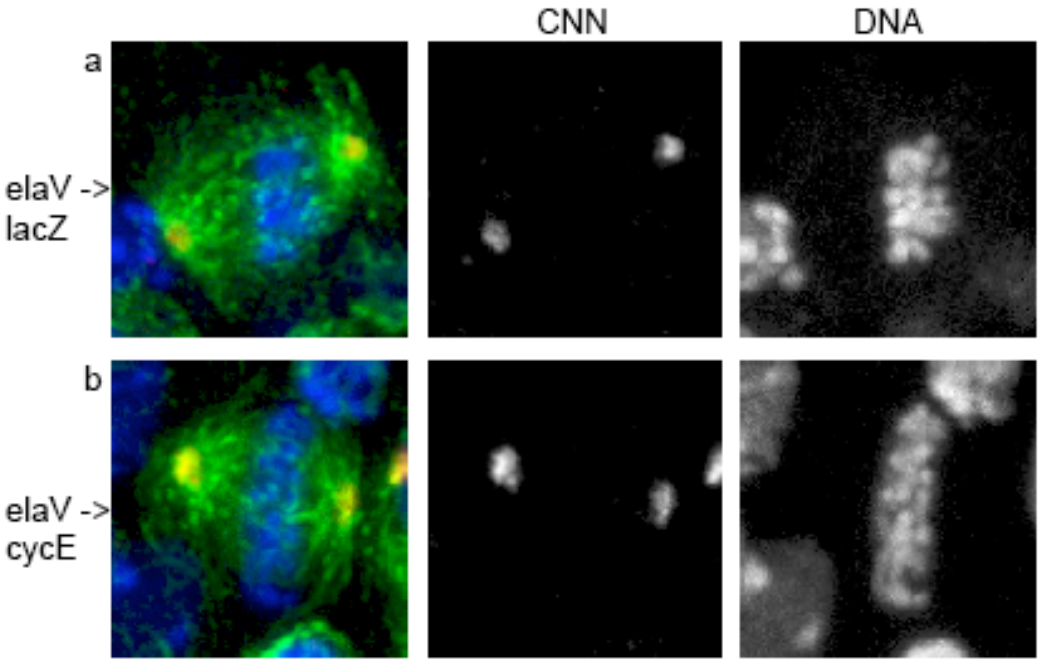

Figure 4-3. CycE-Myc does not cause centrosome amplification in neuroblasts. An elaV-Gal4 driver was used to drive expression of either lacZ (a) or cycE-Myc (b) in Drosophila neuroblasts. Both samples have bipolar spindles with one centrosome at the end of each spindle pole (CNN panel) and properly aligned chromosomes on the metaphase plate (DNA panel). Neuroblasts were stained for a-tubulin (green), CNN (red), and DNA (blue).

commonly used for somatic expression. Further supporting this notion, cycE-Myc does not seem to cause any obvious chromosome segregation defects in the neuroblast cells (Figure 4-3).

Genetic interaction between ST and overexpressed cycE-Myc

Next, we wanted to determine the phenotypes induced by cycE overexpression in an ST background. We hypothesized that if a cycE heterozygous mutant in an ST-expressing embryo enhances embryonic lethality, then overexpressing cycE may suppress ST-induced phenotypes. To further support this hypothesis, a duplication covering cycE, resulting in 3 wild type cycE copies, suppressed all ST phenotypes. However, this duplication covers many genes, therefore any one of these genes or a combination of genes covered in the duplication could be responsible for the suppression. To eliminate the uncertainty of the role of cycE in suppressing the phenotypes, we expressed the cycE-Myc transgene in an ST background.

Since ST at 29°C results in maximal expression, suppression of the phenotypes would be best tested at this temperature, and the duplication suppressed ST phenotypes at this temperature. However, at 29°C, cycE itself is lethal, thereby complicating interpretation of any results. Therefore, we chose to perform experiments at 27°C, an intermediate temperature that compromises the overexpression of cycE-Myc but still expresses high enough ST to confer ST phenotypes. At 27°C, the opposite of our hypothesis occurred, overexpressed cycE-Myc in an ST embryo enhances the phenotypes of ST.

Several ST-associated phenotypes were enhanced, including centrosome amplification, chromosome segregation and alignment defects, and increased astral

microtubule length and density (Figure 4-4 and 4-5). Embryos had increased centrosome amplification, as would be expected because cycE alone results in the same phenotype, although this occurs at the very early mitotic cycles (Figure 4-4a-c). Similar to the heterozygous cycE mutant expressed with ST, ST + cycE-Myc embryos have misaligned chromosomes on and off the mitotic spindle (Figure 4-4a,b and Figure 4-5b). A novel phenotype observed in ST + cycE-Myc embryos is CNN filaments associated with microtubules (Figure 4-4c). The nature of these filaments is unknown, as the phenotype has never been observed before for CNN. The majority of embryos arrest with only polar bodies or meiotic spindles or exhibited large asters organized by single centrosomes at the cortex of the embryo with little to no DNA, similar to phenotypes seen in PP2A A, B, and C heterozygous mutants expressed with ST (Figure 4-5a). Even more dramatic was the polymerized microtubules throughout an embryo with no meiotic or mitotic products and DNA that appeared to have uncontrollably replicated (Figure 4-5c). Overall, cycE-Myc overexpression in an ST-background enhances ST-associated phenotypes similar to heterozygous PP2A subunit mutants.

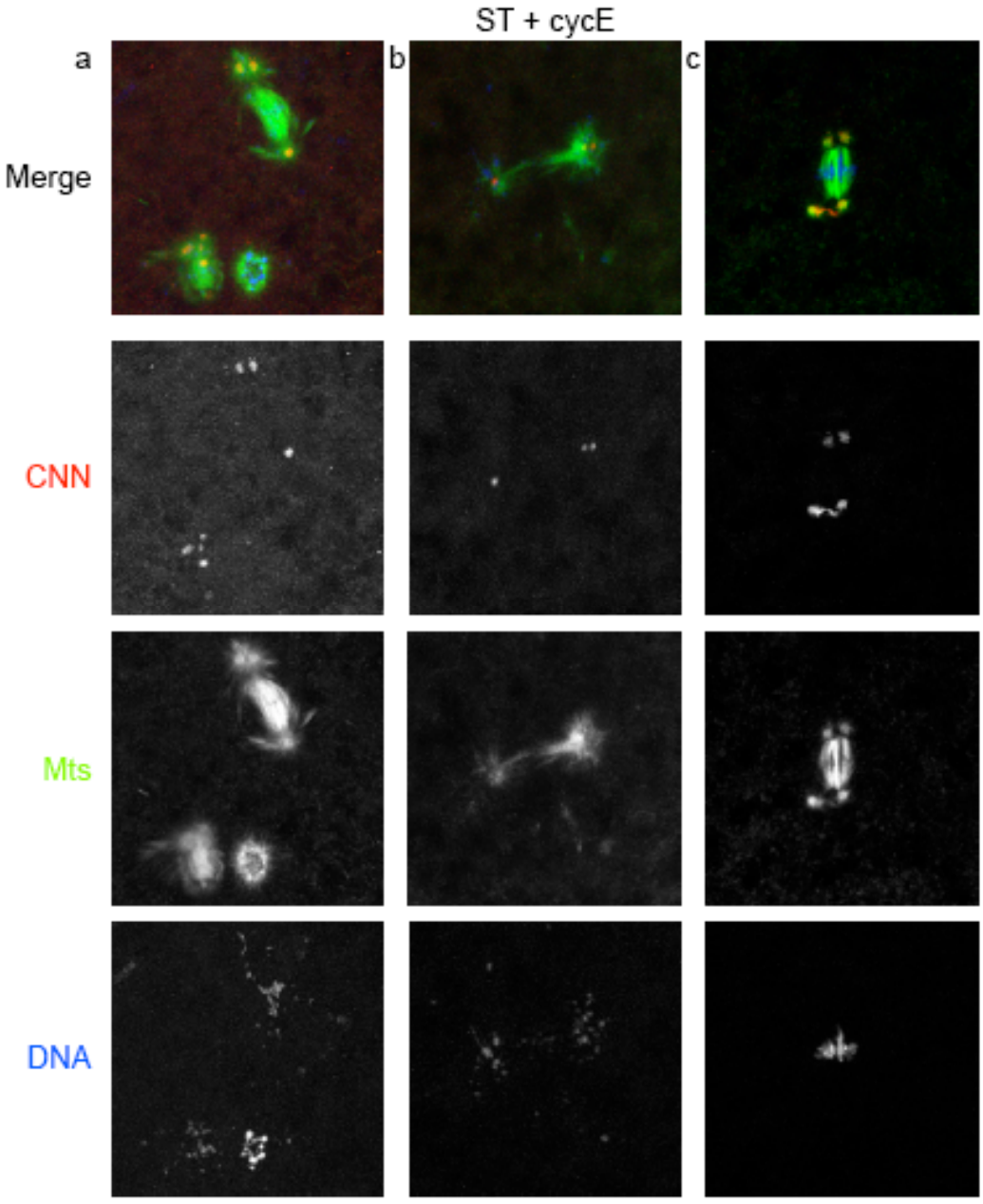

Figure 4-4. CycE-Myc overexpression in an ST background enhances ST-associated phenotypes. ST + cycE-Myc results in enhanced centrosome amplification (a-c), chromosome segregation defects (a,b), and stabilized microtubules (a,b). Note the

filamentous CNN between the two centrosomes in (c). CNN for centrosomes is stained in red, α-tubulin for microtubules (Mts) in green, and DNA in blue.

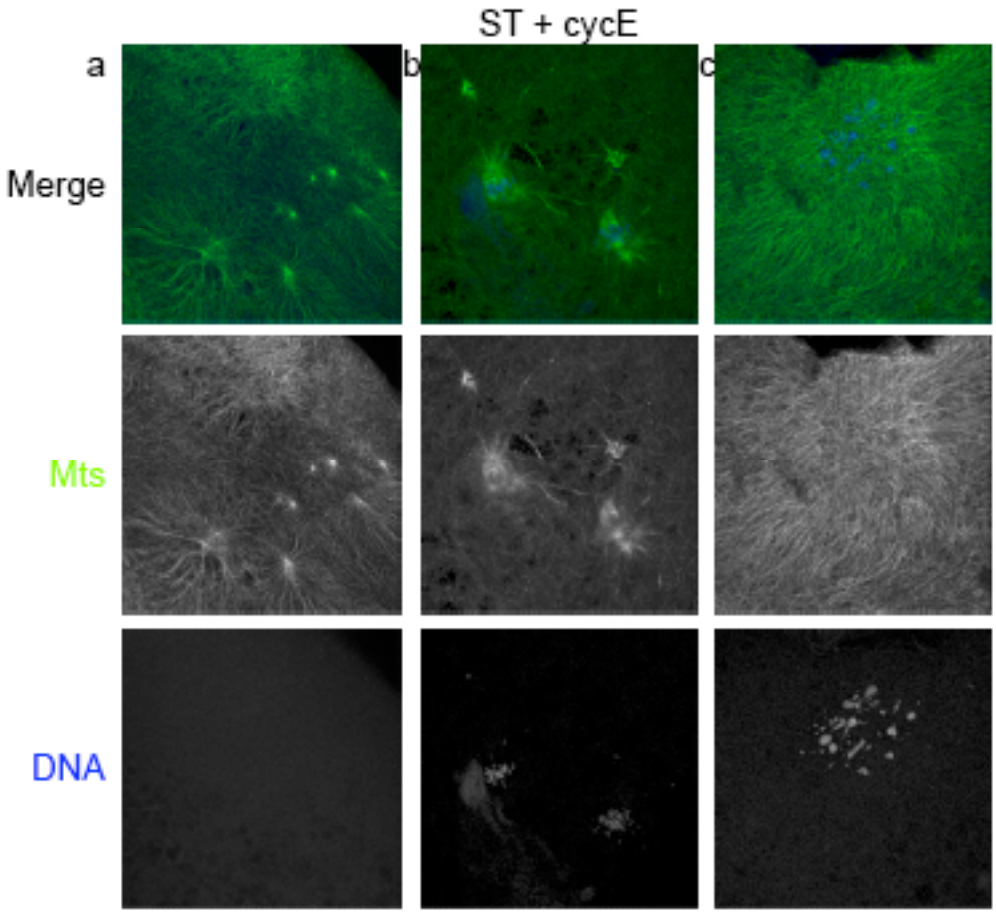

Figure 4-5. CycE-Myc overexpression in an ST background results in larger and longer astral microtubules. Embryos were hand divitellenized to preserve microtubule integrity. Embryos show large asters on the cortex of the embryo from overduplicated centrosomes with no associated DNA (a), increased microtubule asters from the spindle poles (b), and stabilized microtubules associated with endoreduplicated DNA in an embryo with no meiotic products (c). Embryos were stained for a-tubulin (mts) (green) and DNA (blue).

C. Discussion

Genetic interactions in Drosophila can place different genes in similar pathways. The strength of the genetic interaction with ST was demonstrated with PP2A subunit mutants (see Figure 2-10). Therefore, downstream components of ST/PP2A-mediated pathogenesis should give a similar genetic interaction, perhaps even enhancing specific phenotypes associated with one downstream pathway of PP2A.

ST increases cycE expression

ST increases cycE levels and this may cause some of the ST phenotypes. Increased cycE is known to generate CIN and centrosome amplification, both ST-associated phenotypes (Hinchcliffe, Li et al. 1999; Lacey, Jackson et al. 1999; Spruck, Won et al. 1999; Mussman, Horn et al. 2000; Loeb, Kostner et al. 2005; Tsou and Stearns 2006). ST + cycE-Myc further enhances phenotypes caused by ST similar to heterozygous PP2A subunit mutants, suggesting that increased cycE is one downstream mechanism of PP2A disruption. Interestingly, cycE-Myc enhanced the larger and longer astral microtubule phenotype of ST, a phenotype specifically associated with the $PP2A^{B}$ subunit. While PP2A affects cell cycle regulation, it is not known to regulate cyclin levels (Janssens and Goris 2001; Mumby 2007). $PP2A^{B}$ may target a yet unknown substrate that negatively regulates cyclin expression and activity; therefore disrupting the PP2A A-B-C complex would result in increased cycE expression and the subsequent phenotypes. To further support this hypothesis, cycE protein levels should be assayed for in ST + $PP2A^{A+/-}$, $PP2A^{B+/-}$, and $PP2A^{C+/-}$ embryos. Additionally, cycE-Myc can be expressed in a heterozygous mutant PP2A A, B, or C background to detect a genetic interaction. If the

phenotypes are similar to ST + cycE-Myc, then this would suggest that cycE is epistatic to PP2A. To determine a substrate of $PP2A^{B}$ that may be responsible for regulating cycE protein levels requires a large-scale screening approach.

ST interaction with cycE

ST also genetically interacts with mutant cycE, which is quite unexpected given the ST interaction with overexpressed cycE. These opposing results suggest that ST is interacting with cycE in two different ways. First, the heterozygous cycE mutant only enhances the chromosome segregation and alignment defects, whereas overexpressed cycE enhances all the ST-associated phenotypes. Moreover, the majority of ST + $cycE^{+/-}$ embryos arrest in the mitotic syncytial cycles 1-3, whereas most ST + cycE-Myc embryos arrest with free-floating centrosomes that nucleate large asters at the cortex without mitotic products. These different phenotypes suggest that decreasing cycE may affect cell cycle progression. Therefore, the heterozygous cycE mutant expressed in an ST background may cause an arrest in embryogenesis, which then indirectly causes chromosomal defects. However, to really explain the cause for the genetic interaction, further experiments need to be performed to determine other phenotypes caused by ST + $cycE^{+/-}$. Conversely, the increased cycE may have an abnormal gain of function phenotype when it is improperly expressed during the cell cycle. CycE may be limiting for Cdks, therefore overexpressing cycE would bind and activate excess Cdk2 or other Cdks to cause unforeseen phenotypes. To measure a possible increase in cycE activity, individual Cdks could be isolated from embryo extracts to determine phosphorylation towards known substrates, such as Histone H1 for Cdk2 (Bhattacharjee, Banks et al. 2001).

The genetic interaction between ST and cycE revealed a novel function of ST. Using Drosophila allowed us to rapidly and easily characterize the interaction both in the context of decreased and increased cycE expression. Through this approach, we identified two possibly distinct ST pathways associated with one gene. Genetic screens for enhancers and suppressors for ST should reveal other novel interactions with ST and mechanisms for ST pathogenesis.

D. Materials and Methods

Fly Stocks and crosses

Transgenic flies were made by BestGene and by standard procedures. The cycE mutants, $cycE^{AR95}$ and $cycE^{k0500}$, were obtained from the Bloomington Stock Center. Expression of transgenes from pUASp vectors in embryos was achieved by crossing transgenic lines to nos-GAL4VP16 or elaV-Gal4, which expresses GAL4VP16 in ovaries from the *nanos* promoter or Gal4 in the central nervous system from the *elaV* promoter. Females from the nos-Gal4VP16 cross were mated to wild-type males and incubated at either 25˚C or 29˚C (to vary the level of expression). Larvae from the elaV-Gal4 crosses were collected after incubation at either 25˚C or 29˚C (to vary the level of expression).

Plasmids

The maternal cycE cDNA clone was obtained from the Drosophila Genome Resource Center and was amplified by PCR and cloned into pENTR/D-TOPO. Entry clones were then recombined into a vector containing a C-terminal 6X-Myc tag (pPWM) using LR-recombination with the Gateway system (Invitrogen).

Immunofluorescent Staining

Embryos were collected on apple juice/agar plates for 3 hours. They were then fixed with methanol/heptane. For optimal astral microtubule fixation, embryos were fixed 2-3 min with 37% formaldehyde and the vitelline membrane removed by hand. Embryos were blocked in PBT (PBS + 0.1% Tween-20) + 5 mg/ml BSA for 1 hour at room temperature, incubated with primary antibodies in PBT + 5 mg/ml BSA overnight at room temperature, and incubated with secondary antibodies in PBT + 1 mg/ml BSA for two hours at room temperature. After each antibody application, embryos were rinsed twice in PBT and washed two times with PBT for twenty minutes. Embryos were left to settle onto a PBT/90% glycerol cushion overnight at 4°C prior to mounting. Third instar larval brains were dissected in PEM (100mM Pipes pH 6.9, 2mM $MgSO_4$, 1mM EDTA) and squashed with coverslips in 4 μl PEM + 1 μl 1:1 37% formaldehyde:PEM. Brains were adhered to slides in liquid nitrogen and then fixed in 100% Methanol for 10 minutes at -20°C. Brains were incubated with primary and secondary antibody in PBS + 5 mg/ml BSA + 0.1% saponin for 1 hour at room temperature. After each antibody staining, brains were washed three times for 5 minutes in PBS. Embryos and neuroblasts were imaged on a Leica SP2 confocal microscope using a 63X /NA1.4 oil immersion objective.

Embryo Hatching

Embryos were collected on apple juice/agar plates, and then lined up on fresh apple juice/agar plates. The plates were kept at room temperature for two days and were then counted under a dissecting scope to score hatching.

Antibodies

The following antibodies were used for immunofluorescence staining: Rabbit anti-centrosomin (Zhang and Megraw 2007) 1:2000, Rabbit anti-Bld10 (generated by V. Mottier) 1:1000, α-tubulin DM1a 1:1000 (Sigma), Draq5 1:1000 (Axxora). Secondary antibodies included Alexa 488 and 546 coupled goat antibodies used at 1:400 (Invitrogen).

CHAPTER FIVE

A SMALL REGION OF THE FOURTH CHROMOSOME REQUIRED FOR LOCOMOTION IN *DROSOPHILA MELANOGASTER*

A. Introduction

The Drosophila fourth chromosome is the smallest autosome, often referred to as the "dot" chromosome. The euchromatic region of the fourth chromosome contains eighty-two genes located within 1.2 megabases of sequence, a small fraction of the 116.8 megabases of euchromatin in the entire Drosophila genome (Misra, Crosby et al. 2002). Classical genetic approaches have identified essential genes on the fourth chromosome, yet the complete lack of meiotic recombination on the fourth chromosome has made mapping of these genes difficult (Bridges 1935). While tools to study genes on the fourth chromosome have been limited in the past, the complete sequence of the *Drosophila melanogaster* genome, the mapping of new transposon insertions (Bellen, Levis et al. 2004; Thibault, Singer et al. 2004), and the recent generation of large overlapping deficiencies (Podemski, Sousa-Neves et al. 2004; Sousa-Neves, Lukacsovich et al. 2005) has augmented the investigation of genes on the fourth chromosome.

Here we have generated an ~75kb deletion on the fourth chromosome, resulting in the elimination of six genes, four of which have predicted molecular functions based on homology to orthologous genes. Homozygotes develop into fertile adults, however they exhibit acute adult locomotive dysfunction. A sole contribution to this phenotype by

one of the deleted genes was eliminated by using an available transposon insertion mutant.

B. Results

The protein encoded by CG1674 was reported to have a high confidence interaction with γ-tubulin 23C (γ-tub23C), a conserved tubulin variant and a component of centrosomes, that functions in microtubule nucleation (Stearns, Evans et al. 1991; Sunkel, Gomes et al. 1995). To investigate the functional importance of this association, we knocked down CG1674 expression by RNAi in Drosophila Kc cells. CG1674 knockdown by RNAi resulted in a centrosome amplification phenotype (Figure 5-1). This result suggested that CG1674 functions in centrosome replication control, an activity also reported for γ-tubulin (Starita, Machida et al. 2004).

To examine a potential *in vivo* function of CG1674 in centrosome replication control, we took advantage of a P-element transposon insertion in the first intron of the gene, P{SUPor-P}KG00711. This allele of CG1674, $CG1674^{KG00711}$, and the Df(4)17-1 allele, discussed below, are homozygous viable and fertile and exhibit no centrosome replication or mitotic spindle assembly defects (data not shown). To generate a strong allele of CG1674, we mobilized the P-element associated with $CG1674^{KG00711}$ and screened for deletion mutations generated due to imprecise excision of the transposon. From 232 excision chromosomes isolated in this screen, most were precise excisions, but 50 were imprecise, resulting in a deletion of genomic sequences surrounding the insertion

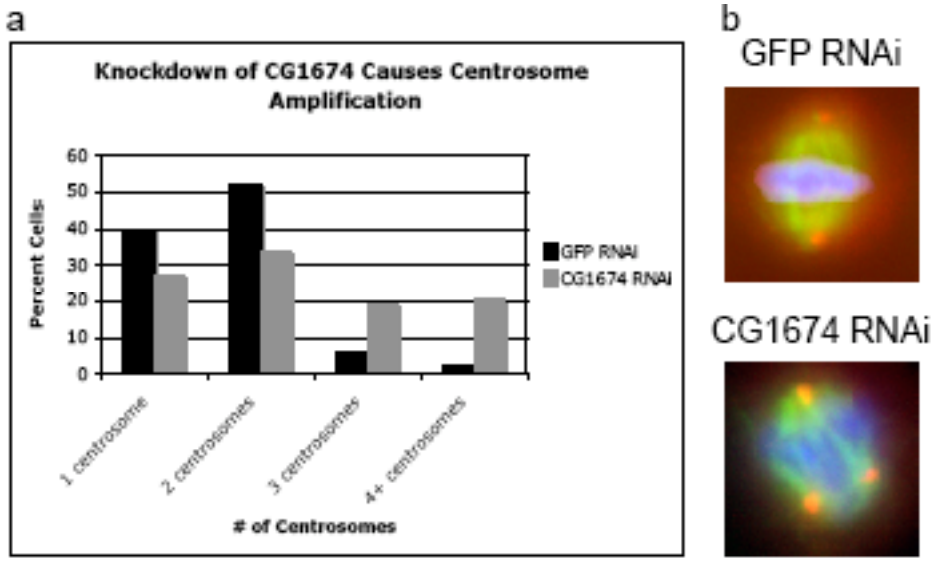

Figure 5-1. Knockdown of CG1674 results in amplified centrosomes. (a) Knockdown of CG1674 with RNAi results in an increase in the number of cells with 3 or 4+ centrosomes as compared to GFP RNAi. (b) An example of a cell treated with GFP RNAi or CG1674 RNAi. CG1674 RNAi results in cells with an abnormal number of centrosomes and a tripolar spindle. Cells are stained for γ-tubulin for centrosomes in red, α-tubulin for microtubules in green, and DNA in blue.

site of the P element. Of these, 48 were missing sequence immediately surrounding the transposon insertion site, but were small deletions that retained the start codons for *CG1674* and *yellow-h* (see Figure 5-2). We recovered only one line with a deletion that extended into the *yellow-h* gene, but the proximal extent of this deletion beyond *yellow-h* was not determined. This mutant was homozygous viable and fertile and had normal body pigmentation.

The remaining deletion produced from this screen, was an ~75 kb deletion, with its proximal breakpoint at or near the position of the original P element (mapped to a 437 bp region between the 3' end of *yellow-h* and the P element insertion site), and the distal breakpoint ~75 kb away near the 5' end of *Synaptotagmin7* (*Syt7*). We refer to this deletion hereafter as Df(4)17-1 (Fig. 5-2). *yellow-h*, the gene to the left of *CG1674*, remains intact in this mutant. At the distal end of this deletion, the *Rad23* ORF is intact (Figure 5-2b). From this analysis we mapped the distal breakpoint of Df(4)17-1 to a 2588 bp region between the 5' end of *Syt7* and the 5' end of *Rad23*. In summary, the PCR analysis showed that the breakpoints for the deletion are between 251083 bp and 251520 bp at the 5' end and between 326624 bp and 329212 bp at the 3' end (base pairs correspond to FlyBase genome annotation R5.6).

Homozygous Df(4)17-1 flies were viable and fertile and were maintained as a stock. However, homozygous Df(4)17-1 flies exhibited visible locomotion defects and a propensity to become stuck in the food substrate. Therefore, we quantified the ability of mutants to walk and fly. To test for ambulatory defect, we measured the competence of the mutant flies in the startle-induced negative geotaxis assay by measuring the percent flies that walk four centimeters in an empty vial devoid of food within thirty seconds

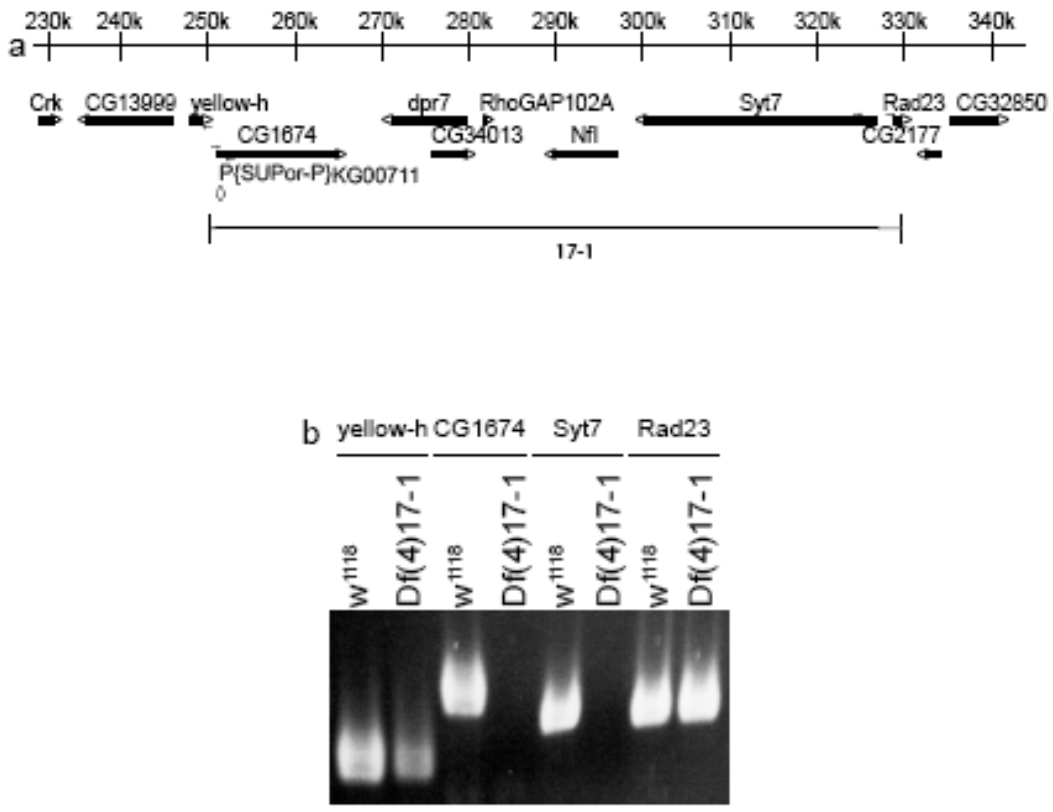

Figure 5-2. Region of fourth chromosome deleted in Df(4)17-1. (a) The region of the fourth chromosome surrounding the P-element insertion (annotated by the diamond, P{SUP-P}KG00711). The black line indicates the region that was excised in the 17-1 mutant and the gray lines indicate where the breakpoints have been mapped. The numbers in the ruler are in kilobase pairs. (b) PCR products for the indicated genes in either wild type, w^{1118}, or mutant, Df(4)17-1, flies. The yellow-h gene and part of the rad23 gene are present in the mutant, whereas CG1674 and syt7 are absent, indicating the approximate size of the excision, ~75kb. Arrows in (a) indicate the location of each primer pair for the specified gene in (b).

(Bainton, Tsai et al. 2000; Leal and Neckameyer 2002). The parental P-element insertion line had ~70% of the flies walk past the four centimeter mark, however the Df(4)17-1 had less than 3% (Fig. 5-3a). The mutant flies generally remained at the bottom of the vial or had difficulty scaling the walls of the vial. We next tested flight capabilities of the mutant flies. To execute this, flies were dumped into a 500ml graduated cylinder coated with oil (Walker and Benzer 2004). In this assay, flies fall to the bottom and stick in the oil or, if their motor skills are intact, they recover horizontal flight and stick to the sides of the graduated cylinder. In the original P-element insertion line, the majority of the flies recover flight and stick to the sides of the graduated cylinder near the top, compared to the Df(4)17-1 flies that mostly fall to the bottom of the graduated cylinder (Fig. 5-3b,c). From these data, we conclude that the mutant flies are defective in ambulatory and flight locomotion.

a

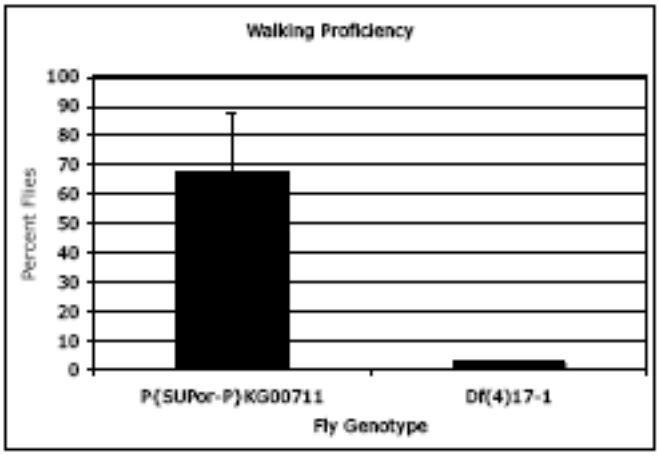
Walking Proficiency
Percent Flies
100
90
80
70
60
50
40
30
20
10
0
P{SUPor-P}KG00711
Df(4)17-1
Fly Genotype

b

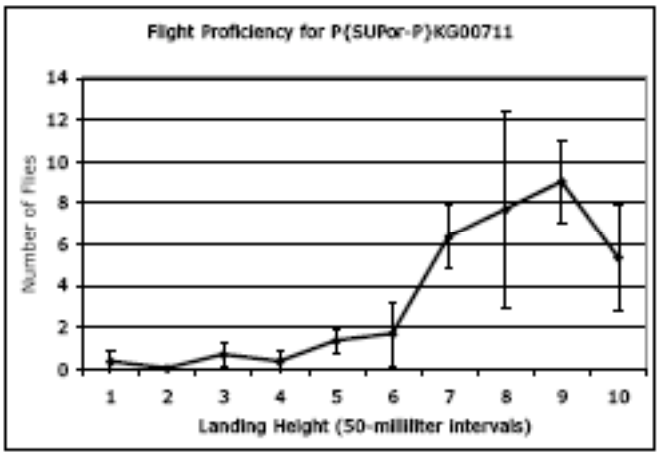
Flight Proficiency for P{SUPor-P}KG00711
Number of Flies
14
12
10
8
6
4
2
0
1
2
3
4
5
6
7
8
9
10
Landing Height (50-milliliter intervals)

c

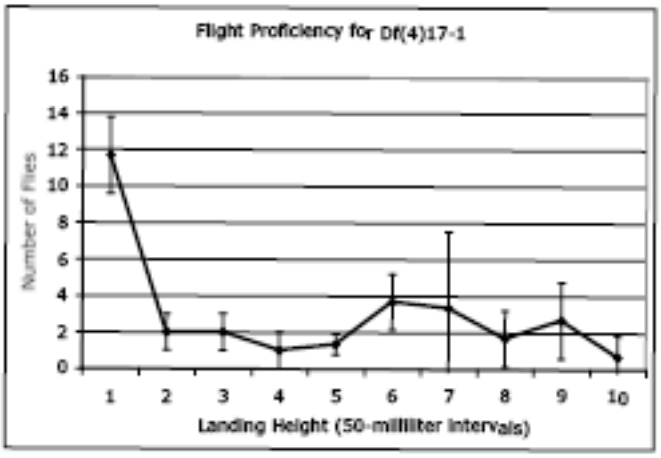
Flight Proficiency for Df(4)17-1
Number of Flies
16
14
12
10
8
6
4
2
0
1
2
3
4
5
6
7
8
9
10
Landing Height (50-milliliter intervals)

Figure 5-3. The Df(4)17-1 mutant has locomotive defects. (a) Flies were tested for walking defects by assaying their ability to walk 4 centimeters in thirty seconds in an empty vial. The original P-element insertion line has 69.7% +/- 19.7% (mean +/- standard deviation for three independent trials) flies reach the 4 centimeter mark, whereas the Df(4)17-1 mutant has 2.4% +/- 0.5% (mean +/- standard deviation for three independent trials) flies. (b,c) Flies were tested for their ability to fly by allowing them to fly in a graduated cylinder coated with oil. (b) The original P-element insertion had the majority of flies stick to the sides of the graduated cylinder near the top, indicating they flew, versus (c) the Df(4)17-1 mutant flies, which mostly fell to the bottom and stuck.

C. Discussion

In this study a small deletion of the fourth chromosome was generated, disrupting the coding sequence for six genes and possibly a seventh gene. Flies homozygous for this deletion are viable and fertile but have locomotive dysfunction. Five of these genes have been assigned a putative function, whereas two have yet unknown functions.

The six genes deleted in the mutant are CG1674, dpr7, CG34013, RhoGAP102A, NfI, and Syt7. The Rad23 coding sequence is intact in Df(4)17-1, however the expression of Rad23 could be affected given the proximity of the breakpoint to the 5' end of this gene. Complementation tests must first be performed to confirm that the missing region is in fact the cause for the ambulatory defects and not another P element mediated insertion or excision elsewhere in the genome. Overlapping deficiencies generated by another group will allow us to determine if this is the case (Sousa-Neves, Lukacsovich et al. 2005). A deficiency that begins from the CG1674 coding region and extends to the end of the fourth chromosome, Df(4)B2-7A, is expected to result in the same ambulatory problems in adult flies. Another deficiency, beginning in the Syt7 gene and extending to the end of the fourth chromosome, Df(4)B2-2D, will narrow down the region responsible for the phenotype. A deficiency that deletes the 5' region of the fourth chromosome and extends into CG1674, Df(4)M101-62f, will only give the ambulatory defects if CG1674 is solely responsible for the phenotype. Finally, a deficiency in a region of the fourth chromosome that does not overlap with Df(4)17-1, Df(4)B6-4A, should not result in the same locomotion defects.

The characterized genes have been given their nomenclature due to sequence homology to related proteins in the Drosophila genome. In the case of *dpr7*, it has homology within its Ig domains to *dpr1*, *defective proboscis extension response 1* (Nakamura, Baldwin et al. 2002). No further characterization has been reported for *dpr7*. RhoGAP102A was initially identified by its putative GAP domain. RNAi was used to knockdown expression of RhoGAP102A *in vivo*, yet no phenotypes were reported with ubiquitous or tissue-specific expression (Billuart, Winter et al. 2001). NfI, nuclear factor I, is a member of a family of site-specific DNA-binding proteins that can repress or activate transcription (Gronostajski 2000). While NfI has four orthologues in mice, there exists only one NfI gene in Drosophila with highly conserved DNA-binding domains. The NfI gene has not been characterized in Drosophila. Syt7, Synaptotagmin 7, was found to be a conserved synaptotagmin family member in Drosophila and other vertebrates (Adolfsen, Saraswati et al. 2004). Synaptotagmins are believed to function in synaptic vesicle fusion at the synapse. Syt7 is pan-neuronally expressed and also expressed in other tissues. Given its expression pattern and its predicted role in neurotransmission, we considered Syt7 as a candidate for the cause of the locomotive dysfunction in Df(4)17-1. However, Syt7 is not expressed at synapses (Adolfsen, Saraswati et al. 2004), and a transposon insertion allele of Syt7, Mi{ET1}Syt7^{MB01453}, inserted within a coding exon near the 5' end of all 6 predicted transcripts for Syt7, did not produce locomotive defects as a homozygote or in trans over Df(4)17-1. However, we did not confirm lowered or loss of Syt7 protein expression in these flies. Rad23 has not been studied *in vivo* in Drosophila. However, in other organisms, such as yeast and humans, it is a DNA-repair gene involved in nucleotide-excision repair (Madura 2004).

In addition, Rad23 has been implicated to interact with the proteasome and has been shown to regulate substrate degradation (Madura 2004). A study in Drosophila S2 cells where the proteasome was inhibited resulted in Rad23 upregulation, indicating that it may have a similar role (Lundgren, Masson et al. 2005). CG1674 and CG34013 have no function predicted from their primary sequence. From this analysis we conclude the candidate genes responsible for the locomotive dysfunction associated with Df(4)17-1 are therefore CG1674, dpr7, RhoGAP102A, CG34013, NfI, or Rad23, or a combined contribution from two or more of the genes deleted in the deficiency.

D. Materials and Methods

Generation of fourth chromosome deletions

A w^+-marked P-element, P{SUPor-P}KG00711 (Bellen, Levis et al. 2004) was mobilized with Δ2-3 transposase located on TMS, and w- progeny were selected. The resulting excision alleles were maintained over ci^D or P{ActGFP}unc-13^{GJ} to generate stocks.

PCR

The following primers were used to map the breakpoints of the deletions we generated:

Yellow-h F: 5'-CGA AAC CAT ACA CTC GAG CA-3'

Yellow-h R: 5'-TGT AAC GGA CGC AAA TAC CA-3'

CG1674 F: 5'-CAG GTA GGG AGC GTG TTC TT-3'

CG1674 R: 5'-TCC ACA CTG TCC ACA TGC TT-3'

Syt7 F: 5'-CGC TGT CAT AAA GGT TGC AG-3'

Syt7 R: 5'-TCC CCC TAA GTT CCG ATT TT-3'

Rad23 F: 5'-CAC GCG ATT CGT CTA GTT CA-3'

Rad23 R: 5'-CCG GAG GGG ATT AGA CTA GG-3'

RNAi and cytology

The culture of Drosophila Kc cells, the production of dsRNA, RNAi treatment of cells, and immunostaining of cells were preformed as described in Kao and Megraw (Kao and Megraw 2004). The following primers were used for synthesis of templates for in vitro transcription:

GFP F: 5'-TAA TAC GAC TCA CTA TAG GGA GAG CAA GGG CGA GGA GCT GT-3'

GFP R: 5'-TAA TAC GAC TCA CTA TAG GGA CCA TGT GAT CGC GCT TCT CG-3'

CG1674 F: 5'-TAA TAC GAC TCA CTA TAG GGA ACC AGC GCC TTG AAC TAG A-3'

CG1674 R: 5'-TAA TAC GAC TCA CTA TAG GGA TTC GAG TGA ATT TCG CAC TG-3'

Monoclonal antibodies to γ-tubulin (GTU-88) and α-tubulin (DM1a) were obtained from Sigma and used at a 1:1000 dilution each. DNA was stained with DAPI (Sigma) at a concentration of 1 μg/ml. Images were captured with a 63X NA1.4 objective on a Zeiss Axiophot Mot2 microscope equipped with a Coolsnap CCD camera and Metamorph imaging software.

Measurement of geotaxis

Empty vials were marked 4 centimeters from the bottom. Flies (no more than thirty) were added to the vial and the vial was tapped down to bring all the flies to the bottom of the vial. This invokes a startle response and flies respond by climbing the walls of the vial (negative geotaxis) (Bainton, Tsai et al. 2000; Leal and Neckameyer 2002). Flies that passed the 4-centimeter mark within thirty seconds were scored. The assay was repeated 3 times in 3 independent experiments.

Measurement of flight capability

This assay was performed as described by Walker and Benzer (Walker and Benzer 2004).

CHAPTER SIX

CONCLUSIONS AND FUTURE DIRECTIONS

DNA tumor viruses, such as SV40, HPV, and adenovirus, cause transformation by expressing viral oncoproteins that misregulate key cellular processes that control cell growth, cell cycle progression, and apoptosis (Saenz-Robles, Sullivan et al. 2001; Frisch and Mymryk 2002; Lavia, Mileo et al. 2003; Lupberger and Hildt 2007; Matsuoka and Jeang 2007; Wise-Draper and Wells 2008). While tumor virus proteins have been extensively studied in mammalian systems, no experimental data has been generated with lower organisms. However, other model organisms may reveal new mechanisms that tumor virus proteins use to cause tumors or allow infection. Furthermore, many proteins in the Drosophila genome are known to be well-conserved in mammals, especially those involved in basic cellular machinery, suggesting that mechanisms found in lower organisms are likely to be conserved in humans. In this regard, we used Drosophila to study ST. Drosophila offers several experimental advantages, including quick experimental implementation, availability of mutants, and well-developed genetic tools. Using Drosophila as a model system, we have discovered novel properties of ST that aids our understanding in SV40 pathogenesis. Therefore, utilizing Drosophila to study tumor virus proteins is an excellent way to determine mechanisms for oncogenesis, viral infection, and disruption of development.

Mechanisms of oncogenesis

ST, with LT, causes transformation due to disruption of PP2A, a tumor suppressor gene (Chen, Possemato et al. 2004; Arroyo and Hahn 2005). Disruption of PP2A results in oncogenesis due to key substrates no longer being dephosphorylated (Mumby 2007). Here we demonstrate that the ST PP2A-binding domain causes many cell cycle related phenotypes, thereby suggesting other mechanisms by which ST may confer transformation.

A novel phenotype associated with ST is centrosome amplification. Dating back to Boveri's theory, centrosome amplification has been implicated in tumorigenesis, however whether the phenotype is a cause or consequence of cancer has yet to be determined (Fukasawa 2007). Centrosome overduplication could cause transformation by generating multipolar spindles. Multipolar spindles result in inaccurate chromosome segregation, aneuploidy, and CIN, all common features of cancer cells (Brinkley 2001; Pihan, Purohit et al. 2001; Lingle, Barrett et al. 2002; Nigg 2002; Fukasawa 2007). Data implicating centrosome amplification as a cause of tumorigenesis comes from tumor virus proteins. E7 from HPV, E1A from human adenovirus, Tax from HTLV-1, and HBx from hepatitis B all share in common the ability to cause centrosome amplification and an increased incidence of multipolar spindles (Duensing, Lee et al. 2000; De Luca, Mangiacasale et al. 2003; Forgues, Difilippantonio et al. 2003; Yun, Cho et al. 2004; Ching, Chan et al. 2006; Wen, Golubkov et al. 2008). ST from SV40 now joins the repertoire of viral proteins that increase centrosome numbers. Therefore, centrosome amplification could be a common mechanism by which tumor virus proteins induce transformation. Further understanding of the fundamental mechanisms of centrosome

duplication could bring about a better understanding of the consequences of amplification.

Another phenotype caused by ST is CIN, a predominant cancerous cell phenotype. CIN leads to an abnormal number of chromosomes inherited into daughter cells, which could result in an increase in oncogenes or a decrease in tumor suppressor genes, resulting in cell survival and transformation (Weaver, Silk et al. 2007). The CIN phenotype may be generated due to centrosome amplification or alternatively, is caused by a separate mechanism. Arguing for CIN as an independent phenotype is that amplified centrosomes tend to cluster at the poles, suggesting that centrosome coalescence is mainly intact, and therefore multipolar spindles infrequently occur. Further, ST results in increased cycE protein levels, a phenotype known to generate CIN (Spruck, Won et al. 1999; Loeb, Kostner et al. 2005). In accordance with this phenotype, further increasing cycE levels in ST embryos generated worse chromosomal defects. ST is known to increase cyclins in mammalian systems; therefore the interaction between ST and cyclins may be conserved in higher organisms and may have similar consequences (Sauer, Knoblich et al. 1995; Porras, Bennett et al. 1996; Watanabe, Howe et al. 1996; Skoczylas, Henglein et al. 2005). Finally, when a heterozygous cycE mutant is expressed in an ST background, chromosome segregation and alignment defects increase significantly, while centrosome amplification does not, suggesting that ST generates CIN independently of centrosome amplification through a pathway involving cycE.

A possibly novel understanding of ST tumor formation is its interaction with kinesin-1. If ST acts as a viral type B-subunit and binds kinesin-1 as a substrate for PP2A, then the dephosphorylation of kinesin-1 may misregulate its activity (Hollenbeck

1993). While kinesin-1 has not been shown to be a tumor suppressor gene, inhibiting the microtubule motor could result in severe consequences. If ST misregulates kinesin-1, proteins and organelles will not be properly localized in the cytoplasm, which could lead to improper cell signaling. Once the interaction between ST and kinesin-1 is better characterized, the possible role of kinesin-1 in transformation can be resolved.

Drosophila was previously shown to be effective in causing tumors in larvae and then revealing metastasis by tumors arising in tissues different from the original site (Brumby and Richardson 2003; Brumby and Richardson 2005). To further understand how DNA tumor virus proteins induce transformation, expressing these proteins in different tissues of Drosophila with another "hit" could induce tumors and metastatic activity in larvae. Furthermore, large-scale genetic screens could be performed to reveal secondary "hits" necessary for viral oncoproteins to cause tumors. Through these experiments, the transforming capabilities of tumor virus proteins and novel tumor suppressor genes and oncogenes can be discovered.

SV40 infection

Viruses tend to hijack cellular machinery to propagate the viral genome. Once efficient viral production has taken place, the virions are released and infect neighboring cells (Greber and Way 2006). Each viral protein is produced to expand infection. Expressing these proteins in Drosophila may reveal interactions with endogenous genes that viruses utilize to confer pathogenesis.

Here, we discovered a novel binding partner for ST, kinesin-1. Given that most viruses traffic along microtubules to move around the cytoplasm of the cell, it was surprising that kinesin-1 would bind ST rather than an SV40 viral coat protein expressed

on the outer surface of the virion (Dohner, Nagel et al. 2005; Greber and Way 2006). Furthermore, ST was found to inhibit motor activity. This interaction reveals a possibly very interesting relationship between viral proteins and core cellular machinery.

Many viruses colocalize with microtubules during infection and more specifically, associate with dynein (Dohner, Nagel et al. 2005; Greber and Way 2006). Dynein directs the viral particles to the MTOC, where viruses assemble into virions for infection. In the case of vaccinia virus, after viral assembly takes place, the virus uses kinesin-1 to move to the periphery of the cell for lysis (Schepis, Stauber et al. 2007). Therefore, for efficient vaccinia virus production, the virus must first assemble a large amount of virions for infection before moving to the cell periphery. SV40 may be using a similar mechanism. ST could inhibit the kinesin-1 motor early in infection to allow viral particles to cluster at the centrosomes. After an allotted time for viral production, ST expression could be decreased or localized to the nucleus to relieve kinesin-1 inhibition and move virions to the cell membrane for lysis.

Biochemical assays conducted in these studies have revealed a property for ST that may be involved in pathogenesis. In the same regard, the novel genetic interactions shown here suggest that ST alters cell cycle progression, which may benefit SV40 infection. ST increases cycE expression and genetically interacts with cycE, suggesting that SV40 may use ST to disrupt the cell cycle. Previously, ST was also shown to induce expression of other cyclins (Sauer, Knoblich et al. 1995; Porras, Bennett et al. 1996; Watanabe, Howe et al. 1996; Skoczylas, Henglein et al. 2005). Therefore, ST may use this property to drive quiescent cells to reenter the cell cycle (Sullivan and Pipas 2002). Reentry into the cell cycle results in the expression of genes necessary for DNA synthesis

and replication, an important step in the viral life cycle. Moreover, reentry into the cell cycle results in abnormal cell proliferation and an increased amount of host cells for infection. SV40 expression of ST may be necessary for viral production by disrupting cell cycle dynamics.

Animal development

Drosophila are a great organism to study development of specific tissues due to tools that allow temporal and spatial expression of transgenes (Phelps and Brand 1998). Moreover, many tissues are dispensable for adulthood, including the eyes and wings. These properties permit the discovery of genetic interactions through large-scale genetic screens. While our studies here concentrated on the Drosophila embryo, the experiments can be repeated in other tissues to discover new genetic enhancers and suppressors for ST.

Many important genes are indispensable for development. Therefore, null mutants do not develop past the early stages of the Drosophila life cycle. By expressing viral proteins, which are known to bind global regulators of development such as p53 and Rb, different stages of development can thoroughly be studied (Frisch and Mymryk 2002; Sullivan and Pipas 2002; Wise-Draper and Wells 2008). A prime example is shown here with ST. ST is often used as a tool to study PP2A, an essential phosphatase (Pallas, Shahrik et al. 1990; Yang, Lickteig et al. 1991). With ST, the early embryonic phenotypes caused by PP2A disruption are possible to assess *in vivo*, with the only other options being RNAi and hypomorphic mutants, which often give an incomplete analysis. Furthermore, ST expression could be driven in several tissues to uncover various PP2A

roles. By utilizing a variety of viral proteins, which have multiple and different binding partners, several genes can be studied in all stages of development.

In this study, we show that ST disrupts early embryogenesis and neural development. The early embryo is a syncytial blastoderm where actin forms cages to separate mitotic spindles and the centrosome is known to be a part of this process (Sullivan, Fogarty et al. 1993; Rothwell and Sullivan 2000). By expressing ST, we further support the role of the centrosome in properly organizing actin cages and microtubule length, thus providing more evidence for PP2A involvement in early embryogenesis. By conducting genetic interactions with candidate genes of centrosomal proteins and actin-modulating proteins, as well as other cell cycle-related proteins, the mechanism by which the embryo divides its centrosomes and properly regulates actin dynamics can be determined.

To better understand the ST-kinesin-1 interaction, we looked to the developing neural system. The function of kinesin-1 in Drosophila larval motor neurons has been well characterized; therefore we utilized the same system to study the effect of ST on kinesin-1 activity (Saxton, Hicks et al. 1991; Hurd and Saxton 1996; Cavalli, Kujala et al. 2005; Horiuchi, Barkus et al. 2005; Pilling, Horiuchi et al. 2006; Horiuchi, Collins et al. 2007). In doing so, we discovered that ST causes abnormal accumulations of the kinesin heavy chain. Further characterization of this phenotype may uncover a better understanding of kinesin-1 activity and its role in neural development.

Furthermore, by shifting the ST-expressing larvae from lower temperatures to a maximal temperature, we were able to control ST expression, as well as larval development. These same experiments could be performed to both look at the effect of

PP2A inhibition at different stages of development while avoiding lethality, and with ubiquitous drivers to better understand PP2A's role in Drosophila development as a whole organism.

Finally, we discovered a genetic interaction between ST and cycE, an important regulator of the cell cycle, DNA replication, and ultimately proper development (Moroy and Geisen 2004). CycE has been well-characterized in eye development (Richardson, O'Keefe et al. 1995). Therefore, ST expression in the eye could reveal mechanisms of development, especially when determining genetic enhancers and suppressors. The interaction in the embryo revealed that ST might interact with cycE in two different pathways; repeating the genetic interaction experiments in the eye could further clarify pathways of development unforeseen in the embryo.

Here we show the efficacy of Drosophila as a model organism for studying tumor virus proteins. Viral proteins can be studied *in vivo* in Drosophila similar to the experiments performed with ST to reveal mechanisms of transformation, viral infection, and animal development.

ACKNOWLEDGMENTS

I would like to acknowledge my mentor, Timothy Megraw, for his guidance and scientific knowledge and supporting me to become an independent scientist. I would like to thank Ling-Rong Kao for generating the $PP2A^{B'}$ single and double mutants. Further, Ling was especially helpful with scientific advice and perspective on life. To the rest of the Megraw lab members, both past and present, I thank you for your assistance, kindness, and generosity. A very special thanks to Robert Hammer and Sarah Comerford, our collaborators, who have guided me through life, both scientifically and personally. They have done more for me than I could possibly ever deserve. I would like to thank the following labs for reagents and experimental advice: Helena Richardson, Estelle Sontag, Hui Zou, Stefan Heidmann, Kristen Johansen, Hugo Bellen, William Saxton, Kristen Verhey, Joe Gindhart, and Rui Sousa-Neves. Thank you to my committee, Robert Hammer, Hongtao Yu, and Hui Zou, for being so understanding. Thank you to Nicola Reading for the editing and revision of this dissertation. Thank you to Tom Wilkie for initiating the building of a sidewalk. Finally, thank you to my friends, especially past, present, and honorary roommates of 127, and family for keeping life exciting and reminding me that there are endless possibilities to explore.

BIBLIOGRAPHY

Adolfsen, B., S. Saraswati, et al. (2004). "Synaptotagmins are trafficked to distinct subcellular domains including the postsynaptic compartment." J Cell Biol 166(2): 249-60.

Ahuja, D., M. T. Saenz-Robles, et al. (2005). "SV40 large T antigen targets multiple cellular pathways to elicit cellular transformation." Oncogene 24(52): 7729-45.

Arroyo, J. D. and W. C. Hahn (2005). "Involvement of PP2A in viral and cellular transformation." Oncogene 24(52): 7746-55.

Asbury, C. L., A. N. Fehr, et al. (2003). "Kinesin moves by an asymmetric hand-over-hand mechanism." Science 302(5653): 2130-4.

Asenjo, A. B., Y. Weinberg, et al. (2006). "Nucleotide binding and hydrolysis induces a disorder-order transition in the kinesin neck-linker region." Nat Struct Mol Biol 13(7): 648-54.

Aylon, Y. and M. Oren (2007). "Living with p53, dying of p53." Cell 130(4): 597-600.

Azimzadeh, J. and M. Bornens (2007). "Structure and duplication of the centrosome." J Cell Sci 120(Pt 13): 2139-42.

Bainton, R. J., L. T. Tsai, et al. (2000). "Dopamine modulates acute responses to cocaine, nicotine and ethanol in Drosophila." Curr Biol 10(4): 187-94.

Bargonetti, J., I. Reynisdottir, et al. (1992). "Site-specific binding of wild-type p53 to cellular DNA is inhibited by SV40 T antigen and mutant p53." Genes Dev 6(10): 1886-98.

Basto, R., J. Lau, et al. (2006). "Flies without centrioles." Cell 125(7): 1375-86.

Bellen, H. J., R. W. Levis, et al. (2004). "The BDGP gene disruption project: single transposon insertions associated with 40% of Drosophila genes." Genetics 167(2): 761-81.

Berger, C., S. Renner, et al. (2007). "The commonly used marker ELAV is transiently expressed in neuroblasts and glial cells in the Drosophila embryonic CNS." Dev Dyn 236(12): 3562-8.

Bettencourt-Dias, M., A. Rodrigues-Martins, et al. (2005). "SAK/PLK4 is required for centriole duplication and flagella development." Curr Biol 15(24): 2199-207.

Bhattacharjee, R. N., G. C. Banks, et al. (2001). "Histone H1 phosphorylation by Cdk2 selectively modulates mouse mammary tumor virus transcription through chromatin remodeling." Mol Cell Biol 21(16): 5417-25.

Billuart, P., C. G. Winter, et al. (2001). "Regulating axon branch stability: the role of p190 RhoGAP in repressing a retraction signaling pathway." Cell 107(2): 195-207.

Blasius, T. L., D. Cai, et al. (2007). "Two binding partners cooperate to activate the molecular motor Kinesin-1." J Cell Biol 176(1): 11-7.

Brand, A. H. and N. Perrimon (1993). "Targeted gene expression as a means of altering cell fates and generating dominant phenotypes." Development 118(2): 401-15.

Bridges, C. B. (1935). "The mutants and linkage data of chromosome four of Drosophila melanogaster." Biol Zh 4: 401-420.

Brinkley, B. R. (2001). "Managing the centrosome numbers game: from chaos to stability in cancer cell division." Trends Cell Biol 11(1): 18-21.

Brumby, A. M. and H. E. Richardson (2003). "scribble mutants cooperate with oncogenic Ras or Notch to cause neoplastic overgrowth in Drosophila." EMBO J 22(21): 5769-79.

Brumby, A. M. and H. E. Richardson (2005). "Using Drosophila melanogaster to map human cancer pathways." Nat Rev Cancer 5(8): 626-39.

Callaini, G. and M. G. Riparbelli (1990). "Centriole and centrosome cycle in the early Drosophila embryo." J Cell Sci 97 (Pt 3): 539-43.

Cavalli, V., P. Kujala, et al. (2005). "Sunday Driver links axonal transport to damage signaling." J Cell Biol 168(5): 775-87.

Chen, F., V. Archambault, et al. (2007). "Multiple protein phosphatases are required for mitosis in Drosophila." Curr Biol 17(4): 293-303.

Chen, W., R. Possemato, et al. (2004). "Identification of specific PP2A complexes involved in human cell transformation." Cancer Cell 5(2): 127-36.

Chen, Y., Y. Xu, et al. (2007). "Structural and biochemical insights into the regulation of protein phosphatase 2A by small t antigen of SV40." Nat Struct Mol Biol 14(6): 527-34.

Ching, Y. P., S. F. Chan, et al. (2006). "The retroviral oncoprotein Tax targets the coiled-coil centrosomal protein TAX1BP2 to induce centrosome overduplication." Nat Cell Biol 8(7): 717-24.

Cho, U. S., S. Morrone, et al. (2007). "Structural basis of PP2A inhibition by small t antigen." PLoS Biol 5(8): e202.

Cho, U. S. and W. Xu (2007). "Crystal structure of a protein phosphatase 2A heterotrimeric holoenzyme." Nature 445(7123): 53-7.

Clurman, B. E., R. J. Sheaff, et al. (1996). "Turnover of cyclin E by the ubiquitin-proteasome pathway is regulated by cdk2 binding and cyclin phosphorylation." Genes Dev 10(16): 1979-90.

Comerford, S. A., D. E. Clouthier, et al. (2003). "Induction of hepatocyte proliferation and death by modulation of T-Antigen expression." Oncogene 22(16): 2515-30.

Crawford, J. M., N. Harden, et al. (1998). "Cellularization in Drosophila melanogaster is disrupted by the inhibition of rho activity and the activation of Cdc42 function." Dev Biol 204(1): 151-64.

Daniels, R., D. Sadowicz, et al. (2007). "A very late viral protein triggers the lytic release of SV40." PLoS Pathog 3(7): e98.

De Luca, A., R. Mangiacasale, et al. (2003). "E1A deregulates the centrosome cycle in a Ran GTPase-dependent manner." Cancer Res 63(6): 1430-7.

Delattre, M., S. Leidel, et al. (2004). "Centriolar SAS-5 is required for centrosome duplication in C. elegans." Nat Cell Biol 6(7): 656-64.

Desai, A. and T. J. Mitchison (1997). "Microtubule polymerization dynamics." Annu Rev Cell Dev Biol 13: 83-117.

Dohner, K., C. H. Nagel, et al. (2005). "Viral stop-and-go along microtubules: taking a ride with dynein and kinesins." Trends Microbiol 13(7): 320-7.

Doronkin, S., I. Djagaeva, et al. (2003). "The COP9 signalosome promotes degradation of Cyclin E during early Drosophila oogenesis." Dev Cell 4(5): 699-710.

Duensing, A., Y. Liu, et al. (2007). "Centriole overduplication through the concurrent formation of multiple daughter centrioles at single maternal templates." Oncogene 26(43): 6280-8.

Duensing, S., A. Duensing, et al. (2004). "Cyclin-dependent kinase inhibitor indirubin-3'-oxime selectively inhibits human papillomavirus type 16 E7-induced numerical centrosome anomalies." Oncogene 23(50): 8206-15.

Duensing, S., L. Y. Lee, et al. (2000). "The human papillomavirus type 16 E6 and E7 oncoproteins cooperate to induce mitotic defects and genomic instability by uncoupling centrosome duplication from the cell division cycle." Proc Natl Acad Sci U S A 97(18): 10002-7.

Duensing, S. and K. Munger (2003). "Human papillomavirus type 16 E7 oncoprotein can induce abnormal centrosome duplication through a mechanism independent of inactivation of retinoblastoma protein family members." J Virol 77(22): 12331-5.

Forgues, M., M. J. Difilippantonio, et al. (2003). "Involvement of Crm1 in hepatitis B virus X protein-induced aberrant centriole replication and abnormal mitotic spindles." Mol Cell Biol 23(15): 5282-92.

Frisch, S. M. and J. S. Mymryk (2002). "Adenovirus-5 E1A: paradox and paradigm." Nat Rev Mol Cell Biol 3(6): 441-52.

Frost, J. A., A. S. Alberts, et al. (1994). "Simian virus 40 small t antigen cooperates with mitogen-activated kinases to stimulate AP-1 activity." Mol Cell Biol 14(9): 6244-52.

Fujii, R., C. Zhu, et al. (2006). "HBXIP, cellular target of hepatitis B virus oncoprotein, is a regulator of centrosome dynamics and cytokinesis." Cancer Res 66(18): 9099-107.

Fukasawa, K. (2007). "Oncogenes and tumour suppressors take on centrosomes." Nat Rev Cancer 7(12): 911-24.

Gaillard, S., K. M. Fahrbach, et al. (2001). "Overexpression of simian virus 40 small-T antigen blocks centrosome function and mitotic progression in human fibroblasts." J Virol 75(20): 9799-807.

Giacinti, C. and A. Giordano (2006). "RB and cell cycle progression." Oncogene 25(38): 5220-7.

Gindhart, J. G. (2006). "Towards an understanding of kinesin-1 dependent transport pathways through the study of protein-protein interactions." Brief Funct Genomic Proteomic 5(1): 74-86.

Girardi, A. J., B. H. Sweet, et al. (1962). "Development of tumors in hamsters inoculated in the neonatal period with vacuolating virus, SV-40." Proc Soc Exp Biol Med 109: 649-60.

Goetz, F., Y. J. Tzeng, et al. (2001). "The SV40 small t-antigen prevents mammary gland differentiation and induces breast cancer formation in transgenic mice; truncated large T-antigen molecules harboring the intact p53 and pRb binding region do not have this effect." Oncogene 20(18): 2325-32.

Goodrich, D. W. (2006). "The retinoblastoma tumor-suppressor gene, the exception that proves the rule." Oncogene 25(38): 5233-43.

Greber, U. F. and M. Way (2006). "A superhighway to virus infection." Cell 124(4): 741-54.

Gronostajski, R. M. (2000). "Roles of the NFI/CTF gene family in transcription and development." Gene 249(1-2): 31-45.

Hahn, W. C., S. K. Dessain, et al. (2002). "Enumeration of the simian virus 40 early region elements necessary for human cell transformation." Mol Cell Biol 22(7): 2111-23.

Hammond, J. W., K. Griffin, et al. (2008). "Co-operative versus independent transport of different cargoes by Kinesin-1." Traffic 9(5): 725-41.

Hancock, W. O. and J. Howard (1998). "Processivity of the motor protein kinesin requires two heads." J Cell Biol 140(6): 1395-405.

Hannus, M., F. Feiguin, et al. (2002). "Planar cell polarization requires Widerborst, a B' regulatory subunit of protein phosphatase 2A." Development 129(14): 3493-503.

Hinchcliffe, E. H., C. Li, et al. (1999). "Requirement of Cdk2-cyclin E activity for repeated centrosome reproduction in Xenopus egg extracts." Science 283(5403): 851-4.

Hollenbeck, P. J. (1993). "Phosphorylation of neuronal kinesin heavy and light chains in vivo." J Neurochem 60(6): 2265-75.

Hong, S., L. C. Wang, et al. (2007). "Heptad repeats regulate protein phosphatase 2a recruitment to I-kappaB kinase gamma/NF-kappaB essential modulator and are targeted by human T-lymphotropic virus type 1 tax." J Biol Chem 282(16): 12119-26.

Horiuchi, D., R. V. Barkus, et al. (2005). "APLIP1, a kinesin binding JIP-1/JNK scaffold protein, influences the axonal transport of both vesicles and mitochondria in Drosophila." Curr Biol 15(23): 2137-41.

Horiuchi, D., C. A. Collins, et al. (2007). "Control of a kinesin-cargo linkage mechanism by JNK pathway kinases." Curr Biol 17(15): 1313-7.

Horn, V., J. Thelu, et al. (2007). "Functional interaction of Aurora-A and PP2A during mitosis." Mol Biol Cell 18(4): 1233-41.

Hurd, D. D. and W. M. Saxton (1996). "Kinesin mutations cause motor neuron disease phenotypes by disrupting fast axonal transport in Drosophila." Genetics 144(3): 1075-85.

Janssens, V. and J. Goris (2001). "Protein phosphatase 2A: a highly regulated family of serine/threonine phosphatases implicated in cell growth and signalling." Biochem J 353(Pt 3): 417-39.

Jiang, D., A. Srinivasan, et al. (1993). "SV40 T antigen abrogates p53-mediated transcriptional activity." Oncogene 8(10): 2805-12.

Kao, L. R. and T. L. Megraw (2004). "RNAi in cultured Drosophila cells." Methods Mol Biol 247: 443-57.

Kelkar, N., C. L. Standen, et al. (2005). "Role of the JIP4 scaffold protein in the regulation of mitogen-activated protein kinase signaling pathways." Mol Cell Biol 25(7): 2733-43.

Kemp, C. A., K. R. Kopish, et al. (2004). "Centrosome maturation and duplication in C. elegans require the coiled-coil protein SPD-2." Dev Cell 6(4): 511-23.

Kirkham, M., T. Muller-Reichert, et al. (2003). "SAS-4 is a C. elegans centriolar protein that controls centrosome size." Cell 112(4): 575-87.

Kleylein-Sohn, J., J. Westendorf, et al. (2007). "Plk4-induced centriole biogenesis in human cells." Dev Cell 13(2): 190-202.

Klueg, K. M., D. Alvarado, et al. (2002). "Creation of a GAL4/UAS-coupled inducible gene expression system for use in Drosophila cultured cell lines." Genesis 34(1-2): 119-22.

Knoblich, J. A., K. Sauer, et al. (1994). "Cyclin E controls S phase progression and its down-regulation during Drosophila embryogenesis is required for the arrest of cell proliferation." Cell 77(1): 107-20.

Koepp, D. M., L. K. Schaefer, et al. (2001). "Phosphorylation-dependent ubiquitination of cyclin E by the SCFFbw7 ubiquitin ligase." Science 294(5540): 173-7.

Lacey, K. R., P. K. Jackson, et al. (1999). "Cyclin-dependent kinase control of centrosome duplication." Proc Natl Acad Sci U S A 96(6): 2817-22.

Lane, D. P. and L. V. Crawford (1980). "The complex between simian virus 40 T antigen and a specific host protein." Proc R Soc Lond B Biol Sci 210(1180): 451-63.

Lavia, P., A. M. Mileo, et al. (2003). "Emerging roles of DNA tumor viruses in cell proliferation: new insights into genomic instability." Oncogene 22(42): 6508-16.

Leal, S. M. and W. S. Neckameyer (2002). "Pharmacological evidence for GABAergic regulation of specific behaviors in Drosophila melanogaster." J Neurobiol 50(3): 245-61.

Lee, K. D. and P. J. Hollenbeck (1995). "Phosphorylation of kinesin in vivo correlates with organelle association and neurite outgrowth." J Biol Chem 270(10): 5600-5.

Leidel, S., M. Delattre, et al. (2005). "SAS-6 defines a protein family required for centrosome duplication in C. elegans and in human cells." Nat Cell Biol 7(2): 115-25.

Leidel, S. and P. Gonczy (2003). "SAS-4 is essential for centrosome duplication in C elegans and is recruited to daughter centrioles once per cell cycle." Dev Cell 4(3): 431-9.

Liao, Y. and M. C. Hung (2004). "A new role of protein phosphatase 2a in adenoviral E1A protein-mediated sensitization to anticancer drug-induced apoptosis in human breast cancer cells." Cancer Res 64(17): 5938-42.

Lingle, W. L., S. L. Barrett, et al. (2002). "Centrosome amplification drives chromosomal instability in breast tumor development." Proc Natl Acad Sci U S A 99(4): 1978-83.

Linzer, D. I. and A. J. Levine (1979). "Characterization of a 54K dalton cellular SV40 tumor antigen present in SV40-transformed cells and uninfected embryonal carcinoma cells." Cell 17(1): 43-52.

Loeb, K. R., H. Kostner, et al. (2005). "A mouse model for cyclin E-dependent genetic instability and tumorigenesis." Cancer Cell 8(1): 35-47.

Lundgren, J., P. Masson, et al. (2005). "Identification and characterization of a Drosophila proteasome regulatory network." Mol Cell Biol 25(11): 4662-75.

Lupberger, J. and E. Hildt (2007). "Hepatitis B virus-induced oncogenesis." World J Gastroenterol 13(1): 74-81.

Madura, K. (2004). "Rad23 and Rpn10: perennial wallflowers join the melee." Trends Biochem Sci 29(12): 637-40.

Mateer, S. C., S. A. Fedorov, et al. (1998). "Identification of structural elements involved in the interaction of simian virus 40 small tumor antigen with protein phosphatase 2A." J Biol Chem 273(52): 35339-46.

Matsuoka, M. and K. T. Jeang (2007). "Human T-cell leukaemia virus type 1 (HTLV-1) infectivity and cellular transformation." Nat Rev Cancer 7(4): 270-80.

Mayer-Jaekel, R. E., H. Ohkura, et al. (1993). "The 55 kd regulatory subunit of Drosophila protein phosphatase 2A is required for anaphase." Cell 72(4): 621-33.

McCormick, F. and E. Harlow (1980). "Association of a murine 53,000-dalton phosphoprotein with simian virus 40 large-T antigen in transformed cells." J Virol 34(1): 213-24.

Misra, S., M. A. Crosby, et al. (2002). "Annotation of the Drosophila melanogaster euchromatic genome: a systematic review." Genome Biol 3(12): RESEARCH0083.

Moberg, K. H., D. W. Bell, et al. (2001). "Archipelago regulates Cyclin E levels in Drosophila and is mutated in human cancer cell lines." Nature 413(6853): 311-6.

Morfini, G., G. Szebenyi, et al. (2002). "Glycogen synthase kinase 3 phosphorylates kinesin light chains and negatively regulates kinesin-based motility." EMBO J 21(3): 281-93.

Moroy, T. and C. Geisen (2004). "Cyclin E." Int J Biochem Cell Biol 36(8): 1424-39.

Mumby, M. (2007). "PP2A: unveiling a reluctant tumor suppressor." Cell 130(1): 21-4.

Mungre, S., K. Enderle, et al. (1994). "Mutations which affect the inhibition of protein phosphatase 2A by simian virus 40 small-t antigen in vitro decrease viral transformation." J Virol 68(3): 1675-81.

Mussman, J. G., H. F. Horn, et al. (2000). "Synergistic induction of centrosome hyperamplification by loss of p53 and cyclin E overexpression." Oncogene 19(13): 1635-46.

Nakamura, M., D. Baldwin, et al. (2002). "Defective proboscis extension response (DPR), a member of the Ig superfamily required for the gustatory response to salt." J Neurosci 22(9): 3463-72.

Nigg, E. A. (2002). "Centrosome aberrations: cause or consequence of cancer progression?" Nat Rev Cancer 2(11): 815-25.

Nigg, E. A. (2006). "Cell biology: a licence for duplication." Nature 442(7105): 874-5.

Nigg, E. A. (2007). "Centrosome duplication: of rules and licenses." Trends Cell Biol 17(5): 215-21.

Nitta, T., M. Kanai, et al. (2006). "Centrosome amplification in adult T-cell leukemia and human T-cell leukemia virus type 1 Tax-induced human T cells." Cancer Sci 97(9): 836-41.

Nunbhakdi-Craig, V., L. Craig, et al. (2003). "Simian virus 40 small tumor antigen induces deregulation of the actin cytoskeleton and tight junctions in kidney epithelial cells." J Virol 77(5): 2807-18.

O'Connell, K. F., C. Caron, et al. (2001). "The C. elegans zyg-1 gene encodes a regulator of centrosome duplication with distinct maternal and paternal roles in the embryo." Cell 105(4): 547-58.

Pagliarini, R. A. and T. Xu (2003). "A genetic screen in Drosophila for metastatic behavior." Science 302(5648): 1227-31.

Pallas, D. C., L. K. Shahrik, et al. (1990). "Polyoma small and middle T antigens and SV40 small t antigen form stable complexes with protein phosphatase 2A." Cell 60(1): 167-76.

Peel, N., N. R. Stevens, et al. (2007). "Overexpressing centriole-replication proteins in vivo induces centriole overduplication and de novo formation." Curr Biol 17(10): 834-43.

Pelletier, L., N. Ozlu, et al. (2004). "The Caenorhabditis elegans centrosomal protein SPD-2 is required for both pericentriolar material recruitment and centriole duplication." Curr Biol 14(10): 863-73.

Phelps, C. B. and A. H. Brand (1998). "Ectopic gene expression in Drosophila using GAL4 system." Methods 14(4): 367-79.

Pihan, G. A., A. Purohit, et al. (2001). "Centrosome defects can account for cellular and genetic changes that characterize prostate cancer progression." Cancer Res 61(5): 2212-9.

Pilling, A. D., D. Horiuchi, et al. (2006). "Kinesin-1 and Dynein are the primary motors for fast transport of mitochondria in Drosophila motor axons." Mol Biol Cell 17(4): 2057-68.

Pim, D., P. Massimi, et al. (2005). "Activation of the protein kinase B pathway by the HPV-16 E7 oncoprotein occurs through a mechanism involving interaction with PP2A." Oncogene 24(53): 7830-8.

Podemski, L., R. Sousa-Neves, et al. (2004). "Molecular mapping of deletion breakpoints on chromosome 4 of Drosophila melanogaster." Chromosoma 112(8): 381-8.

Porras, A., J. Bennett, et al. (1996). "A novel simian virus 40 early-region domain mediates transactivation of the cyclin A promoter by small-t antigen and is required for transformation in small-t antigen-dependent assays." J Virol 70(10): 6902-8.

Poulin, D. L. and J. A. DeCaprio (2006). "Is there a role for SV40 in human cancer?" J Clin Oncol 24(26): 4356-65.

Raff, J. W. and D. M. Glover (1989). "Centrosomes, and not nuclei, initiate pole cell formation in Drosophila embryos." Cell 57(4): 611-9.

Rajagopalan, H. and C. Lengauer (2004). "Aneuploidy and cancer." Nature 432(7015): 338-41.

Reed, S. I. (1997). "Control of the G1/S transition." Cancer Surv 29: 7-23.

Richardson, H., L. V. O'Keefe, et al. (1995). "Ectopic cyclin E expression induces premature entry into S phase and disrupts pattern formation in the Drosophila eye imaginal disc." Development 121(10): 3371-9.

Richardson, H. E., L. V. O'Keefe, et al. (1993). "A Drosophila G1-specific cyclin E homolog exhibits different modes of expression during embryogenesis." Development 119(3): 673-90.

Robinow, S. and K. White (1988). "The locus elav of Drosophila melanogaster is expressed in neurons at all developmental stages." Dev Biol 126(2): 294-303.

Robinow, S. and K. White (1991). "Characterization and spatial distribution of the ELAV protein during Drosophila melanogaster development." J Neurobiol 22(5): 443-61.

Rodrigues-Martins, A., M. Riparbelli, et al. (2007). "Revisiting the role of the mother centriole in centriole biogenesis." Science 316(5827): 1046-50.

Rorth, P. (1998). "Gal4 in the Drosophila female germline." Mech Dev 78(1-2): 113-8.

Rothwell, W. F. and W. Sullivan (2000). "The centrosome in early Drosophila embryogenesis." Curr Top Dev Biol 49: 409-47.

Saenz-Robles, M. T., C. S. Sullivan, et al. (2001). "Transforming functions of Simian Virus 40." Oncogene 20(54): 7899-907.

Sager, R., K. Tanaka, et al. (1983). "Resistance of human cells to tumorigenesis induced by cloned transforming genes." Proc Natl Acad Sci U S A 80(24): 7601-5.

Sauer, K., J. A. Knoblich, et al. (1995). "Distinct modes of cyclin E/cdc2c kinase regulation and S-phase control in mitotic and endoreduplication cycles of Drosophila embryogenesis." Genes Dev 9(11): 1327-39.

Saxton, W. M., J. Hicks, et al. (1991). "Kinesin heavy chain is essential for viability and neuromuscular functions in Drosophila, but mutants show no defects in mitosis." Cell 64(6): 1093-102.

Schepis, A., T. Stauber, et al. (2007). "Kinesin-1 plays multiple roles during the vaccinia virus life cycle." Cell Microbiol 9(8): 1960-73.

Schlaitz, A. L., M. Srayko, et al. (2007). "The C. elegans RSA complex localizes protein phosphatase 2A to centrosomes and regulates mitotic spindle assembly." Cell 128(1): 115-27.

Schuchner, S. and E. Wintersberger (1999). "Binding of polyomavirus small T antigen to protein phosphatase 2A is required for elimination of p27 and support of S-phase induction in concert with large T antigen." J Virol 73(11): 9266-73.

Schuh, M., C. F. Lehner, et al. (2007). "Incorporation of Drosophila CID/CENP-A and CENP-C into centromeres during early embryonic anaphase." Curr Biol 17(3): 237-43.

Skoczylas, C., K. M. Fahrbach, et al. (2004). "Cellular targets of the SV40 small-t antigen in human cell transformation." Cell Cycle 3(5): 606-10.

Skoczylas, C., B. Henglein, et al. (2005). "PP2A-dependent transactivation of the cyclin A promoter by SV40 ST is mediated by a cell cycle-regulated E2F site." Virology 332(2): 596-601.

Sluder, G. and J. J. Nordberg (2004). "The good, the bad and the ugly: the practical consequences of centrosome amplification." Curr Opin Cell Biol 16(1): 49-54.

Snaith, H. A., C. G. Armstrong, et al. (1996). "Deficiency of protein phosphatase 2A uncouples the nuclear and centrosome cycles and prevents attachment of

microtubules to the kinetochore in Drosophila microtubule star (mts) embryos." J Cell Sci 109 (Pt 13): 3001-12.

Sontag, E. (2001). "Protein phosphatase 2A: the Trojan Horse of cellular signaling." Cell Signal 13(1): 7-16.

Sontag, E., S. Fedorov, et al. (1993). "The interaction of SV40 small tumor antigen with protein phosphatase 2A stimulates the map kinase pathway and induces cell proliferation." Cell 75(5): 887-97.

Sontag, E., V. Nunbhakdi-Craig, et al. (1995). "A novel pool of protein phosphatase 2A is associated with microtubules and is regulated during the cell cycle." J Cell Biol 128(6): 1131-44.

Sontag, J. M. and E. Sontag (2006). "Regulation of cell adhesion by PP2A and SV40 small tumor antigen: an important link to cell transformation." Cell Mol Life Sci 63(24): 2979-91.

Sousa-Neves, R., T. Lukacsovich, et al. (2005). "High-resolution mapping of the Drosophila fourth chromosome using site-directed terminal deficiencies." Genetics 170(1): 127-38.

Spruck, C. H., K. A. Won, et al. (1999). "Deregulated cyclin E induces chromosome instability." Nature 401(6750): 297-300.

Starita, L. M., Y. Machida, et al. (2004). "BRCA1-dependent ubiquitination of gamma-tubulin regulates centrosome number." Mol Cell Biol 24(19): 8457-66.

Stearns, T., L. Evans, et al. (1991). "Gamma-tubulin is a highly conserved component of the centrosome." Cell 65(5): 825-36.

Strohmaier, H., C. H. Spruck, et al. (2001). "Human F-box protein hCdc4 targets cyclin E for proteolysis and is mutated in a breast cancer cell line." Nature 413(6853): 316-22.

Sullivan, C. S., P. Cantalupo, et al. (2000). "The molecular chaperone activity of simian virus 40 large T antigen is required to disrupt Rb-E2F family complexes by an ATP-dependent mechanism." Mol Cell Biol 20(17): 6233-43.

Sullivan, C. S. and J. M. Pipas (2002). "T antigens of simian virus 40: molecular chaperones for viral replication and tumorigenesis." Microbiol Mol Biol Rev 66(2): 179-202.

Sullivan, W., P. Fogarty, et al. (1993). "Mutations affecting the cytoskeletal organization of syncytial Drosophila embryos." Development 118(4): 1245-54.

Sunkel, C. E., R. Gomes, et al. (1995). "Gamma-tubulin is required for the structure and function of the microtubule organizing centre in Drosophila neuroblasts." EMBO J 14(1): 28-36.

Sweet, B. H. and M. R. Hilleman (1960). "The vacuolating virus, S.V. 40." Proc Soc Exp Biol Med 105: 420-7.

Thibault, S. T., M. A. Singer, et al. (2004). "A complementary transposon tool kit for Drosophila melanogaster using P and piggyBac." Nat Genet 36(3): 283-7.

Thimmappaya, B., V. B. Reddy, et al. (1978). "The structure of genes, intergenic sequences, and mRNA from SV40 virus." Cold Spring Harb Symp Quant Biol 42 Pt 1: 449-56.

Thompson, W. C., L. Wilson, et al. (1981). "Taxol induces microtubule assembly at low temperature." Cell Motil 1(4): 445-54.

Tournebize, R., S. S. Andersen, et al. (1997). "Distinct roles of PP1 and PP2A-like phosphatases in control of microtubule dynamics during mitosis." Embo J 16(18): 5537-49.

Tsou, M. F. and T. Stearns (2006). "Controlling centrosome number: licenses and blocks." Curr Opin Cell Biol 18(1): 74-8.

Tsou, M. F. and T. Stearns (2006). "Mechanism limiting centrosome duplication to once per cell cycle." Nature 442(7105): 947-51.

Van Doren, M., A. L. Williamson, et al. (1998). "Regulation of zygotic gene expression in Drosophila primordial germ cells." Curr Biol 8(4): 243-6.

van Drogen, F., O. Sangfelt, et al. (2006). "Ubiquitylation of cyclin E requires the sequential function of SCF complexes containing distinct hCdc4 isoforms." Mol Cell 23(1): 37-48.

Viquez, N. M., C. R. Li, et al. (2006). "The B' protein phosphatase 2A regulatory subunit well-rounded regulates synaptic growth and cytoskeletal stability at the Drosophila neuromuscular junction." J Neurosci 26(36): 9293-303.

Walker, D. W. and S. Benzer (2004). "Mitochondrial "swirls" induced by oxygen stress and in the Drosophila mutant hyperswirl." Proc Natl Acad Sci U S A 101(28): 10290-5.

Watanabe, G., A. Howe, et al. (1996). "Induction of cyclin D1 by simian virus 40 small tumor antigen." Proc Natl Acad Sci U S A 93(23): 12861-6.

Weaver, B. A., A. D. Silk, et al. (2007). "Aneuploidy acts both oncogenically and as a tumor suppressor." Cancer Cell 11(1): 25-36.

Welcker, M., J. Singer, et al. (2003). "Multisite phosphorylation by Cdk2 and GSK3 controls cyclin E degradation." Mol Cell 12(2): 381-92.

Wen, Y., V. S. Golubkov, et al. (2008). "Interaction of hepatitis B viral oncoprotein with cellular target HBXIP dysregulates centrosome dynamics and mitotic spindle formation." J Biol Chem 283(5): 2793-803.

Wiese, C. and Y. Zheng (2006). "Microtubule nucleation: gamma-tubulin and beyond." J Cell Sci 119(Pt 20): 4143-53.

Wilson, L., H. P. Miller, et al. (1985). "Taxol stabilization of microtubules in vitro: dynamics of tubulin addition and loss at opposite microtubule ends." Biochemistry 24(19): 5254-62.

Wise-Draper, T. M. and S. I. Wells (2008). "Papillomavirus E6 and E7 proteins and their cellular targets." Front Biosci 13: 1003-17.

Won, K. A. and S. I. Reed (1996). "Activation of cyclin E/CDK2 is coupled to site-specific autophosphorylation and ubiquitin-dependent degradation of cyclin E." EMBO J 15(16): 4182-93.

Xu, Y., Y. Xing, et al. (2006). "Structure of the protein phosphatase 2A holoenzyme." Cell 127(6): 1239-51.

Yang, C. S., M. J. Vitto, et al. (2005). "Simian virus 40 small t antigen mediates conformation-dependent transfer of protein phosphatase 2A onto the androgen receptor." Mol Cell Biol 25(4): 1298-308.

Yang, S. I., R. L. Lickteig, et al. (1991). "Control of protein phosphatase 2A by simian virus 40 small-t antigen." Mol Cell Biol 11(4): 1988-95.

Yasuda, J., A. J. Whitmarsh, et al. (1999). "The JIP group of mitogen-activated protein kinase scaffold proteins." Mol Cell Biol 19(10): 7245-54.

Yildiz, A., M. Tomishige, et al. (2004). "Kinesin walks hand-over-hand." Science 303(5658): 676-8.

Yun, C., H. Cho, et al. (2004). "Mitotic aberration coupled with centrosome amplification is induced by hepatitis B virus X oncoprotein via the Ras-mitogen-activated protein/extracellular signal-regulated kinase-mitogen-activated protein pathway." Mol Cancer Res 2(3): 159-69.

Zhang, J. and T. L. Megraw (2007). "Proper recruitment of gamma-tubulin and D-TACC/Msps to embryonic Drosophila centrosomes requires Centrosomin Motif 1." Mol Biol Cell 18(10): 4037-49.